GEOLOGY, MINERALOGY AND PROVENANCE OF ALLUVIAL GOLD MINERALIZATION IN RIVER GAGARE DRAINAGE BASIN, WONAKA SCHIST BELT, NORTHWESTERN NIGERIA

BY

HARUNA MUHAMMED, GREMA, B.Sc. GEOLOGY (ABU), 2012
(P13SCGL8012)

A THESIS SUBMITTED TO THE SCHOOL OF POSTGRADUATE STUDIES, AHMADU BELLO UNIVERSITY, ZARIA; IN PARTIAL FULFILMENT OF THE REQUIREMENTS FOR THE AWARD OF MASTER OF SCIENCE DEGREE IN GEOLOGY

DEPARTMENT OF GEOLOGY,
FACULTY OF PHYSICAL SCIENCES,
AHMADU BELLO UNIVERSITY,
ZARIA - NIGERIA

NOVEMBER, 2017

DECLARATION

I declare that this thesis entitled "Geology, Mineralogy and Origin of Alluvial Gold Mineralization in River Gagare Drainage Basin, Wonaka Schist Belt, Northwestern Nigeria" was carried out by me in the Department of Geology, Ahmadu Bello University, Zaria. The information derived from literatures were duly acknowledged in the text and referenced. No part of this thesis was previously presented for award of any degree, diploma or related certificate(s) at this or other institutions.

H.M., Grema	……	……
Name of Student	Signature	Date

CERTIFICATION

This thesis entitled "Geology, Mineralogy and Origin of Alluvial Gold Mineralization in River Gagare Drainage Basin, Wonaka Schist Belt, Northwestern Nigeria, by HARUNA MUHAMMED, GREMA" meets the regulations governing the award of the degree of Master of Science of the Ahmadu Bello University, Zaria, and is approved for its contribution to knowledge and literary presentation.

Chairman, Supervisory Committee Name)	(Signature)	Date
Member, Supervisory Committee (Name)	(Signature)	Date
Head of Department (Name)	(Signature)	Date
Dean, School of Postgraduate Studies (Name)	(Signature)	Date

ACKNOWLEDGEMENTS

I would like to express my gratitude to God Almighty for giving me the strength needed in this endeavor.

My immeasurable gratitude goes to my supervisors Prof. I. Garba and Prof. P.O. Ogunleye for their patience, understanding and guidance throughout the course of this study.

Many thanks to the external examiner Prof. S. Baba for patiently going through every line of this work. The contributions of the internal examiners, Prof. A Idris, Dr. A.A. Ibrahim are appreciated.

I am grateful to all academic, technical and administrative staff members of the Departments of Geology, Ahmadu Bello University, Zaria and Usmanu Danfodiyo University, Sokoto for their contributions in one way or the other.

My appreciation also to the Grema, Abdulkarim and Usman families for their support and patience.

Friend, colleagues, acquaintances that have contributed in one way or the other are also appreciated.

DEDICATION

To Dr. Ibrahim Hamidu. I am immeasurable grateful.

ABSTRACT

Gold occurrence in Nigeria is known to be associated with the schist belts in the western half of the country. Amongst these is the Wonaka schist belt that has widespread occurrence of placer Au without identified primary sources, which has remained puzzling. This study applied morphological and mineral chemistry analyses of gold grains to characterize and determine the provenance of gold grains within the River Gagare drainage basin and also estimate the transport distances and provide insight into the possible mineralization style. Analytical techniques and methods employed include transmitted light microscopy, sieve analysis, binocular microscopy, scanning electron microscopy, and energy dispersive spectroscopy. These were used to carry out petrographic examination of the rocks, sedimentological studies of the gold-bearing stream sediments and heavy mineral concentrates and also to determine gold grain surface characteristics such as roundness, flatness, outline, surface texture and composition. The study area comprises of metasediments (quartz-mica schist, phyllite, metasandstone), granitoids (porphyritic granite, and diorite) and granitic gneiss, with aplite, quartz and quartzo-feldspathic veins as the minor rock occurrences. The dominant tectonic fabric within the metasediments and the granite gneiss are the steeply dipping, N-S, NW-SE and NE-SW trending, phyllitic cleavage, schistose foliations (S1) and gneissocity respectively. Gold grains from class 1, 4, and 5 are all of the B and C types, with similar flatness indices ranging from 2.5 to 11. Most of the gold grains from these classes are equant and elongated having moderately smoothen surfaces and regular outlines, suggesting short to moderate transport distances (300 m – 15 km). Rivers Kutiri and Gagare have 75% of the gold grains within them belonging to the C-type group, with catchment area consisting of all the classes, and flatness indices between 3 and 46. Primitive and trunk placers give them a multisource. The sources may be more distant than indicated by the ratios of A-type to B-type and B-type to C-type grains determined by the morphological characteristics. Lack of delicate secondary growth, pristine type, sharply crystalline Au grains, and Au overgrowth are indicative of detrital origin. All the representative gold grains plotted in the mesothermal field of the ternary Au-Agx10-Cux100 plot with low Cu and enriched Ag contents. Additionally, 70% of the recovered Au grains were less than 60 μm in size typical for Au from Archean granite-greenstone terrains.

TABLE OF CONTENTS

DECLARATION i
CERTIFICATION ii
ACKNOWLEDGEMENTS iii
DEDICATION iv
ABSTRACT v
LIST OF PLATES x
LIST OF FIGURES xii
LIST OF APPENDIXES xiv
CHAPTER ONE 1
INTRODUCTION AND GENERAL INFORMATION 1
1.1 PREAMBLE 1
1.2 LOCATION AND ACCESSIBILITY 2
1.3 RELIEF AND DRAINAGE 2
1.4 CLIMATE AND VEGETATION 2
1.5 STATEMENT OF RESEARCH PROBLEM 3
1.6 JUSTIFICATION OF THE STUDY 3
1.7 AIM AND OBJECTIVES 3
CHAPTER TWO 4
LITERATURE REVIEW 4
2.1 REGIONAL SETTING 4
2.1.1 The Migmatite-Gneiss Complex 4
2.1.2 The Schist Belts (Metasedimentary and Metavolcanic Rocks) 5
2.1.3 The Older Granites (Pan African Granitoids) 6
2.1.4 Undeformed Acid and Basic Dykes 7
2.1.5 Younger Granites 8
2.1.6 Sedimentary Basins 8
2.2 GOLD AND ITS OCCURENCE 8
2.2.1 Determination of Grain Surface Characteristics 14
2.2.2 Sediment Transport and Gold Deposition 14
2.2.3 Surface Characteristics of Au Grains Related to Stream Transport. 16
2.2.3.1 Roundness and Flatness 16
2.2.3.2 Outline and Surface Texture 18
2.3 GOLD MINERALIZATION IN NIGERIA 19

2.3.1 Gold mineralization in Wonaka Schist Belt 22
CHAPTER THREE 25
MATERIALS AND METHODS 25
3.1 MATERIALS USED 25
3.2 DESK STUDY 25
3.3 FIELD GEOLOGICAL MAPPING 25
3.4 SAMPLE COLLECTION 26
3.5 ANALYTICAL TECHNIQUES/METHODS 29
3.5.1 Transmitted Light Microscopy 29
3.5.2 Sieve Analysis 29
3.5.2.1 Method and Procedure 30
3.5.2.2 Description of the Parameters and Sets 30
3.5.3 Binocular Microscopy 32
3.5.4 Scanning Electron Microscopy (SEM) 33
3.5.5 Energy Dispersive Spectrometry (EDS) 34
3.5.6 Gold Grain Study and Classification Scheme 35
3.6 MAP DIGITIZATION 38
CHAPTER FOUR 39
RESULTS AND INTERPRETATION 39
4.1 FIELD GEOLOGY AND PETROGRAPHY 39
4.1.1 Quartz-Mica schist 39
4.1.2 Phyllite 42
4.1.3 Metasandstone 44
4.1.4 Medium – Coarse Grained Porphyritic Granite 46
4.1.5 Granite Gneiss 49
4.1.6 Diorite 51
4.1.7 Aplite Dykes 53
4.1.8 Quartz and Quartzo-feldspathic veins 55
4.2 STRUCTURAL GEOLOGY 58
4.2.1 Foliations 58
4.2.2 Joints 58
4.2.3 Faults 62
4.2.4 Folds 63
4.2.5 Lineament Analysis 64

4.3 SEDIMENTOLOGY OF GOLD BEARING STREAM SEDIMENTS 69
4.4 GOLD-BEARING HEAVY MINERALS 70
4.4.1 Description of Heavy Minerals 70
4.5 GOLD GRAIN MORPHOLOGY ..... **Error! Bookmark not defined.**
4.5.1 Class One: ..... **Error! Bookmark not defined.**
4.5.2 Class Four: ..... **Error! Bookmark not defined.**
4.5.3 Class Five: ..... **Error! Bookmark not defined.**
4.5.4 River Kutiri (RK) and River Gagare (RG) ..... **Error! Bookmark not defined.**
CHAPTER FIVE ..... **Error! Bookmark not defined.**
DISCUSSION ..... **Error! Bookmark not defined.**
5.1 GEOLOGY OF THE STUDY AREA ..... **Error! Bookmark not defined.**
5.2 STRUCTURAL FEATURES AND PATTERNS ..... **Error! Bookmark not defined.**
5.3 STREAM SEDIMENTS ..... **Error! Bookmark not defined.**
5.4 ORIGIN OF THE GAGARE BASIN ALLUVIAL GOLD GRAINS ..... **Error! Bookmark not defined.**
5.5 POSSIBLE GENETIC ORIGIN OF THE RIVER GAGARE BASIN GOLD. **Error! Bookmark not defined.**
5.6 DISTANCES TO SOURCE ..... **Error! Bookmark not defined.**
5.6.1 Distance to source: Class One ..... **Error! Bookmark not defined.**
5.6.2 Distance to Source: Class Four ..... **Error! Bookmark not defined.**
5.6.3 Distance to Source: Class Five ..... **Error! Bookmark not defined.**
5.6.4 Distance to Source: Rivers Kutiri and Gagare ..... **Error! Bookmark not defined.**
CONCLUSIONS AND RECOMMENDATIONS ..... **Error! Bookmark not defined.**
6.1 CONCLUSIONS ..... **Error! Bookmark not defined.**
6.2 RECOMMENDATIONS 78
REFERENCES 79
APPENDIXES 89

LIST OF TABLES

Table 2.1: Physico-chemical properties of gold…….....10

Table 2.2: Morphological and compositional characteristics of Au grains associated with distance from source…….19

Table 3.1: The grade scale for interpretation of graphic standard deviation……..32

Table 3.2: The grade scale for the interpretation of graphic skewness (GS)……..33

Table 3.3: The grade scale for the interpretation of GK values……23

Table 4.1: Modal mineral composition of rocks in the study area……..…….....44

Table 4.2: Heavy minerals within gold-bearing samples in the study area……..…67

Table 4.3: Statistical summary of grain morphology analysis of representative Au grains from class one……..70

Table 4.4: Spectral EDS microanalyses of some Au grains from class one in element concentration in wt.
%.....71

Table 4.5: Statistical summary of grain morphology analysis of representative Au grains from class four…….74

Table 4.6: Spectral EDS microanalyses of some class four Au grains element concentration in wt.%.....74

Table 4.7: Statistical summary of grain morphology analysis of representative Au grains from class five……..……76

Table 4.8: Spectral EDS microanalyses of some class five Au grains element concentration (wt.%)……..77

Table 4.9: Statistical summary of grain morphology analysis of representative Au grains from River Kutiri (RK) and River Gagare (RG)…….....79

Table 4.10: Spectral EDS microanalyses of some Rivers Kutiri and Gagare Au grains element concentration in wt.%.....81

LIST OF PLATES

Plate 2.1: Artisanal mining of Au from the pebble placer accumulation in the bed of River Gagare, a common practice in the area (Geoprobe 2014b)……..….24

Plate 2.2: Photographs of artisanal mining activities…….....…25

Plate 3.1: Photographs of sample collection and panning……..…28

Plate 4.1: Photograph of N-S trending, steeply dipping schist as seen in a stream channel at Kofa N12^0 15' 36.9", E06^0 56' 36.2"…….43

Plate 4.4: Photograph of thin beds of calc-silicate rocks, layered within the quartz-mica schist N 12^0 12' 57.5", E 6^0 54' 12.4"…….....44

Plate 4.3: Photomicrographs of quartz-mica schist in XPL (A) and PPL (B)…….....45

Plate 4.4: Photograph of phyllite occurring within a stream channel N12^0 14' 42.4", E06^0 58' 37.1"…….....47

Plate 4.5: Photomicrograph of phyllite in PPL (A) and XPL (B)…….....48

Plate 4.6: Photograph of metasandstone, exposed along stream channel. Weathering has reduced some occurrences into low lying, reddish pink friar rock……..…49

Plate 4.7: Photomicrographs of metasandstone in XPL (A) and PPL (B)……..…50

Plate 4.8: Photograph porphyritic granite at Dakace N12^0 14' 09.4", E06^0 51' 0.6"…….....…..51

Plate 4.9: Hand specimen of the porphyritic granite. N12^0 14' 09.4", E06^0 51' 0.6"…….....…52

Plate 4.10: Photomicrographs of different sections of the porphyritic granite…….....53

Plate 4.11: Photograph of granite gneiss (N 12^0 11' 13.8", E06^0 50' 34.4")……..…..…54

Plate 4.12: Photomicrographs of Granite gneiss in XPL (A) and PPL (B)……..…….55

Plate 4.13: Photograph of weathered diorite boulder at Shamori N12^0 06' 41.4", E06^0 54' 52.8". Inset is a hand specimen of the rock…….....56

Plate 4.14: Photomicrograph of diorite in XPL (A) and PPL (B)…….57

Plate 4.15: Photograph sharp boundary between medium grained granite (right) and aplite (left) N12^0 14' 09.4", E06^0 51' 0.6"…….....58

Plate 4.16: Aplite within granite gneiss (N 12^0 11' 13.8", E06^0 50' 34.4")…….59

Plate 4.17: Photograph of quartzo-feldspathic veins trending NW-SE. (N12^0 15' 36.9", E06^0 56' 36.2"). Inset is a hand specimen of quartz vein with empty vugs……..….60

Plate 4.18: Photograph of quartz veins within quartz –mica schist at Wonaka (N12^0 16' 34.7", E06^0 56' 47.3")……..61

Plate 4.19: Photograph of vein stringers, trending NW-SE within the quart-mica schist (N12^0 13' 42.0", E06^0 58' 29.7")……...61

Plate 4.20: Photograph of quartz-mica schist with NE-SW trending parallel joint sets in (N12^0 12' 06.6", E06^0 57' 55.8")……...63

Plate 4.21: Photograph of metasandstone with conjugal joints (N12^0 05' 51.6", E06^0 51' 12.7")……...65

Plate 4.22: Photograph of a mafic xenolith, displaced by an aplite dyke which was subsequently faulted within low lying medium grained granite at Takasaba (N 12^0 17' 48.6", E 6^0 48' 54.6")……...……67

Plate 4.23: A) Ptygmatitic folding within granite gneiss (N12^0 10' 30.1", E06^0 50' 11.2"). B) Folded phyllite exposed along stream channel (N12^0 14' 50.3", E06^0 59' 14.5")……...68

Plate 4.24: Incident light images of heavy mineral concentrates. ……..……76

Plate 4.25: incident light images of heavy mineral concentrate……...……..77

Plate 4.26: BSE images of representative Au grains of each morphological type from class one…...82

Plate 4.27: BSE images of representative Au grains of each morphological type from class four……...……..85

Plate 4.28: BSE images of representative Au grains of each morphological type from class five……..88

Plate 4.29: BSE images of representative Au grains of each morphological type from RK and RG……..92

LIST OF FIGURES

Figure 1.1: Location map of the study area…….3

Figure 2.1: Schist Belt localities in Nigeria within the context of the regional geology of parts of West Africa……7

Figure 2.2: Types of primary and secondary Au deposits and emplacement environment…..……13

Figure 2.3: Types of Au grain outlines used in this study……...……...…….20

Figure 2.4: Regional geology and structure of western half of Nigeria……...21

Figure 2.5: Spatial distribution of gold grades around Mada area……...24

Figure 3.1: Drainage map of the study area, showing distribution of the sampling points…….29

Figure 3.2: Schematic illustration of interactions of an electron beam with a solid sample..……...35

Figure 3.3: Ternary Au-Cu x100-Ag x10 plot for Au grains from three bedrock source types from central Cordillera, Chile…….....….38

Figure 3.4: Ternary Au-Cu-Ag plots of the compositions of Au grains from the Batouri gold district……...40

Figure 4.1: Geologic map of the study area……...…42

Figure 4.2.: Rose diagram of joint trends in quartz-mica schist of the study area……..63

Figure 4.3: Rose diagram of joints observed within phyllite of the study area……...64

Figure 4.4: Rose diagram of joint trends of the granite gneiss of the study area……...66

Figure 4.5: Rose diagram of joint trends within granite in the study area…….....……..66

Figure 4.6: Lineament trends of structures in the study area…….……....70

Figure 4.7: Lineament density map of the study area……..……....….71

Figure 4.8: Lineament intersection density map of the study area…….…….…….72

Figure 4.9: Pie charts illustrating the distribution of heavy minerals per slide……...….75

Figure 4.10: Distribution of the samples into classes, based on corresponding watershed.....….79

Figure 4.11: Morphological histogram summarizing the Au grains outline from class one…….....80

Figure 4.12: Morphological histogram summarizing the Au grains outline from class four…..….84

Figure 4.13: Morphological histogram summarizing the Au grains outline from class five……...87

Figure 4.14: Morphological histogram summarizing the Au grains outline from Rivers Kutiri and Gagare……90

LIST OF APPENDIXES

Appendix 1.1: Joint readings on granite……115

Appendix 1.2: Joint reading on quartz-mica schist……115

Appendix 1.3: Joints reading on phyllite……115

Appendix 1.4: Joints reading on granite gneiss……...116

Appendix 1.5: DEM shaded relief images of A: 0^0 (N), B: 45^0 (NE), C: 90^0 (E), and D: 135^0 (SE)……....117

Appendix 1.6: DEM shaded relief images of A: 180^0 (S), B: 225^0 (SW), C: 270^0 (W) and D: 315^0 (NW)……118

Appendix 1.7: Combined shaded relief images of N, NE, E, and SE……118

Appendix 1.8: Combined shaded relief images of S, SW, W and NW……119

Appendix 1.9: Automatically extracted lineament from shaded relief images of N, NE, E, and SE……...120

Appendix 1.10: Automatically extracted lineament from shaded relief images of S, SW, W, and NW……120

Appendix: 1.11: Final reclass and B; Level of coincidence image……....121

Appendix 2.1: Sieve analysis data from the stream sediments samples……..122

Appendix 3.1: Cumulative frequency curves of weight % vs. phi values……...125

CHAPTER ONE

INTRODUCTION AND GENERAL INFORMATION

1.1 PREAMBLE

Gold (Au) occurrence in Nigeria is known to be related to the schist belts in the western half of the country. Historical records show that about 12,000 kg of gold was produced between 1914 and 1980 (Bungwon, 1984). Much of the production was from alluvial sources related to primary vein mineralization. However, since Au has been reported to occur in both alluvial and eluvial forms in addition to primary sources in Nigeria (Garba 2003), it is worth studying the nature of occurrence and economic potential of the alluvial placers that have yielded not only large Au deposits worldwide but are relatively the easiest to mine and process.

Several schist belts in NW Nigeria were reported to be endowed with Au mineralization (Elueze 1981, Garba 2002a). Amongst these is the Wonaka schist belt, which is characterized by unique occurrence of hornfelsic schists, phyllites and large masses of Pan-African granitoids (Turner 1983). Another unique feature of the Wonaka schist belt (though not given much attention) is the widespread occurrence of placer Au without identified primary sources. The Au mineralization within this schist belt is essentially hosted in the alluvium along the valley of River Gagare and its tributaries, notably at Gidan Boss, Dutsen Butsa, Mada, Kutcheri, Dankaya, Wonaka, Fura-Girke, River Yankuzau, and Gidan Chido (Amuda *et al.,*2013; Geoprobe, 2014a, 2014b; and Usman, 2014). The alluvial gold along the River Gagare have been seasonally exploited by artisanal miners by panning of pebbly wash alluvial accumulation in the river bed below thick seasonally deposited sands. The intensive artisanal activity and its impressive tenor of the gold output would require sufficiently large or widespread primary gold sources.

1.2 LOCATION AND ACCESSIBILITY

The study was undertaken along the River Gagare and its tributaries in the area east of Gusau (Fig. 1.1), bounded between 12^0 03' 46"N - 12^0 24' 10"N and 06^0 49' 00"E - 07^0 00' 32"E, within the Federal Survey Map Sheets 54 Gusau (NE and SE).

The area covers about 632 Km^2, and is accessible via the Kotorkoshi - Mada road that stems from the federal road (A126) that links Funtua and Gusau. Accessibility within the study area however, is provided by the network of numerous roads and tracks that consist of untarred, lateritized roads and all season footpaths

1.3 RELIEF AND DRAINAGE

The study area is generally undulating, straddling the major valley of the Gagare River, filled with alluvial terraces. The Gagare River system in the study area consists of River Kutiri (Mada) and its tributaries drain into Butsa and Fura Girke that subsequently empties into the larger Gagare River. This River system drains the highlands of the Wonaka Schist Belt and flows in the northwest direction, eventually joining the Rima River system which subsequently empties into the River Niger. The Gagare River valley is flanked by a rather undulating, more rugged terrain to the southeast towards Fura Girke and Kofa villages. The Kotorkoshi hills and Chafe Hills bound the study area on all but the northern part. The Gagare River system flows seasonally between the months of May/June and October/November.

1.4 CLIMATE AND VEGETATION

The area of study is within the tropical climatic region of the Sudan Savannah Zone. It is characterized by two distinct seasons. The dry season, with relatively low humidity, lasts from November to April while the rainy season commences in May and ends in September/October with mean annual rainfall between 450-550mm. Vegetation is mostly of the transition zone of the Sudan

and Sahel Savannah types, characterized by thorny bushes, shrubs, sparse tree cover and fringing forests concentrated along water course were moist soil exists.

Figure 1.1: Location map of the study area (Google Earth, 2017)

1.5 STATEMENT OF RESEARCH PROBLEM

The alluvial gold mineralization in the Gagare River basin which drains mostly the Wonaka schist belt has remained puzzling without identified primary sources in both proximal and distal areas.

1.6 JUSTIFICATION OF THE STUDY

Past efforts in the study area of the occurrence of gold mineralization in the Wonaka Schist belt have not succeeded in establishing the primary source of the rich placer gold mineralization nor characterize the gold grains. As such, it was thought that a thorough sedimentological study of the placer deposits could provide insight into the possible sources of the gold mineralization being exploited by artisanal miners along the Gagare river basin.

1.7 AIM AND OBJECTIVES

The aim of this research is to establish the provenance of the gold grains in the study area.

Objectives:

a) Determine the relationship between the mineralization within the stream sediments and the surrounding (host) rocks, if any exist.
b) Systematically characterize placer gold grain morphologies and geochemical composition of the River Gagare drainage basin gold grains.
c) Document all current artisanal mining areas and establish recognition criteria if any exist and continuity of Au mineralization beyond the mining areas.

CHAPTER TWO

LITERATURE REVIEW

2.1 REGIONAL SETTING

The Wonaka Schist Belt is within the Nigerian Basement Complex, which is part of the Pan-African mobile belt, situated east of the West African Craton and north-west of the Congo Craton. The basement complex is intruded by Mesozoic Calc-Alkaline Ring Complexes (Younger Granites) and unconformably overlain by Cretaceous and younger sediments. The Nigerian Basement Complex was affected by the c. 600 Ma Pan-African orogeny which resulted in a reactivated region, a product of plate collision between the passive continental margin of West African Craton and that of the active Pharusian Continental Margin (Burke and Dewey, 1972; Dada, 2006). The rocks are believed to be the results of at least four major orogenic cycles of deformation, metamorphism and remobilization, corresponding to the Liberian (c. 2,700 Ma), the Eburnean (c. 2,000 Ma), the Kibaran (c. 1,100 Ma), and the Pan-African cycles (c. 600 Ma). Consequently, four major lithological units can be distinguished, namely:

1. The Migmatite – Gneiss Complex
2. The Schist Belt (Metasedimentary and Metavolcanic rocks)
3. The Older Granites (Pan African Granitoids) and
4. Undeformed Acid and Basic Dykes.

2.1.1 The Migmatite-Gneiss Complex

The Migmatite gneiss Complex is the oldest basement complex unit which comprises of Archean and Birrimian polycyclic grey gneiss of granodioritic to tonalitic composition, considered to be the basement *sensu stricto* (Rahaman, 1988, Dada, 2006). It is the most widespread of all the components units in the complex, accounting for 60% of the basement rocks. Evidence from petrography and

geochronology suggest that the Pan- African reworking led to recrystallization of many constituent minerals of the migmatite- gneiss complex by partial melting with majority of the rocks displaying medium to upper amphibolite facies metamorphism.

2.1.2 The Schist Belts (Metasedimentary and Metavolcanic Rocks)

Known also as the Newer Metasediments (Oyawoye, 1964) or Younger Metasediments (McCurry, 1976), the Schist Belts (Ajibade 1976, Turner 1983) consist of low to medium grade metasediments and metavolcanic belts trending N-S (or NNE-SSW) in a zone about 300 km wide, best developed in the western half of Nigeria (west of longitude 8◦E), though smaller occurrences are found to the east albeit sporadically. The major schist belts of Nigeria are: Zungeru-Birnin Gwari, Kushaka, Malumfashi (Karaukarau), Kazaure, Wonaka, Maru, Anka, Zuru, Ushama, Iseyin-Oyan River, Ife-Ilesha, and the Igarra-Kabba-Lokoja belts (Fig. 2.1).

The schist belts are considered to be Upper Proterozoic supracrustal rocks infolded into the older migmatite-gneiss complex and both intruded by syn- to late-tectonic granitoids (Older Granites) (Garba 2002b). They comprise of coarse to fine grained clastics, pelitic schists, phyllites, banded iron formation, carbonate rocks (marbles/dolomitic marbles) and mafic metavolcanics (greenstones and amphibolites). Some include fragments of ocean floor material from small back-arc basins. Oyawoye (1972) and McCurry (1976) considered the schists belts as relicts of a single supracrustal cover; while multiple basins of deposition was suggested by Rahaman (1976) and Grant (1978). Structurally, Olade and Elueze (1979) related the schist belts to be fault-controlled rift-like structures while Truswell and Cope (1963) explained the structural relationships between the schist belts and the basement to be conformable metamorphic fronts.

2.1.3 The Older Granites (Pan African Granitoids)

The Older Granites of Nigeria are widespread throughout the Basement Complex and occur commonly as large circular masses consisting of an extensive spectrum of rocks varying in composition from tonalite through granodiorite to granite, syenite and charnockite (Truswell and Cope 1963).

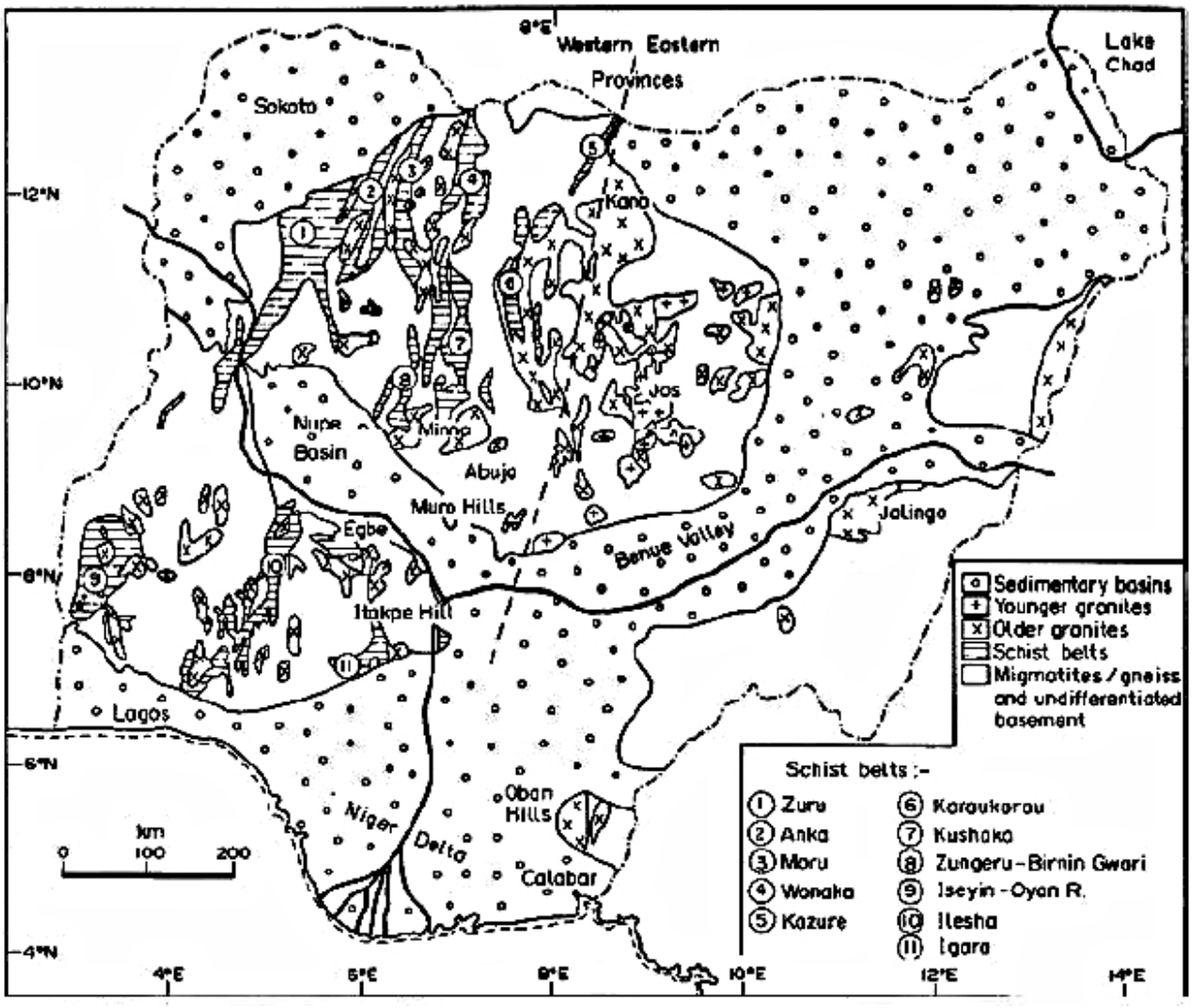


Figure 2.1: Schist Belt localities in Nigeria within the context of the regional geology of parts of West Africa (after Woakes *et al.,* 1987).

The north-south linear aggregation of many large batholiths of the Older Granites suggests that they may be related to deeply seated pre-existing plutonic episode controlled by deep mantle structures (Ogezi, 1977).

The Older Granites are the most obvious manifestation of the Pan-African orogeny and represent significant additions of materials (up to 70% in some places) to the crust (Rahaman, 1988). Compositionally, the granites plot in the field of calc-alkaline rocks on the AFM diagram and although they contain significant amount of alkalis, they are also often slightly corundum normative (Rahaman, 1988). The Older Granites have been dated by several authors at 500-700 Ma (Van Breeman et *al.,* 1977, Rahaman *et al.,* 1983, Kroner, 1984).

2.1.4 Undeformed Acid and Basic Dykes

The undeformed acid and basic dykes are late to post-tectonic Pan-African, cross-cutting the Migmatite-Gneiss Complex, the Schist Belts and the Older Granites. The undeformed acid and basic dykes comprise of:

i. Felsic dykes that are associated with Pan African granitoids on the terrain such as the muscovite, tourmaline and beryl bearing pegmatites, microgranites, aplites and syenite dykes (Dada, 2006)
ii. Basic dykes that are generally regarded as the youngest units in the Nigerian basement such as dolerite and the less common basaltic, felsic and lamprophyric dykes.

The age of the felsic dykes was put at between 580 Ma and 535 Ma from Rb-Sr studies on whole rocks (Matheis and Caen-Vachette, 1983; Dada, 2006), while the basic dykes have a much lower suggested age of 500 Ma (Grant, 1970).

2.1.5 Younger Granites

These are high level intrusions termed the Mesozoic ring complexes of Nigeria that intruded the late Precambrian to Lower Palaeozoic basement rocks. They form part of the wider province of anorogenic alkaline magmatism that intruded the Basement Complex discordantly to form high level steeped hills, occurring in a zone 200 km wide and 1600 km long from Niger Republic to Nigeria. Over 95% of the rocks can be classified as rhyolites, quartz-syenites or granites, with basic rocks forming the remaining 5%. Many of the rocks have strongly alkaline to peralkaline compositions; others are aluminous to per aluminous (Bowden and Kinnaird, 1984).

Initial stages in development of the ring complexes involved intrusion of vast amounts of acid lavas, tuffs and ignimbrites. Almost everywhere these rhyolitic rocks directly overlie the Pan-African basement, which means that the Younger Granites were emplaced in uplifted areas that were undergoing erosion. Granitic ring dykes are the major component of most of the complexes, ranging from 5 or less to over 30 km in diameter, and varying in plan from the polygonal to circular or crescent, and through more irregular shapes to simple stocks and bosses (Obaje 2009).

2.1.6 Sedimentary Basins

The sedimentary basins, containing sediments of Cretaceous to Tertiary ages, comprise the Niger Delta, Anambra Basin, the Benue Trough (the Lower, Middle and Upper Benue Basins), Chad Basin, Sokoto Basin, Bida (Nupe) Basin and Dahomey Basin (Zaborski, 2000).

2.2 GOLD AND ITS OCCURENCE

Gold (Au) is a highly reflective, yellow transition metal, with atomic number 79 and atomic mass of 196.96655 g/mol. which lies between Pt and Hg in the Periodic Table. It is a strongly siderophilic element that consequently tend to occur in the metallic state or in metal alloys, generally regarded as

a noble chemically inert metal (Table 2.1). Gold occurs predominantly in native form but is often alloyed with silver or copper and contains impurities of other metals including but not limited to,

Table 2.1: Physico-chemical properties of gold

S/No.	PROPERTY	DESCRIPTION
1	Chemical symbol	Au
2	Atomic number	79
3	Atomic weight	197
4	Density	19.32 g/cc @300k
5	Specific heat	0.128 j/gK
6	Melting point	1064.58 ^{0}C
7	Hardness	2 to 3 on Mohr's scale
8	Molar volume	10.2 cm^3/mole
9	Resistivity	2.2 x 10^{-8}
10	Crustal abundance	0.005ppm
11	Seawater abundance	4 to 8 x 10^{-6}ppm
12	Tensile strength	138 mega Pascal when annealed
13	Lustre	Metallic
14	Magnetic susceptibility	Low
15	Crystal system	Cubic (isometric)
16	Twinning	Commonly on octahedral planes
17	Ductility	Can be drawn into thin long wires

18	Malleability	Can be hammered into a sheet so thin that light can pass through
19	Volatility	Commences well below melting point
20	Streak	Golden yellow, shiny
21	Color and transparency	Yellow, becomes lighter with Ag content increase; opaque.
22	Distinguishing features	Color, specific gravity, softness. Not attacked by HCl.

palladium, rhodium, iron, nickel, bismuth and lead (Goldschmidt 1954). Golds tend to concentrate in late crystallites of a magmatic differentiation series and is found mostly in hydrothermal veins and pegmatites. In sedimentary rocks, Au is concentrated in resistates, and due to its high specific gravity, it tends to form rich placer deposits. Gold is also found in manganese nodules. The metal has been known and prized as an object of beauty and for its unique properties of chemical stability, electrical conductivity, malleability and ductility (trivalent and univalent variety) since early existence of man (Goldschmidt 1954). Gold has served for a long time as a standard of value against which to appraise the costs of labour, goods, currency, and national economy.

The average concentration of Au in the Earth's crust is in the order of 5 ppb and occurs mainly in discrete ore deposits. Au-bearing ore deposits fall into two main categories: (i) quartz or quartz-carbonate veins or vein systems, related to igneous activity or other heating events, and (ii) placer (sedimentary) deposits. Auriferous vein-type deposits can be further subdivided, on the basis of structure, geochemistry and mode of emplacement, into replacement or space-filling veins and shallow, low temperature epithermal deposits. Likewise, sedimentary Au deposits can be further divided into true residual placer Au deposits and those in which Au has been chemically transported and reprecipitated during ore deposit weathering, termed supergene ore deposits (Marshal and Fairbridge 1999).

Gold is one of the last minerals to crystallize out under hydrothermal conditions of deposition and thus tends to fill fractures and spaces between other minerals and rocks which it comes into contact with. Thus Au deposits are believed to underlie many modern hot springs and steam vents and are characterized by quartz and carbonate veining which is often broken and disseminated through the extensively chemically altered host rock. The veins are formed by hot waters circulating near a magma body or other heat source, which leach precious metals such as Au and silver from the host rock or magmatic fluids carrying these metals, before rising towards the surface (Fig. 2.2). Epithermal Au-quartz-carbonate mineralization forms as this fluid cools and/or reacts with surrounding host rocks (Fig. 2.2). Typical mineral associations include Au-electrum-quartz-carbonate with silver, arsenic, antimony, and iron sulfides. In the sulfide-rich hydrothermal fluids, including those of relatively low temperature fluids in surface hot springs, Au may be complexed by sulfide ligands (e.g. $Au(HS)_2$: Seward, 1973). Au may be reprecipitated in response to fluid boiling, due to temperature/pressure changes and loss of the sulfide ligand as gaseous HS, or to chemical reactions involving the sulfide ligand such as oxidation in the near-surface or surface environment. Precipitation in the sinters of hot springs and other hydrothermal surface features may also be caused by Au adsorption onto amorphous mineral surfaces.

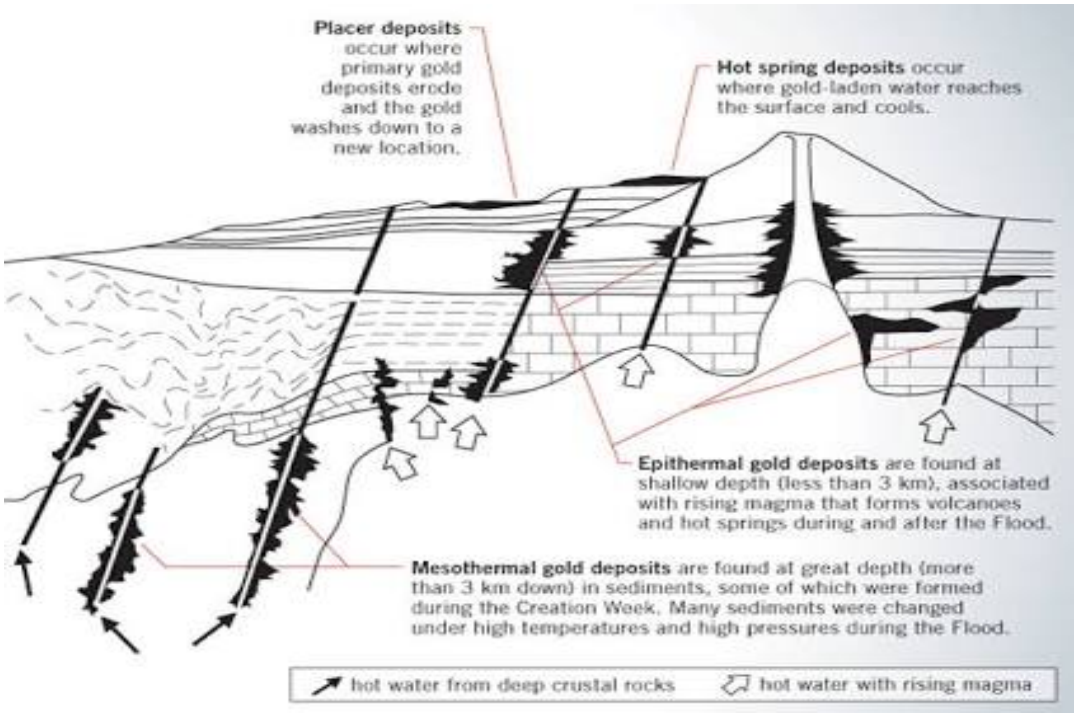


Figure 2.2: Types of primary and secondary Au deposits and emplacement environment (AuResource.com)

Gold sulfide complexing has also been proposed to account for Au transport in fluids forming auriferous quartz veins at higher temperatures and pressures in the Earth's crust. These ore bodies are usually structurally controlled by faulting or other structural features and associated with extensive chemical alteration of the wallrocks. Emplacement of Au-bearing vein is often associated with igneous, particularly porphyry, intrusive, or with metamorphic fluids which remobilize silica and metals from the surrounding rocks. Gold occurs both in the quartz vein and in the altered wallrock adjacent to the vein and typical mineral associations are Au-quartz with iron and copper sulfides. Gold complexed by sulfide can be precipitated in response to decreasing pressures and/or temperatures, as fluids move into fracture zones and/or up the geothermal gradient. Gold may also precipitate when the sulfide ligand reacts with iron in silicate and oxide minerals of the wallrock during chemical alteration of the host rock. Consequently the Au grains are moulded by the

geometry of the opening into aggregates of irregular shape and size and commonly contain inclusions of quartz and other rock forming minerals (Macdonald 2007).

Although Au grain may be crystalline, it occurs more frequently in other forms. These forms include aggregates of irregularly shaped grains in quartz and other hydrothermal minerals, reticulated dendrite, filiform, spongy massive and scales. Size, shape, and surface texture of Au are strongly influenced by their depositional environment and associated minerals. Gold tends to be coarse grained when deposited in quartz veins with only small amounts of pyrite, but may occur in an extremely finely divided state in massive pyrite or other sulphide ores.

In low temperature fluids, the familiar rounded nuggets of Au which occur at or near the surface are usually part of placer, formed by the weathering of vein or epithermal Au deposits. As Au is physically heavy and relatively chemically inert, nuggets and fragments of Au from a weathering vein system tend to remain near to the source while weathering processes remove other rock components. In flat terrain, this can lead to Au enrichment in the soil directly above an ore deposit while in steep terrain, Au enrichment will occur in nearby stream and river systems, and possibly also offshore from the mouth of a large river. While the composition of placer Au can reflect that of the original ore deposits, prolonged exposure to fluvial transport leads to the selective leaching of the more readily soluble components, such as silver and copper, from the Au alloy. This can cause an increase in Au fineness with distance from the original ore deposit.

Au grains in alluvial settings are distinguished by contrasting morphologies that reflect chemical and physical conditions in depositional environments that include regolith, glacial, fluvial, aeolean and shallow marine. When liberated, the type of gross deformation Au grain will undergo is predetermined by its original morphology. Pounding of equant grains produces flattening and cracking, flat grains are folded and pinched; elongated grains, which are transported by rolling, tend to develop into cigar-shaped particles. Lobate projections may represent Au grains that have been

rounded by later supergene processes involving dissolution and re-precipitation of Au with limited fluvial or glacial transport (Lakin *et al.* 1973).

2.2.1 Determination of Grain Surface Characteristics

Gold grains have been recovered from stream sediment as early as the Pre-Romans times, however, the use of these grains characteristics in tracing primary sources have only been employed in the past 40 years, (McClenaghan and Cabri, 2011). Though, other minerals maybe used with varying successes in detecting Au deposits (as pathfinders), Au grains have been known to be the best indicator mineral for the presence of Au deposit (Gleeson and Boyle 1980). This doesn't however, downgrade the importance of using sulphides (pyrite, pyrrohtite, arsenopyrite, chalcopyrite, sphalerite, galena, pyrorgyrite, and cinnabar), PGM, tellurides, scheelite, cassiterite, barite and rutile as well as secondary minerals (jarosite, limonite, goethite, and pyrolusite) as reliable indicators of Au deposits (Youngson *et al.,* 2002 and McClenaghan and Cabri, 2011).

Stream and till sediments are considered the most effective media for using gold grain methods (e.g. Dilabio 1991; Grant *et al.,* 1991; Townley *et al.*, 2003; Chapman and Mortensen, 2006; McClenaghan and Cabri, 2011; Vishiti *et al.,* 2015).

2.2.2 Sediment Transport and Gold Deposition

Fluvial sediments are transported in three ways namely: wash, suspension and traction (Richard, 1982). These modes of transportation lead to smoothening, polishing, rounding, fracturing and fissuring of the sediments as they move (Marshall, 1927). However, different size materials travel with different motion agent during this movement. Cobbles and other larger sized clasts generally tend to be transported as traction loads; however, if the flow magnitude is sufficiently strong, they may be transported in suspension. Traction loads are generally transported by dragging and saltation. In this way, when they are subjected to percussion, grinding and abrasion, they tend to split, fracture

and become polished, (Keunen, 1956; Richard, 1982). These has been the main agents of reshaping of Au grains during transport, which Marshall (1927) relate to the impact as a result of collision between any clasts with another clast or the bedrock. Modification of rock fragments and grains during fluvial transport depends largely on the grain form and the concentration and characteristic of other materials together with which they move. Sand act as an abrasion agent when being transported together with gravel size particles. Impacts during this transport setting, if sufficiently energetic, will result in breaking off of small parts of the grains or as much as a substantial chip of the fragment. This with time will cause the transported materials to be rounded with this attribute increasing with distance and the particle size while only decreasing with hard materials.

When it comes to accumulation of Au grains in water bodies, effect of hydrophobicity is considered because of the unbalance molecular forces at the water-solid interface causing significant tension (McDonald, 2007). In the case of Au, the surfaces are variably hydrophobic depending on the purity. Fine Au particles with high surface to mass ration will float on the surface of water and be lost while larger particles with smaller surface area/mass ration sink.

McDonald (2007) highlighted four important factors that are necessary for the economic concentration of placer Au to be linked to broad groups of Au-bearing rocks in the hinterland. These are:

i. Adequate catchment of source rocks
ii. Sufficient weathering to release the Au
iii. Efficient methods of transportation and
iv. Media and avenue for concentration

Detrital Au and sediments in general are diagnostic of the source and associated country rocks from which they were derived. Regardless of the distance and age of the sediments, certain indicator rock

forming minerals act as pointers to the particular rock types that may represent the source or origin of the Au (McDonald, 2007)

2.2.3 Surface Characteristics of Au Grains Related to Stream Transport.

The surface characteristic of Au grains reflects the grains' history related to growth, dissolution, and deformation (Leake *et al.,* 1991). Newly liberated Au grains are usually irregularly shaped. As a result of the progressive transformation and separation in stream flow, they become semi-spherical, wafer-shaped, and finally flake-shaped. Their surfaces evolve from smooth and clean to pitted, hackly, and, finally, to lobate-textured, although variations in the stream's composition, energy and sediment type somewhat modify this general trend. Flaky and small size particles are easier to transport; distal placers consist of predominantly flake-shape Au of small size classes (Groen *et al*., 1990).

Townley *et al.,* (2003) noted that the characteristic nature of Au, especially malleability allows for the shape changes during weathering and transportation (including mechanical abrasion) in fluvial environments. The Au grains transported by streams are usually describe in terms of their flatness, roundness, outline, and surface texture (fractures, grooves etc.), serving as guide to transport and proximity referencing, (Townley *et al.,* 2003).

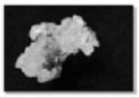
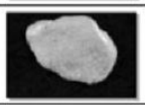
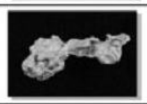
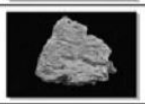
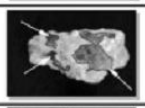
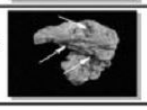
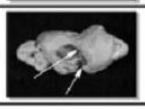
2.2.3.1 Roundness and Flatness

These surface characteristics are achieved primarily by collision of the grains during transportation. Particle roundness refers to the degree to which angular edges have been "smoothed out" rather than the measured grain sphericity (3-D) (Higgins, 2012). Roundness begin immediately as Au grains enter fluvial environment, and tend to be the most dominant of all the factors during the first 10 km of transport (Youngson and Craw, 1999), after which it basically remained unchanged. Flatness in Au grain studies is determined through Cailleux Flatness Index (Cailleux and Tricart, 1959), which is a simple measure of the mass redistribution a malleable particle undergoes in fluvial systems

(Youngson and Craw, 1999). For example if (a), (b) and (c) are the lengths of the long, intermediate and short axes of a particle, respectively, the Cailleux flatness index = (a + b) / 2c. The indices gradually increase with increasing transport downstream. Examples of this are given in Knight *et al.,* (1999), Youngson and Craw, (1999), Youngson *et al.,* (2002), McClenaghan and Cabri (2011) and Higgins (2012). Youngson and Craw (1999) have shown that the Cailleux flatness index ranges from approximately 1 (spherical or cubic) to just over 130 - highly flattened and folded discoids, or elongate/irregularly folded discoids, or sub-spherical/ellipsoidal - for the most far-traveled grains. Based on the data compiled by Youngson and Craw (1999), Au grains with maximum Cailleux flatness values of less than 7 are found in proximal primitive-placer zones and are largely undeformed; they have traveled 1 to 10 km from the lode Au source. Furthermore, grains with maximum Cailleux flatness values of 1 to 3 are found in primary or colluvial sources and have crystalline and delicate morphologies (Table 2.2); they in turn have traveled less than 1 km from the lode Au source. This was measured in this study, using the graduated eyepiece of the binocular microscope and also using ImageJ software.

Furthermore, Knight *et al.,* (1999) reported that Au grain roundness and flatness increase rapidly within the first 3 km from the source. After 5 km, the flatness continues to increase slowly while roundness remains essentially unchanged. This makes roundness a sensitive and more reliable estimator for distances less than 5 km while flatness better at a distance greater than 5 km (McClenaghan and Cabri, 2011). Youngson and Craw (1999) further added that extreme flattening denoted by folding of the Au grains often serve as an indicator of significant transportation in the fluvial environment.

Table 2.2: Morphological and compositional characteristics of Au grains associated with distance from source (after Townley *et al.,* 2003)

Distance to the source	0-50 m	50-300 m	> 300 m
General shape			
Outline			
Surface			
Primary crystal imprints		*Diffuse Evidences*	*Absent*
Associated minerals	*Quartz and Fe Oxides* 	*Fe Oxides* 	*Limonites* 
Flatness index	1-3.6	2.1-6	3.0-7.5

2.2.3.2 Outline and Surface Texture

Outline of Au grain refers to the dimensional description of the grains lying flat on the short axis perpendicular to the surface (Higgins, 2012). The grains of Au tend to have complex outlines close to the source(s), and with subsequent transportation, the outline is transformed by abrasion, resulting in rounding and flattening (Youngson and Craw, 1999). The primary texture of the surfaces of the Au grains display crystalline surface features and angular edges that are characteristic of the proximity to the source (Fig. 2.3). However, as transportation progresses, abrasion destroys these features by smoothening and polishing of the grains. Grooves and other surface markings can persist depending on the materials transported together with the Au grains and dissolution of inclusions and other soluble minerals within the grains.

Thus DiLabio (1991), Knight *et al.,* (1999), Youngson and Craw (1999), Townley *et al., (*2003) and McClenaghan and Cabri (2011) concluded that the degree of rounding, flattening, folding, and polishing of the grains provide valuable information about the stream transport system, with

McClenaghan and Cabri (2011) further stating that mechanical abrasion and collision in general control the shape while with time, roundness, smoothing and in-folding protrusion and increase flatness in such transportation medium.



Figure 2.3: Types of Au grain outlines used in this study (after Youngson and Craw 1999). Branched outline approximates dendritic and irregular crystalline forms. Complex outline approximates the highly irregular shapes in primary, colluvial and primitive forms. Equant outline approximates spherical and discoid grains. Elongate outline approximates prismoidal, rod-shaped, and elongate and wire flakes.

2.3 GOLD MINERALIZATION IN NIGERIA

A number of studies and exploration projects have been carried out on gold mineralization in Nigeria. These includes: Woakes and Bafor (1984), Bungwon (1984), Akande and Fakorede (1988), Garba (1992a, b; 2000a, b; 2002a, b; and 2003), Danbatta (2006), Ramadan and Abdel Fattah (2010), Abubakar (2012), Amuda *et al*., (2013), and Waziri (2014). Alluvial and elluvial placers as well as primary veins host Au in several parts of the supracrustal (schist) belts in the western half of Nigeria, with some of the most important occurrences found in the Maru, Anka, Tsohon Birnin Gwari, Kwaga, Malele, Gurmana-Shiroro, Minna-Suleja, Mahuta, Bin Yauri, Egbe- Isanlu, Iperindo-Igun, Okolom-Dogondaji and Shaki areas (Garba 2003, Ramadan and Abdel Fattah 2010, Geoprobe 2014a & b) (Fig. 2.4), with a few occurrences outside these major areas (Garba, 2003).

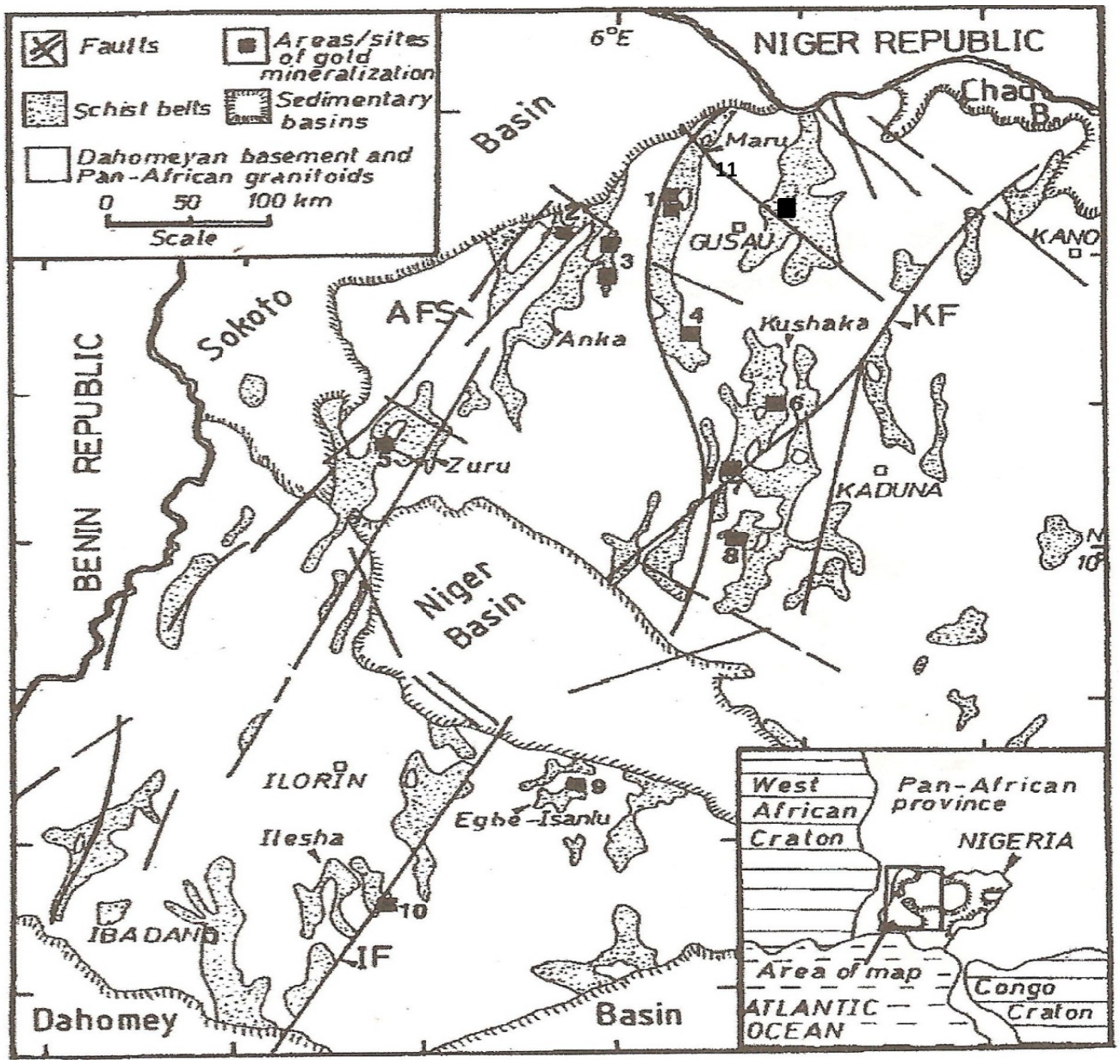


Figure 2.4: Regional geology and structure of western half of Nigeria, showing locations of key sites of Au Mineralization (after Garba 2002) 1, Maru (Duki and Maraba); 2,Anka (Kwali and Jameson); 3, Anka (Zuzzurfa and Kuba); 4, Malele; 5, Bin Yauri; 6,Tsohon Birnin Gwari; 7, Kwaga; 8, Gurmana; 9, Okolom-Dogondaji; 10, Iperindo and 11, Wonaka (Mada and Fura-Girke. AFS = Anka fault system, KFS = Kalangai fault system, IF = Ifewara fault.

Garba (2003) noted that primary Au occurs in veins, stringers, lenses, reefs and similar bodies of quartz, quartz-feldspar and quartz-tourmaline rocks in both the supracrustals and the basement rocks. The veins commonly range in thickness from several centimeters to a few meters, and in

length up to several hundred meters, often displaying lenticular or pinch-and-swell (boudinage) structure. They are invariably steeply inclined and may occur as isolated bodies or as parallel or *en echelon* vein systems (Garba, 2003). The Au-bearing veins, reefs and stringers are often localized by brittle and ductile fault structures commonly associated with fractures and shear zones, and are mainly concordant with regional foliation trends or planes of schistosity that traverse phyllites, schists, quartzites, gneisses and contact aureoles of granitoid masses. There is no systematic correlation between Au mineralization and the type of country rock, no obvious association of Au-bearing veins with Older Granites or particular lithologies among the supracrustal rocks. However, the main areas of Au mineralization occur near major faults and shear zones, spatially related to the two fault systems in the region, namely: Anka and Kalangai Transcurrent Fault Systems. The primary Au veins discovered so far are all small and have been mostly worked at the surface, only a few are large enough to justify underground mining. Placer Au has come from small disseminated pods and veinlets with low Au contents that became concentrated by alluvial processes (Wright *et al.*, 1985).

According to Garba (2003), the similarity of the possible fluid source in all the Au mineralization sites studied in the Nigerian basement may be an indication of Au ore-fluids that were active on a regional scale. The structural settings also suggest the emplacement of the Au mineralization to be late Pan-African, subsequent to peak regional metamorphism and granitoid intrusion. This period was also (c. 500 Ma) characterized by widespread uplift and brittle deformation which gave rise to the development of regional conjugate fault system that host the Au mineralization. The spatial relationship between Au mineralization and transcurrent fault systems that were possible Pan-African crustal sutures suggests a genetic link with collision tectonics (Garba 2002b).

2.3.1 Gold mineralization in Wonaka Schist Belt

The Wonaka schist belt consists of hornfelsic schist mainly fine-grained quartz-biotite schist that contains sillimanite, garnet or cordierite; forming a monotonous expanse with constant foliation trend (McCurry, 1976). It lies northwest of Malumfashi schist belt, and has distinctive composition and metamorphic region than the other schist belts. Thin beds of calc-silicate rocks are widely distributed within it (Fargher, 1966). Metamorphism is of the higher temperature and low pressure type in contrast with other belts. This has been interpreted to be due to its proximity to large granitic batholith of granite and granodiorite which almost engulf the belt. Mudstone occurrences within the belt has been thought to occur as a result of coarse grained clastic materials being progressively reduced westward from Malumfashi through Kazaure to the areas of the Wonaka schist occurrence (Turner, 1983). The Wonaka schist belt is fast becoming one of the most endowed schist belts of Nigeria in terms of Au mineralization due to widespread occurrence of Au placer deposits.

Gold mineralization in the Wonaka schist belt occurs along the stretch of the River Gagare Basin with extensive but non-uniform, erratic distribution (Plate 2.1). In the Wonaka-Fura Girke area, Au mineralization is essentially in alluvial deposits along the channel of River Gagare in form of pebbly wash accumulation covered by top river sands or soil cover of variable thickness (Geoprobe, 2014a). The Au bearing pebble wash, from which artisanal miners are sporadically extracting Au by panning (Plate 2.1), is found both on the river over bank and in the river bed (Figure 2.5) below thick accumulation of seasonally deposited sands (Geoprobe, 2014b). Average placer Au grade in the Fura Girke area is up to 2 ppm, with a resource base of about 175,000 oz. indicated within an area of 645, 000 m^2 along the valley of the River Gagare Valley (Geoprobe, 2014a).

Similarly, the Butsa-Mada region has also being witnessing a lot of seasonal artisanal Au mining activity with little or no trace of the primary vein sources (Plate 2.2). The placers have an average Au grade of about 8 ppm, distributed extensively along the River Gagare channel (Geoprobe, 2014b).



Plate 2.1: Artisanal mining of Au from the pebble placer accumulation in the bed of River Gagare, a common practice in the area (Geoprobe 2014b)

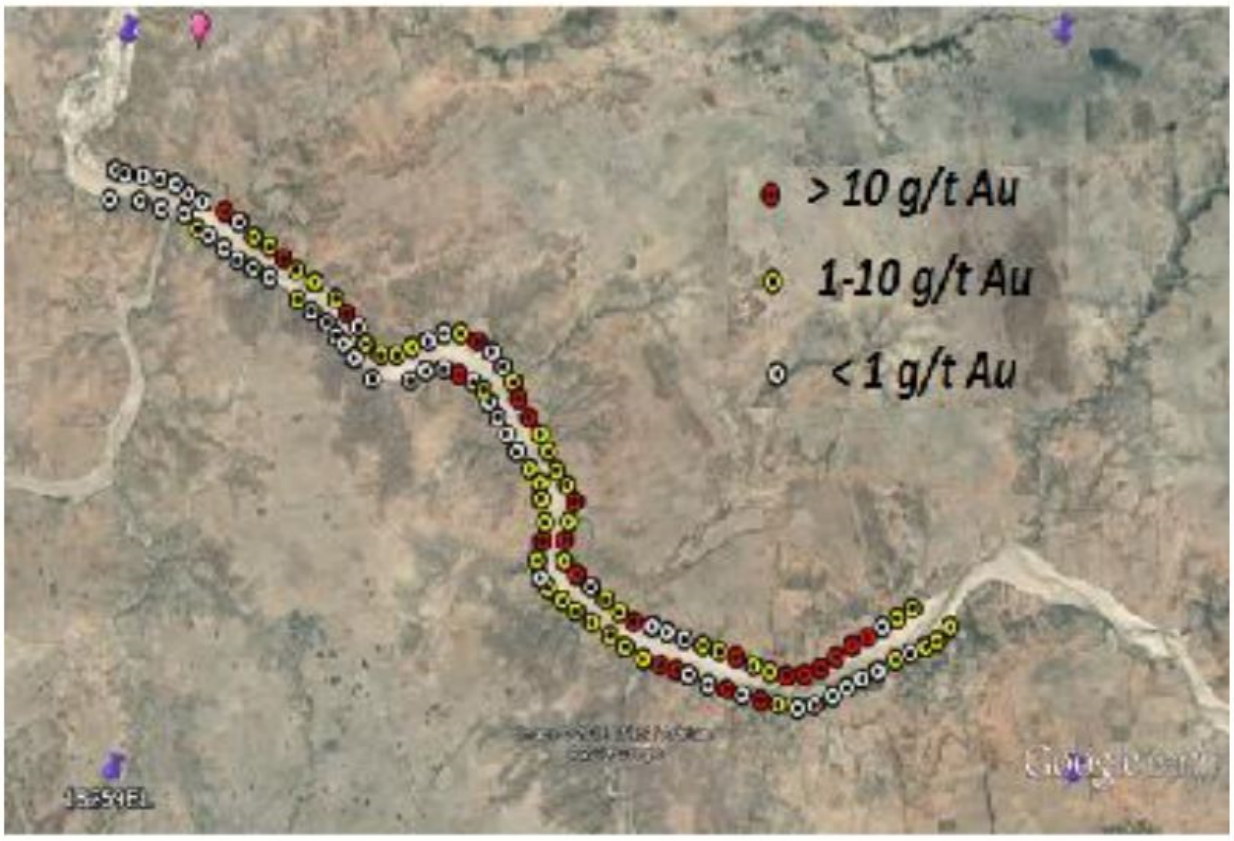


Figure 2.5: Spatial distribution of gold grades around Mada area (Geoprobe, 2014b)

Alluvial Au deposits also occur along River Kaya (Dutsen Burka), Dankaya, River Yankuzau and its tributaries in areas near Gidan Chido, and Gidan Boss (Amuda *et al.,* 2013). Panning of 40 kg sediments from pits in the area around Gidan Boss and Dutsen Burka yielded 0.28 g Au (Amuda *et al.,* 2013).



Plate 2.2: Photographs of artisanal mining activities near (A) Gidan Chido at 11°52'48''N & 07°03'15''E, B) Gidan Boss at 11°51'30''N & 07°02'55''E, C and D) Dutsen Burka at 11°51'22''N & 07°02'40''E (Amuda *et al.,* 2013)

CHAPTER THREE

MATERIALS AND METHODS

This outlines the materials and methods employed in this study. In attempting to characterize the source(s) of the alluvial Au occurrences, analyses of the geology and structural settings of the rocks in the area are combined with sieve analysis of the stream sediments and heavy mineral studies, with Au grain morphological analyses and mineral chemistry:

3.1 MATERIALS USED

Masking tape, polythene and large sample bags, waterproof marker pen and other writing materials, chisel, hammer, stainless steel pan, spade, topographic and geological maps, sampling sheets, GPS, and compass clinometer.

3.2 DESK STUDY

Extensive literature review of published and unpublished works such as Theses, Journal articles, books, field reports, topographic and geological maps, related to Au mineralization and the geology of the research area was carried out.

3.3 FIELD GEOLOGICAL MAPPING

Detailed field mapping employing traversing method was carried out in the study area. Additionally, twenty eight (28) country rock samples (7 quartz mica schist, 5 granite gneiss, 5 porphyritic granite, 4 phyllite, 4 diorite and 3 metasandstone samples) and 19 quartz vein samples, totaling 47 were collected using hammer and chisel. Representative samples were obtained in-situ. Each sample was labeled using masking tape onto which sample number was assigned using a waterproof marker pen and subsequently placed in a sample bag for transportation.

3.4 SAMPLE COLLECTION

Stream sediment samples were collected randomly (not based on a grid) from low order streams channels and from confluences with a higher order (larger) stream to avoid sampling mixed sediments resulting from flood flow. The samples were taken at zones of high energy - indicated by coarser sediment accumulations, at bends within the channels, intersections of tributaries (confluences), and places where flow has been interrupted by rock bars or other natural traps that favour heavy mineral accumulation (Plates 3.1a-c). At each sampling site, spade and pan were washed with the stream water prior to sample collection. About 15 kg of representative composited stream sediment samples were collected at the middle of the channel at a depth of 20 – 55cm – at each location - to avoid the thick accumulation of seasonally deposited sands; spade was used to scope the sample into a stainless steel, flat-bottomed conical pan or sample sac. The heavy mineral concentrates were extracted from the collected material by panning – a circular and pendulum motions of the pan within the channel under the water level (Plate 3.1d). At the site of sampling where surface water was not available, a hole was dug to access water usually to a depth of less than a meter (Plate 3.1c). During repeated shaking cycles, the lighter particles were washed and dispensed while the heavier settled down the pan. This process was repeated until a residue of heavy minerals was obtained (Plate 3.1e). A total of 67 heavy mineral concentrate samples (HMCs) were obtained (including 3 duplicate samples for control) and stored in a clearly labeled polythene plastic bags secured with a loose knot and transported in an upright position. All the sampling sites were located using a GPS (Fig. 3.1). At the base camp, the samples were air dried for a week and repackaged for analysis.

During sampling, sources of contamination such as river and collapsed banks, riparian zones, roads, bridges, habitation and winnowed sediment areas were avoided. Others are areas of limited sediment accumulation, sampler induced contamination from jewelry, pan and shovel, metal sampling box etc.



Plate 3.1: Photographs of sample collection and panning.

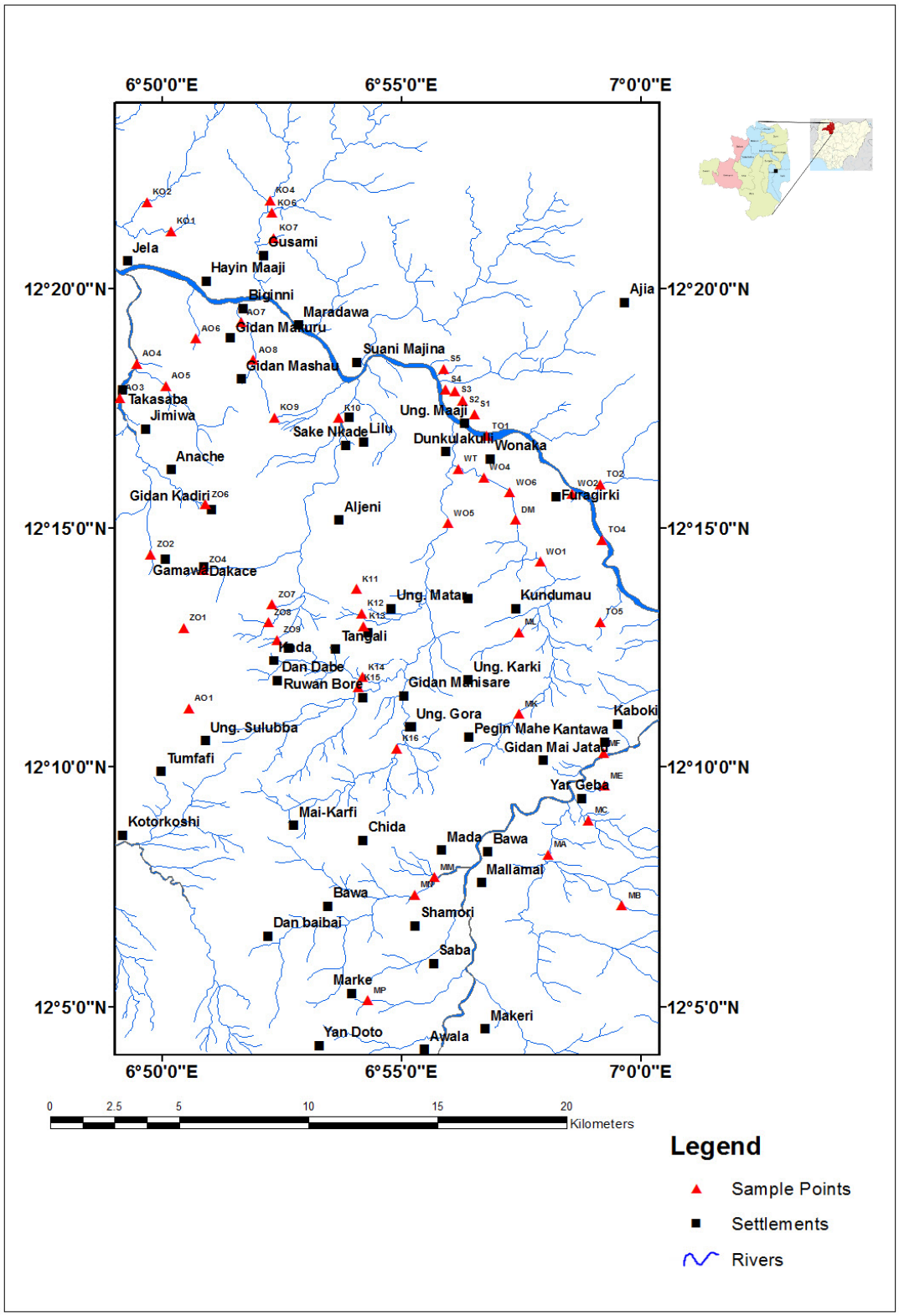


Figure 3.1: Drainage map of the study area, showing distribution of the sampling points

The HMCs were carefully examined with a binocular microscope in order to describe their occurrence, examine their surface morphology and to select suitable gold grains for further study. The HMCs were subjected to microanalyses in line with the recommendation of Youngson and Craw, (1999); Knight *et al., (*1999); Chapman and Mortensen (2006); McClenaghan and Cabri, (2011) and Vishiti *et al.,* (2015). The techniques employed allow for the qualitative and semi-quantitative determination of the morphology, composition and other characteristics of the Au grains. The advantage of the methods employed in this study over traditional geochemical analysis of sediment samples in exploration is that Au grains are visible and can be examined and that the methods are sufficiently sensitive to detect only a few amounts of Au gains in a large bulk samples, equivalent to ppb level, (Chapman *et al.,* 2010; McClenaghan and Cabri, 2011; Moles *et al.,* 2013 and Vishiti *et al.*, 2015). This is especially useful in areas like that of the Gagare streams where numerous regional rocks contribute dilutant sediment concentrates as well as geochemical signals.

3.5 ANALYTICAL TECHNIQUES/METHODS

3.5.1 Transmitted Light Microscopy

Out of the 28 rock samples obtained, Nineteen (19) representative samples were selected for thin section preparation, produced for petrographic studies using transmitted light microscope, to determine the composition, distribution and evolution of the rocks of the study area.

3.5.2 Sieve Analysis

This analysis was carried out using samples from the gold-bearing stream sediments to determine the grain size distribution. Grain size is expressed in Phi (ϕ) unit which is a negative logarithm to the base of 2 of the particle diameter in millimeter (mm), thus ϕ is a dimensionless quantity. Apparatus used include; piston and mortar, electronic weighing balance, set of five sieve mesh and an electronic shaker.

3.5.2.1 Method and Procedure

Portions of the samples were pounded gently in the mortar using the piston to separate the individual grains from each other. The samples were oven dried and 100g of each was then measured using the electronic weighing balance for sieve tests. Set of five Wentworth sieves which were already weighed empty and recorded. The sieves were arranged according to increasing aperture size and the sample poured into them from the top (1mm sieve) and covered, then positioned in the shaker and the machine was operated for 10min during which the samples filtered through the different mesh and retained according to sizes.

After the filtration, the individual test mesh were weighed with the sieved content, then the weight of the empty mesh was subtracted from it to determine the weight of the retained grains. Subsequently at the end of the process, calculations, deductions and interpretations were made based on Fork and Ward (1957) to determine the mean distribution, sorting, skewness and kurtosis.

From the results obtained from the sieve analysis, cumulative curves and histograms were generated following standard procedures. Grain sizes corresponding to the 5th, 16th, 25th, 50th, 75th, 84th and 95th percentiles were obtained and used to compute the graphic mean, median, standard deviation (sorting), inclusive graphic skewness and graphic kurtosis.

3.5.2.2 Description of the Parameters and Sets

Median Grain Size

The median grain size is the grain size that separates 50% of the sample (by weight) from other 50%. It thus, corresponds to ϕ50 (that is, the ϕ value of the 50^{th} percentile). It corresponds to a certain grain size in mm. **Mean:-** $\frac{\phi 16 + \phi 50 + \phi 84}{3}$

Graphic Sorting

It is a measure of the scatter of the grain size about the mean and corresponds with the standard deviation (Table 3.1). It is indicative of the hydrodynamic condition such as range of velocities and degree of turbulence operating in the transporting medium and to some extent suggestive of the distance of travel. **Sorting** $\frac{\phi 84 - \phi 16}{4} + \frac{\phi 95 - \phi 5}{6.6}$

TABLE 3.1: The grade scale for interpretation of graphic standard deviation

GRAPHIC SORTING (Φ)	INTERPRETATION
<0.35	Very well sorted
0.35 – 0.51	Well sorted
0.50 – 0.71	Moderately well sorted
0.71 – 1.0	Moderately sorted
1.0 – 2.0	Poorly sorted
>2.0	Extremely poorly sorted

Graphic Skewness

This is the measure of the bias in the grain size distribution toward the coarser or finer-grained end of the size range. Positively skewed samples (Table 3.2) have an excess of fine grain, while negatively skewed samples have an excess of coarse grain

Skewness: $\frac{\phi 16 + \phi 84 + 2\phi 50}{2(\phi 84 - \phi 16)} + \frac{\phi 5 + \phi 95 - 2\phi 50}{2(\phi 95 - \phi 5)}$

TABLE 3.2: The grade scale for the interpretation of graphic skewness (GS)

GRAPHIC SKEWNESS (Φ)	INTERPRETATION

>0.30	Strongly fine skewed
0.30 – 0.10	Fine skewed
0.10 – -0.10	Near symmetrical
-0.1 – -0.30	Coarse skewed
<-0.30	Strongly coarse skewed

Graphic Kurtosis

This is a measure of the flatness of the grain size distribution as it would appear on a simple frequency curve. Flat distributions are platykurtic (Table 3.3) while peaked distributions are leptokurtic.

Kurtosis: $\frac{\phi 95 - \phi 5}{2.44(\phi 75 - \phi 25)} = \frac{\{4 - (-0)\}}{2.44(2 - .0)} = \frac{4}{4.392}$

TABLE 3.3: The grade scale for the interpretation of GK values

Graphic Kurtosis(ϕ)	**Interpretation**
<0.67	Very platykurtic
0.60 – 0.90	Platykurtic
0.90 – 1.50	Mesokurtic
1.5 – 3.0	Leptokurtic
>3.0	Very leptokurtic

3.5.3 Binocular Microscopy

Binocular microscope is a powerful instrument used in the observation and determination of grain surface characteristics. This technique was used to carry out examination on the surfaces of gold grains in their natural state and coloration. The gold grains were subsequently classified to represent

different surface morphology and representative grains were chosen for detailed analysis of the physical characteristics such as roundness, outline, folding, flatness and composition.

3.5.4 Scanning Electron Microscopy (SEM)

SEM is a powerful technique applied in micro-imaging of a variety of materials. This technique was used in exploring the surface characteristics to determine particle size, texture, inclusions and general morphology on that surface.

Basically, electron microscope employs a beam of electrons and exploits the wavelike properties of electrons to obtain an image. Since the wavelength of the electron beam is much lower than that of visible light, resolution and useful magnification of SEM are much higher. Scanning coils move probe spot across specimen surface to form specimen image. Interaction of electron beam (Fig. 3.2) with sample generates a variety of signals (secondary electrons [SE], backscattered electrons [BSE], characteristic X-rays, etc.).

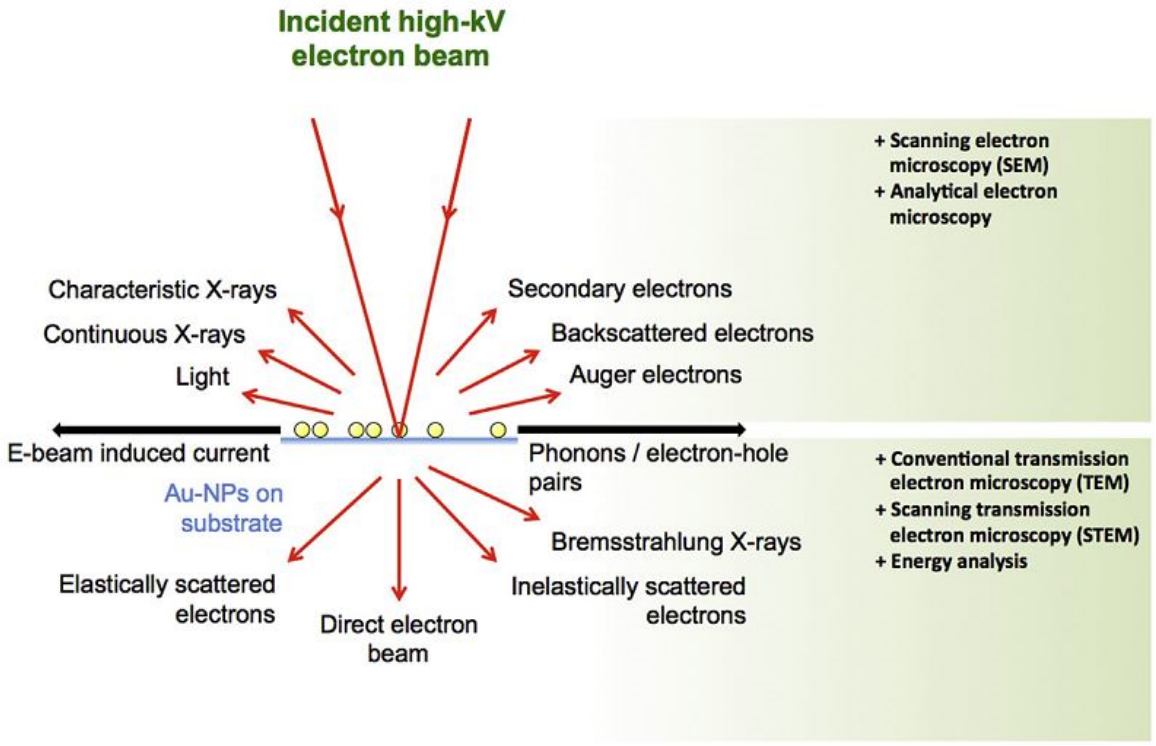


Figure 3.2: Schematic illustration of interactions of an electron beam with a solid sample.

One of main characteristics of chemical elements is their atomic number (Z), which is unique for each element and is a basis for BSE imaging and X-ray (EDS) identification of heavy metal-bearing phases. The number of BSE is controlled by the atomic number of elements in the sample. Elements with higher Z reflect more BSE than elements with lower Z, thus producing the so called Z-contrast or compositional contrast, which enables relative distinction between particles with different elemental composition. Heavy metals are electron dense elements with high atomic number and are effective electron backscatters. In BSE images, a phase with high average atomic number like Au appears white, and most other phases are seen in shades of grey. The study has employed SEM (Phenom ProX) instrument from Ahmadu Bello University, Zaria-Nigeria and Covenant University, Ota-Nigeria for the morphological characterization of Au grains, minerals and recognition of textures for selected stream sediment samples. Characterization of the individual Au grains in the samples was done on two levels; the first is a micro-morphological description of the grain shapes and general appearance which involves studying the visual morphology of the grains. The second being examination of the grain surface at higher magnification to identify micro scale morphological features like fracturing and lines of inclusions.

3.5.5 Energy Dispersive Spectrometry (EDS)

EDS is a technique that is applied in the determination of elemental composition of a surface. This technique makes use of X-rays emitted by elements that are initially excited by bombarding electrons. After localization of heavy metal-bearing grains in the sample with BSE imaging, qualitative and semi-quantitative chemical composition of selected grains was measured using the EDS. EDS detects and processes X-rays that are emitted from constituent elements and are characteristic of each chemical element, dependent on its atomic number, density of the material, beam energy and the emitted X-ray energy. X-ray maps of a surface are often quite valuable in revealing compositional variation across a sample. EDS was used in this study to perform spot

analysis of the elemental composition at different points on the solid surface, and to examine the distribution of the elements on the surface of the minerals via mapping. It is noteworthy to know that mineral polymorphs cannot be distinguished by this method (EDS), and hence are grouped as one species. Example; TiO_2 (i.e. rutile, analase, brookite) or Al_2SiO_5 (andalusite, sillimanite and kyanite) are referred to as rutile and sillimanite respectively. However, the distinction between rutile and ilmenite for example is based entirely on the measured TiO_2 wt% by the EDS (e.g. Keulen *et al.,* 2012). Each grain is classified according to a mineral classification scheme based on the measured element concentration in the grain.

3.5.6 Gold Grain Study and Classification Scheme

Due to the covered nature of the study area, two methods were employed. These are (1) the use of Au grain morphology as a distance to source indicator, and (2) the application of Au grain composition and HMC as discrimination tools for primary source type. The Au grains generally occur as fine-grained discrete grains in native form. The occurrences as silt-sized material of the Au grains enable the use of panning to reduce the amount of sediments in the field. They were studied using Binocular Microscope, SEM and EDS.

Parallel studies of surface characteristics of Au grain, compositional data combined with gangue mineral inclusions examinations in the Au grains provide greater insights to mineralization styles and distinguishing grain populations (Leake *et al*., 1993; Chapman *et al*., 2000, 2009, 2010; Potter and Styles 2003; Townley *et al.,* 2003). This kind of approach was choosen and employed in this study due to the facts provided by these criteria, which reduces the need for large Au grain morphological and compositional dataset.

Morphological characteristics were grouped according to degree of modifications, adopted from the grouping of Au grains from that used by Townley *et al.* (2003), Higgins (2012), and Vishiti *et al.,* (2015) on the basis of surface characteristics. The groups are:

i. **A-type** grains refer to Au grains with very angular to angular edges and irregular shapes, representing the least morphologically evolved. They include block rod, wire, leaf, crystal, star and globule or bleb.

ii. **B-type** grains are those Au grains that retain some aspect of the primary surface textures but edges and protrusions have been folded, rutted and or curled due to transport. They may also be striated. These types include all forms of Au grain occurrence mention A-type but have been modified to varying degrees. The grains are generally sub angular to sub rounded.

iii. **C-type** This group has undergone significant transport that resulted to complete shape modification. All primary surface forms have been damaged in one way or the other, with the grains having rounded to well rounded edges, polished and smoothened surfaces. The group represents the most morphologically evolved of the grains. The grains are flattened to round resulting from repeated folding of leaves, wires and rods. Surfaces may be pitted from impact marks with other grains during transport, with the ultimate end shapes being the typical discoid placer flakes and/or nuggets.

Since the development of using signatures from microchemistry of Au grains by the British Geological Survey (Leake *et al.,* 1995; Chapman *et al.,* 2000; Vishiti *et al.,* 2015; Chapman and Mortensen, 2006), has, together with Au grains' morphological studies become a reliable tool in speculating on the nature of primary Au mineralization through the study of detrital Au grains (Vishiti *et al.,* 2015). The criteria employed are the grains' mineral inclusions and alloyed minerals (Chapman *et al.*, 2000, 2009, 2010; Chapman and Mortensen, 2006; Moles *et al.*, 2013; Vishiti *et al.,* 2015). This suitability, Vishiti *et al.* (2015) reiterated as due to the fact that the composition of Au grains in stream sediments and soil reflects the composition of the Au grains in the lode source or bedrock. This relationship is better represented by the use of the ternary plot (Fig. 3.3), proposed by Townley *et al.* (2003) and developed by latter researchers (Chapman and Mortensen, 2006; Chapman

et al., 2010; Moles *et al.*, 2013; Vishiti *et al.,* 2015). The representation, use the Au grain composition in term of the Au itself, presence of Ag and Cu within it to classify the detrital grains into different type of primary sources.

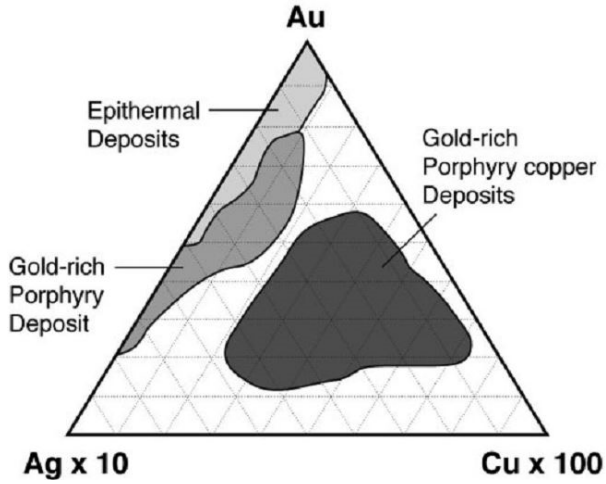


Figure 3.3: Ternary Au-Cu x100-Ag x10 plot for Au grains from three bedrock source types from central Cordillera, Chile (Townley *et al.,* 2003)

In addition to composition of the inclusion, the relative proportion of specific mineral classes (e.g. tellurides, sulphides, sulpharsenides, sulphosalts) in Au grains can be useful for identifying different grain sources (Chapman *et al* . 2009). Abundance of inclusion may decrease due to both post-depositional alteration/weathering in the surficial environment and physical grain degradation with increasing transports downstream (Mortensen *et al.,* 2004). The result of the microanalysis by the EDS was used for the micro-chemical analysis. Correction was done automatically using ZAF (Z=atomic mass, A=absorption, F=florescence) method on the data and further normalized wt% was used instead of atomic wt% because bulk composition of the grain was considered and wt% does not depend on accelerating voltage which was varied during the analysis.

Examples of the application of this classifications scheme include Youngson *et al.* (2002) demonstration of the use of combining Au grain composition with morphology to identify distinct sources of placer grains, Townley *et al.,* (2003) use of Au grain compositional data to distinguish

epithermal, Au-rich porphyry and Au-rich porphyry Cu systems. Potter and Styles (2003) similar study that determined Au signatures associated with grains from skarn mineralization and application by Vishiti *et al.,* (2015) in the exploration pits of Batouri Au district, SE Cameroun to link the relic particulate Au to the primary lode-Au mineralization (Fig. 3.4).

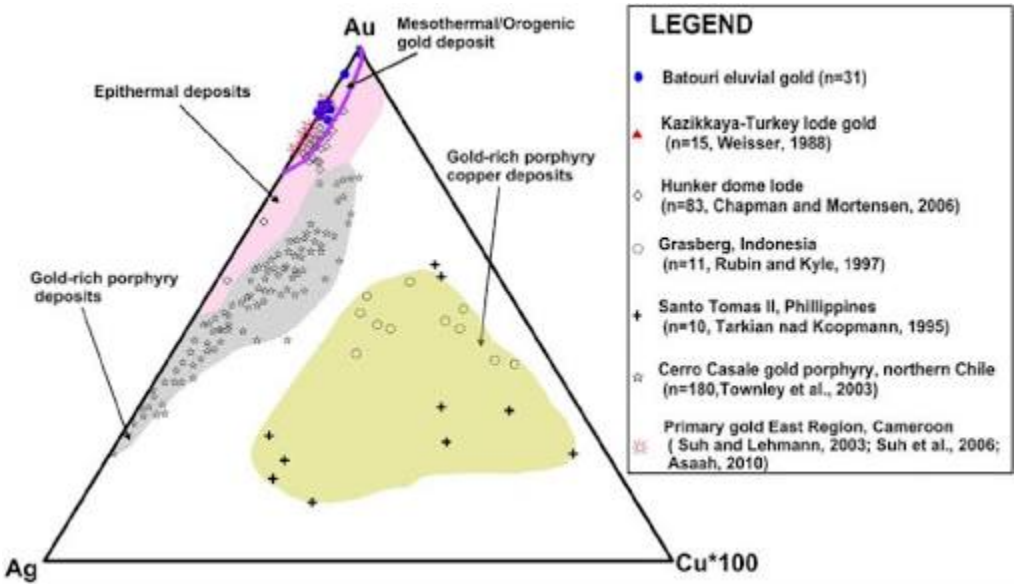


Figure 3.4: Ternary Au-Cu-Ag plots of the compositions of Au grains from the Batouri gold district compared with those from the Kazikkaya-Turkey lode gold, Hunker dome lode, Grasberg, Indonesia, Santo Tomas II, Philippines and Cerro Casale gold porphyry northern Chile. The Batouri gold grain samples showhydrothermal signatures.

3.6 MAP DIGITIZATION

Study area maps of parts of Sheet 54 Gusau NE and SE were scanned and digitized at a scale of 1:50,000 using MapInfo digitizing software (version 11.4) and ArcGIS for the various maps used in this study.

CHAPTER FOUR

RESULTS AND INTERPRETATION

This chapter presents the results of field mapping, petrographic studies, structural analyses, sieve analysis, HMCs studies, grain morphological characterization and mineral chemistry analysis.

4.1 FIELD GEOLOGY AND PETROGRAPHY

The study area comprises of quartz-mica-schist, phyllite, meta-sandstone, medium to coarse grained porphyritic granite, granitic gneiss, and diorite as the five major rock types with aplite, quartz and quartzo-feldspathic veins representing minor rock occurrences(Fig. 4.1).

4.1.1 Quartz-Mica schist

Quartz-mica schist occurs in the central part of the study area, extending from north to south across the Gagare River, covering about 228 km^2 of the study area. The rock is poorly exposed, however, where seen, within the river channel (Plate 4.1), it is low lying. It also occurs as boulders and smaller fragments within the stream channels in the study area. The schist is coarse enough to enable identification of individual mica flakes of dark looking biotite and light muscovite, which together, give a light reflecting vitreous sheen. The rock splits easily along the micaceous films. In some places, reddish brown crystals of garnet dot the rock with some euhedral having the hexagonal outline of the mineral. Generally, the rock is strongly foliated, with the N-S trend direction, mostly defined by the alignment of muscovite with flat platy cleavages. Chlorite occurs together with opaque minerals in a lenticular form by in by the quartz and feldspar crystals.

Figure 4.1: Geologic map of the study area



Plate 4.1: Photograph of N-S trending, steeply dipping schist as seen in a stream channel at Kofa N12^0 15' 36.9", E06^0 56' 36.2". Inset is a hand specimen of the rock with spots of garnet crystals.

Quartz and quartzo-feldspathic veins ranging from 0.8 cm to 86 cm in width transcend the rock in all directions, albeit mostly running in the NW, NE and E directions, with the former parallel to the trend direction of the rock. Color variation was also observed within the schist in the parts of the study area. In the northern and east central parts, the schist appears darker with more of biotite and muscovite occurring within it, while in the central parts, garnet crystals appearing as reddish spots, are dotted all over the rock, while south of Mada and along Yan Doto, the dominant quartzo-

feldspathic nature of the schist makes it appear relatively lighter. Thin beds of concordant calc-silicate rocks were seen within the quartz-mica schist (Plate 4.2).

Microscopic examination of the rock reveals that the schist is medium grained together with opaque minerals exhibiting a well-developed planar foliation and that of quartz and feldspar, however, the foliation is generally moderately to poor with less than 75% of the grains aligned within 10^0 of the common plane (Plate 4.3). It is composed of quartz, biotite, muscovite, plagioclase, chlorite, and garnet (Table 4.1), in addition to opaque minerals. The quartz crystals are sub- to anhedral with the latter dominating; undulose extinction is pronounced within the crystals and together with plagioclase feldspar, has mostly serrate boundaries. The biotite occurs irregularly within both the bands as anhedral crystals with its perfect, one directional cleavage giving it a straight extinction. Strong pleochroism were readily observed in the ppl view. Muscovite alludes clear to pale yellow coloration in ppl with a moderate relief and not pleochroic, appearing stippled, while under xpl, it exhibits parallel extinction. Two part biotite-chlorite occurrence were observed within the thin section, however, where the chlorite is well developed, the crystals exhibit green coloration in ppl with brownish appearance in xpl, showing anomalous interference colors.



Plate 4.2: Photograph of thin beds of calc-silicate rocks, layered within the quartz-mica schist N 12^0 12' 57.5", E 6^0 54' 12.4"

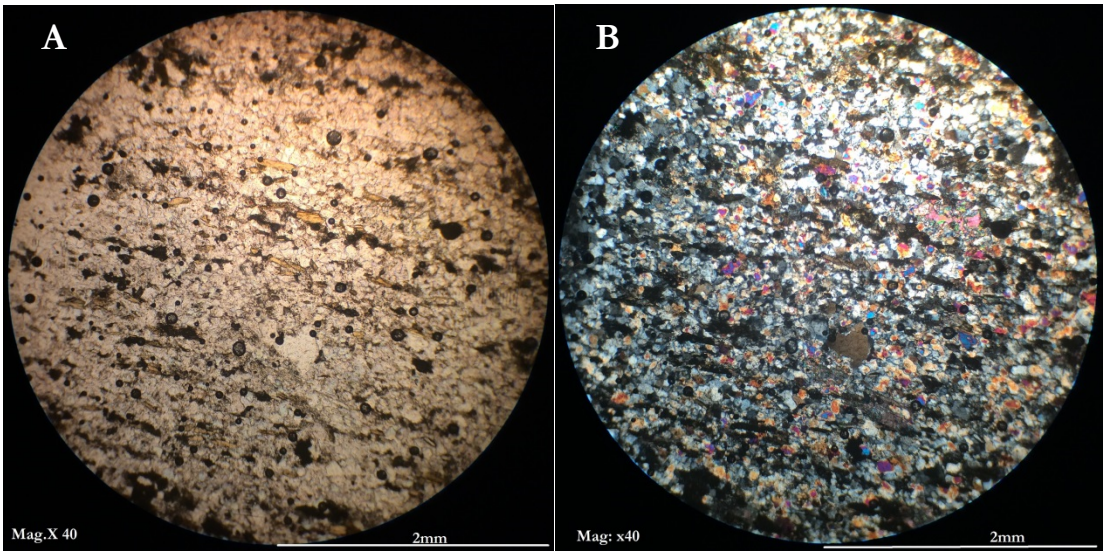


Plate 4.3: Photomicrographs of quartz-mica schist in PPL (A) and XPL (B). Garnet porphyroblast can be seen within the section with quartz, biotite, muscovite and chlorite forming moderate schistosity. QTZ= quartz, BT= biotite, PL= Plagioclase, CHL= chlorite, ORTH= orthoclase, OP= opaque, GT= Garnet.

Table 4.1: Modal mineral composition of rocks in the study area.

4.1.2 Phyllite

Phyllite occurs as low lying outcrops, mostly exposed within stream channels and covering an area of about 14.4 km^2. It is found occurring in the east central part of the study area around Fura-Girke (Fig. 4.1), and is bounded by medium grained granite to the east and around Wonaka, where it is bordered by the quartz mica schist to the west. The rock has the characteristic fine-grained texture, with steeply dipping foliation, trending in the NW direction and silky sheen on the cleavage plane, arising from the micaceous minerals. It is generally grey to dark grey in colour where the exposures along the streams (Plate 4.4). They are cut in almost all directions by quartz veins and stringers that appear to have been deformed together with the rock.

Microscopic observation reveals minerals mostly the mica crystals, with weak pleochroism; light green to colorless hue in plane polarized light (PPL) and parallel extinction in cross polarized light (XPL). Quartz was observed to have undulose extinction in most of the crystals and 1st order grey

interference color with interlocking boundaries (Plate 4.5). Crystals of mica minerals are needle-like and are the most aligned of all the minerals with some having been altered to chlorite.



Plate 4.4: Photograph of phyllite occurring within a stream channel N12^{0} 14' 42.4", E06^{0} 58' 37.1".

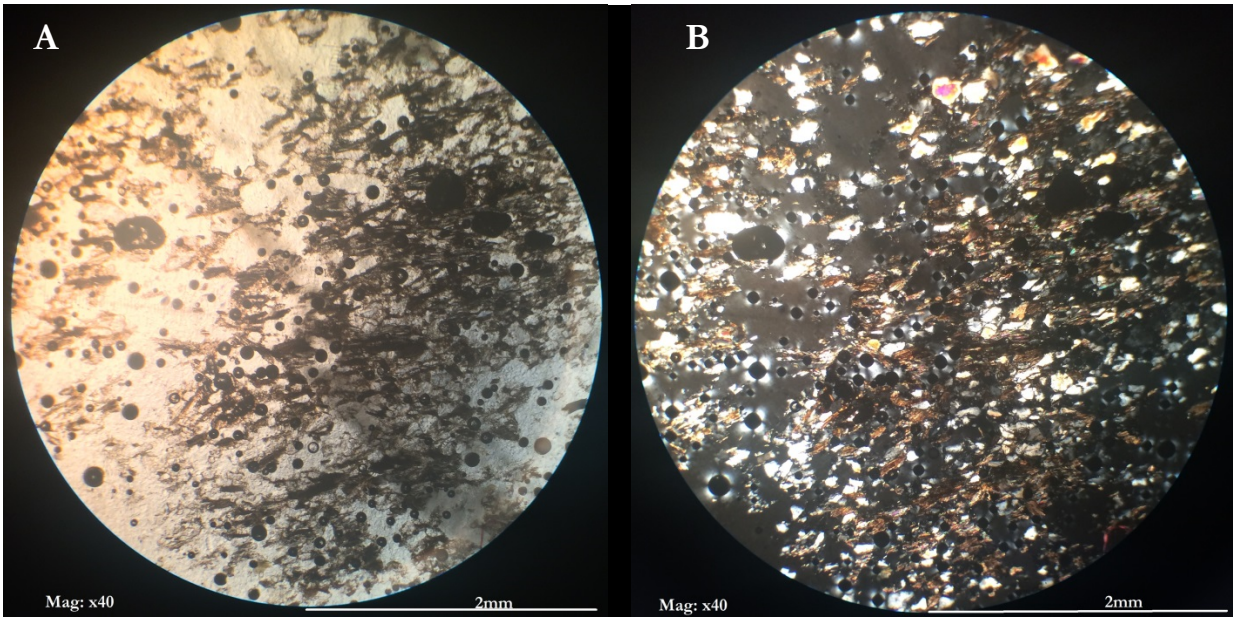


Plate 4.5: Photomicrograph of phyllite in PPL (A) and XPL (B). Crystals of mica and quartz are seen

4.1.3 Metasandstone

This rock occurs as ridges in the southwestern part of the study area and as highly weathered exposures within streams channels, covering about 22 km^2 (Plate 4.6). It is fine grained, pink to reddish brown in color and composed essentially of quartz, feldspar and biotite and minute amount of opaque minerals in hand specimen. The reddish coloration is due to high Fe oxide content of the rock in the study area that has led to ferruginization of the surfaces. The rock trends in N-S and NW-SE directions with dips of 61^0 to 72^0 E. The lack of characteristic interlocking mosaic of quartz crystals, fine grained texture, presence of other minerals other than quartz and presence of sandpaper-like surfaces together with lack of glassy appearance – which reverse are all diagnostic features of quartzite- reveal a sandstone that has undergone some degree of metamorphism rather than complete recrystallization to form quartzite (Plate 4.7). The ridges occurrences have relatively thin layers of highly weathered schist within them, with lateritic capping.

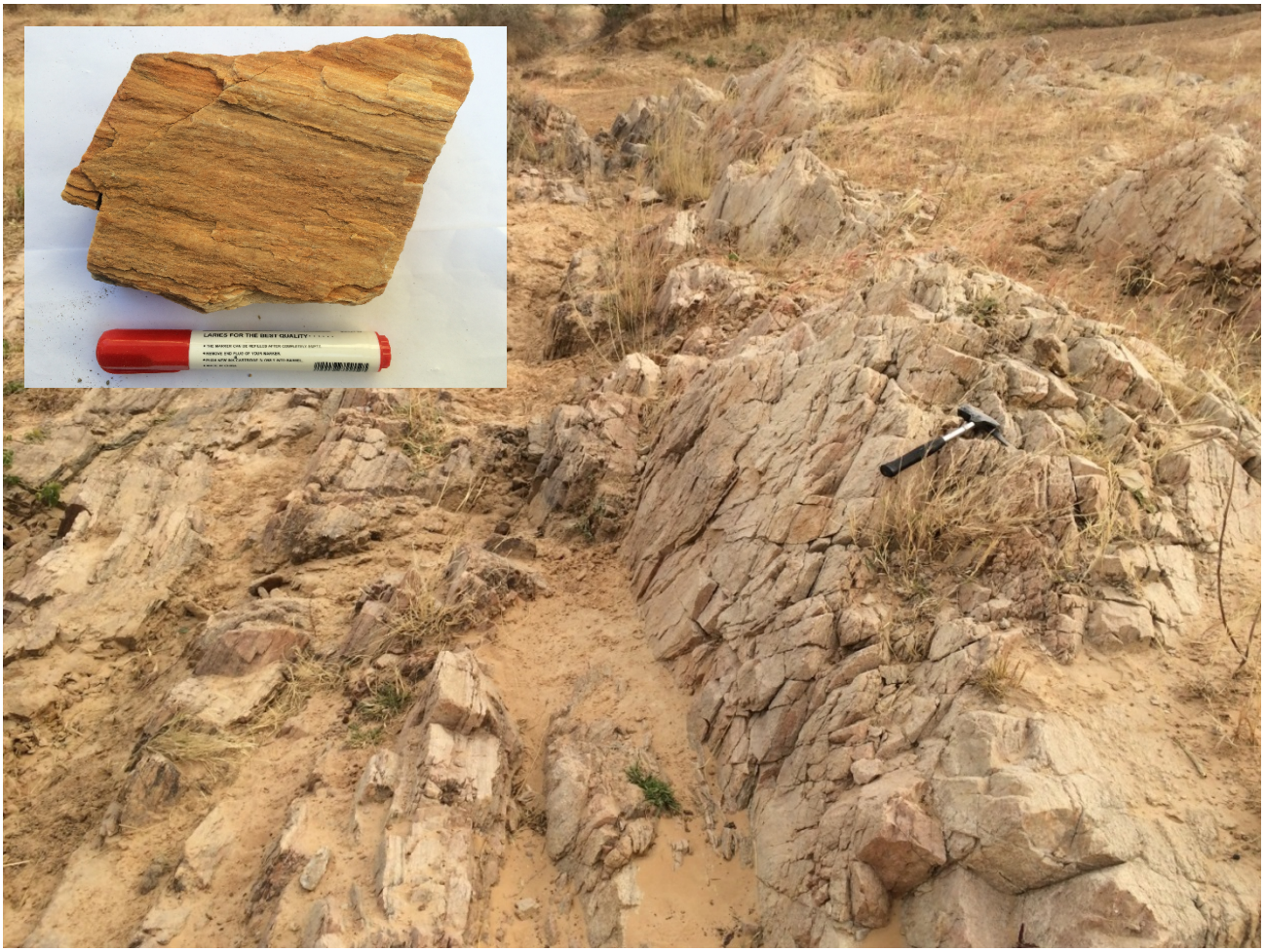


Plate 4.6: Photograph of metasandstone, exposed along stream channel. Weathering has reduced some occurrences into low lying, reddish pink friar rock.

.

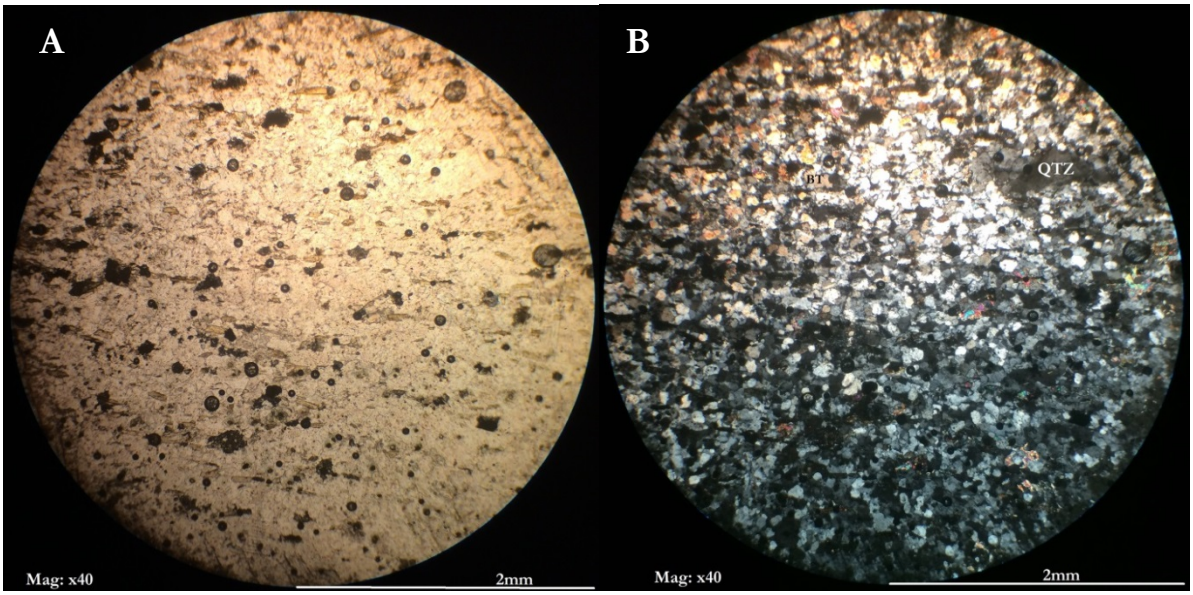


Plate 4.7: Photomicrographs of metasandstone in PPL (A) and XPL (B). QTZ= quartz, OP= opaque.

4.1.4 Medium – Coarse Grained Porphyritic Granite

The medium-coarse grained granite is the most widespread rock is the study area about 47 km^2. The rock occurs in clustered groups of hills and low lying outcrops, of various shapes of which whale backs are more common. The outcrops tend to be elongated in a north-east south-west direction. They are exposed extensively at Gusami village and forming the Awala, Dakace and Anache hills (Plate 4.8). Generally, the rock is medium to coarse grained, pinkish with cavities (druses) within which well-formed crystals are visible (Plate 4.9).



Plate 4.8: Photograph porphyritic granite at Dakace N12^0 14' 09.4", E06^0 51' 0.6"



Plate 4.9: Hand specimen of the porphyritic granite. N12^0 14' 09.4", E06^0 51' 0.6"

In the southeastern part of the study area, isolated occurrence of fine grained variety of this rock is found. It is composed of quartz, feldspar of which large phenocrysts are easily seen with the naked eye, hornblende, biotite and opaque minerals (Plate 4.9). The hills at Awala and Dakace have mostly been broken into large boulders. In some of the outcrops, weathering has turned the rock completely to clay. The exposure around Gusami is medium grained with porphyritic texture, with large crystals of quartz, and feldspars clearly observed.

In thin section, the quartz crystals are sub- to anhedral with some having kink bands, graphic intergrowth with poikilitic orthoclase, enclosing biotite and in some crystals plagioclase (Plate 4.10). Polysynthetic twinning of plagioclase characteristic of albite and cross-hatch twinning is of microcline are distinctive and some of the feldspars altered to sericite. The rock has a hiatal, porphyritic texture seen in some of the zoned feldspar crystals.

Green crystals of hornblende occur with poikilitic inclusions. Fine crystals of muscovites do occur albeit in minute amount. Orthoclase occurs with Carlsbad twins and in some of the crystals, perthite unmixing occur with alteration toward the edges occurring.

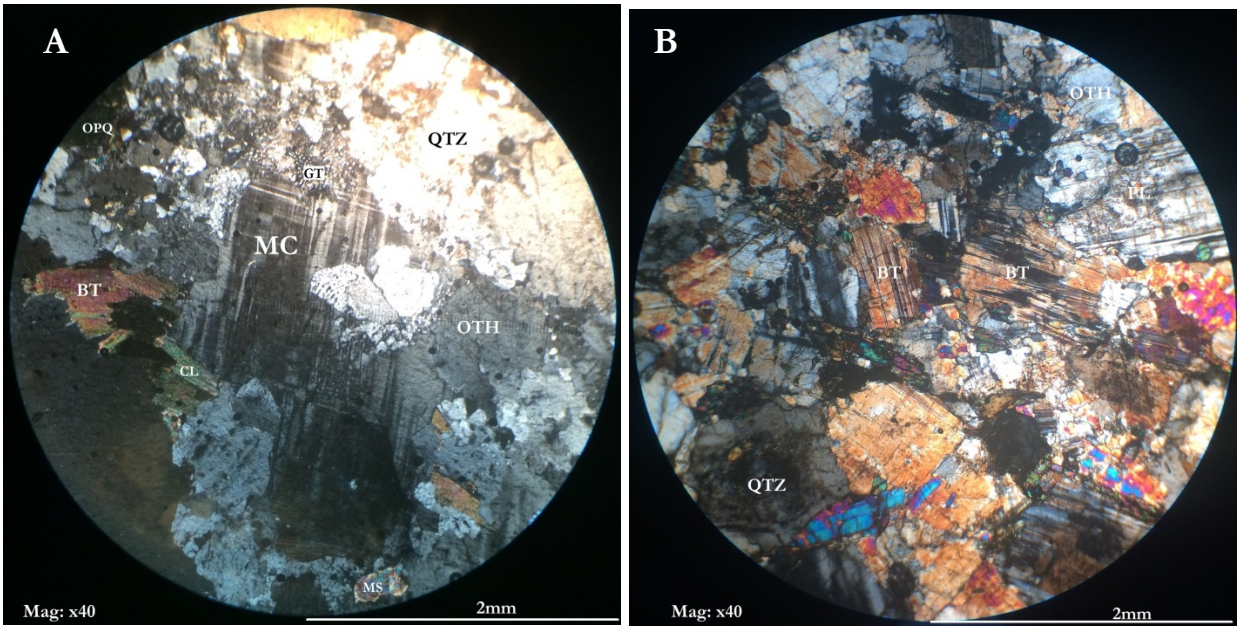


Plate 4.10: Photomicrographs of different sections of the porphyritic granite. QTZ= quartz, BT= biotite, PL= Plagioclase, MC= microcline, CHL= chlorite, OTH= orthoclase, OP= opaque, GT= Graphic texture.

4.1.5 Granite Gneiss

This rock occurs in the southwestern part of the study area, as part of the Kotorkoshi hilly outcrops mostly weathered into boulders and low-lying outcrops. The rock intrude the schists while in some places, the gneissic features include ptygmatitic folds (Plate 4.11). It is mostly light to dark grey and occupies about 25 km^2. In hand specimen, it comprise of feldspars, quartz, biotite, and muscovite, together with other mafic minerals (Table 4.1). Gneissic texture is characterized by streaky banding. The texture is generally medium grained, granoblastic, and often foliated. Bands of quartzo-feldspathic minerals range from mm scale to 8.6cm in thickness. At Tsohowar Mada, it has a sharp contact with the coarse grained porphyritic granite, both having similar fracture patterns and quartzo-feldspathic veining. Biotite dominates the mafic band in hand specimen.

In thin section, the granite gneiss minerals appear deformed and altered, with distinct foliation. Quartz, biotite, microcline, plagioclase, orthoclase, muscovite, pyroxene, sericite all occurring as sub- to anhedral shredded crystals (Table 4.1). Quartz occurs as polycrystalline, sometimes poikiloblastic

mineral, with quartz and biotite smaller inclusions (Plate 4.12), lacking pleochroism and having undulose extinction.



Plate 4.11: Photograph of granite gneiss (N 12^0 11' 13.8", E06^0 50' 34.4"). Banding is so developed in some parts of the rock giving a strong foliation.

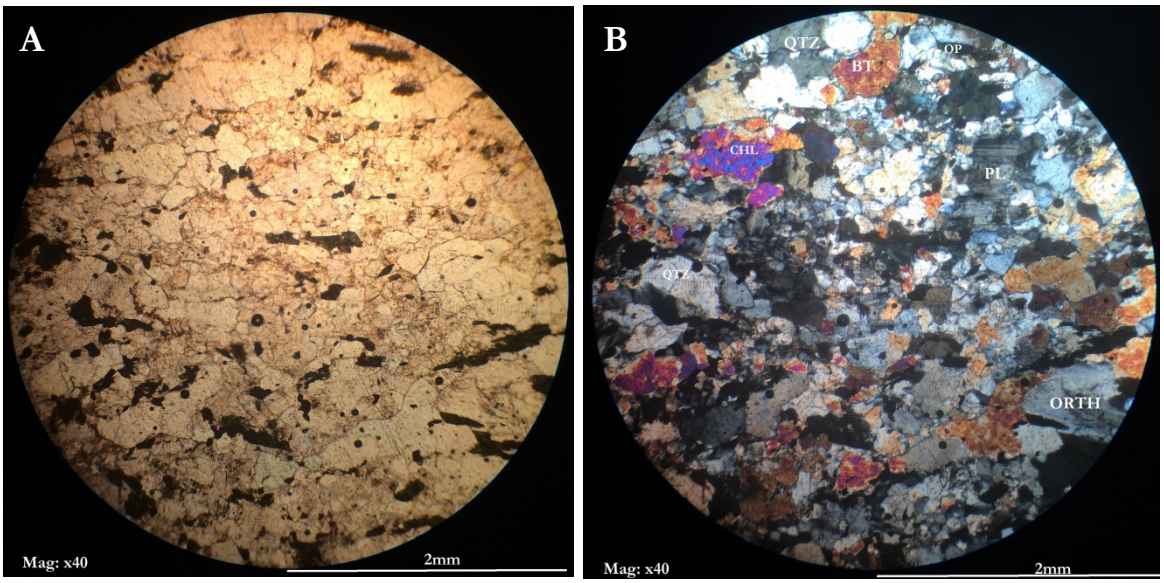


Plate 4.12: Photomicrographs of Granite gneiss in PPL (A) and XPL (B). QTZ= quartz, BT= biotite, PL= Plagioclase, CHL= chlorite, ORTH= orthoclase, MC= microcline, OP= opaque, GT= Graphic texture.

4.1.6 Diorite

Occurrences are at Maske area, southwest of Mada. The rock outcrops as hills that trend in E-W direction and as whaleback in other areas (Plate 4.13). The rock is porphyritic, medium to coarse grained and composed of white plagioclase feldspar and mixture of hornblende, biotite and quartz. In hand specimen, the rock appears speckled black and white and weakly foliated. The outcrops seem to occur with no other associated rock exposure. In some parts of the outcrop, the rock occurs as equigranualr, exhibiting different textural variation within meters on the same exposure.



Plate 4.13: Photograph of weathered diorite boulder at Shamori N12^0 06' 41.4", E06^0 54' 52.8". Inset is a hand specimen of the rock

Microscopic observations show the minerals occurring as sub- to an-hedral. Plagioclase occurs mostly as anhedral crystals. Zoning is common within the plagioclase feldspar crystals, together with Carlsbad and polysynthetic twinning that are well developed. The hornblende crystals occur as subhedral crystal, mm in sizes with some crystals having inclusions and some rimed and intergrowth with plagioclase. Quartz occur as intergranular crystals, often within interstitials together with small

amount of microcline, the latter having tartan twins. The hornblende is pleochroic, exhibiting green to brown pleochroism while the reverse exhibited by biotite (Plate 4.14).

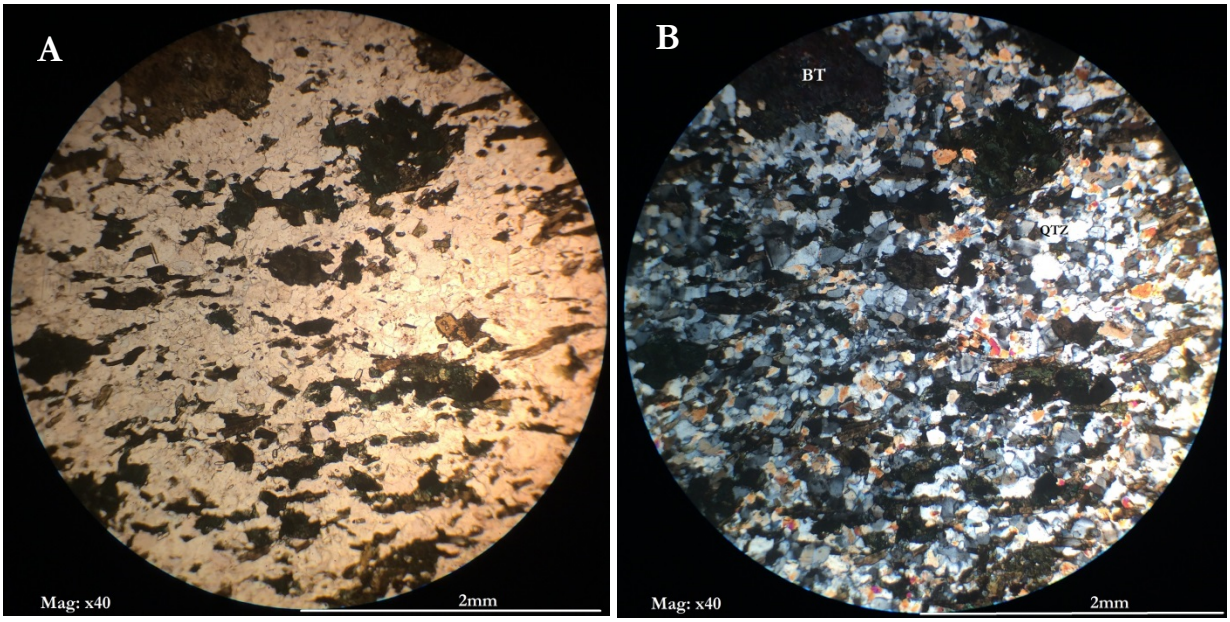


Plate 4.14: Photomicrograph of diorite in PPL (A) and XPL (B). QTZ= quartz, BT= biotite, PL= Plagioclase, ORTH= orthoclase, OP= opaque.

4.1.7 Aplite Dykes

Aplite dykes occur within the granite and the granite gneiss in the study area, occurring as fine grained variety of the rock that have sharp contacts with the host rock (Plate 4.15). The rock is dominated by quartz, alkali feldspar, plagioclase, biotite and opaque minerals and are best developed at Gidan Sani location (Plate 4.16). At Takasaba, an aplite dyke occurs across the entire outcrop as irregular bodies, displacing a xenolith.



Plate 4.15: Photograph of sharp boundary between medium grained granite (right) and aplite (left) N12^0 14' 09.4", E06^0 51' 0.6".

Thin sections of the aplite reveal fine grained, holocrystaline texture. Most of the crystals are anhedral, except for few subhedral feldspar crystals.



Plate 4.16: Aplite within granite gneiss (N 12^0 11' 13.8", E06^0 50' 34.4").

4.1.8 Quartz and Quartzo-feldspathic veins

These are apparently fracture-filling rocks that are found within all the rock units in the study area. They consist of varying sizes and styles with most of the occurrence within quartz-mica schist. Occurrences of within the schist are composed of quartz and feldspar with vugs having well developed crystals of same or empty. They occur in some places as pegmatitic with large interlocking phaneritic crystals of quartz and feldspar, and rarely containing mica (Wonaka, Dunkulakulli), and pyrites (southwest of Mada, Kutiri River occurrence), with varying sizes up to 65 cm in width and can be traced for up to 100 m along strike. They often are covered by over burden (Plate 4.17). They dip almost always vertical with varying width.



Plate 4.17: Photograph of quartzo-feldspathic veins trending NW-SE. (N12^0 15' 36.9", E06^0 56' 36.2"). Inset is a hand specimen of quartz vein with empty vugs.

The mineral composition varies from smoky to milky white variations with stock-work texture within the quartz veins made up of network of discontinuous and closely spaced fractures. The veins are composed of quartz ± feldspar ± hematite ± mica ± sulphide and few salvages of wallrock. Two generations of quartz veins were observed. The first generation are thin (about 1-5cm thick), and folded occurring in the northern and central parts of the study area mainly within the schists (Plate 4.18). The second generation of quartz veins are more abundant throughout the study area with exception of the areas underlain by diorite. They occur in the form of vein swarms in the schist (Plate 4.19) with higher density toward the eastern parts. They occur parallel to and/or cut the foliation with varying angles.



Plate 4.18: Photograph of quartz veins within quartz –mica schist at Wonaka (N12^0 16' 34.7", E06^0 56' 47.3")

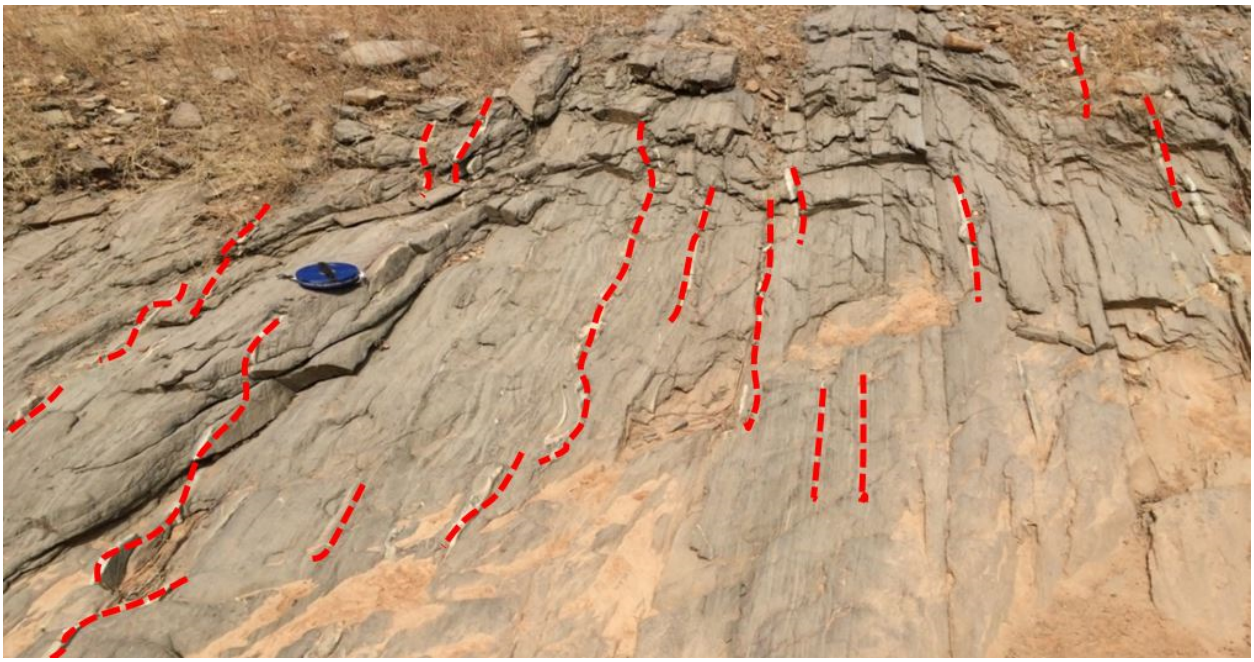


Plate 4.19: Photograph of vein stringers, trending NW-SE within the quart-mica schist (N12^0 13' 42.0", E06^0 58' 29.7")

4.2 STRUCTURAL GEOLOGY

Both ductile and brittle structures were observed in the study area. The structural patterns are dominated on regional scale by NE-SW striking foliations, and N-S striking lineaments. In addition, other types of structures, such as folds, joints and fractures were also observed in different localities in the study area.

4.2.1 Foliations

This is the most prominent structural feature within the metasediments in the study area, defined by the parallel to sub-parallel alignment of the platy mineral grains. The foliations generally trend in similar directions within all the metasediments, largely NNE and NW, with average dip of 60^0E. The bands observed within the granite gneiss have thickness varying from mm size to few tens of a cm (Plate 4.11). Foliation that occur within the quartz-mica schist are, defined by the alignment of the micaceous minerals.

4.2.2 Joints

Joints were observed in all the rocks of the study area and are the most abundant structural features observed (Appendixes 1.1; 1.2; 1.3 and 1.4). They are dense and closely spaced in most of the places and often perpendicular, with a general trend of N-S and NW-SE directions (Fig. 4.2 and Fig. 4.3). Different styles of jointing including conjugal, parallel, systematic, cross and vertical joints occur in the schist, all indicating a largely irregular jointing (Plate 4.20 and Plate 4.21).

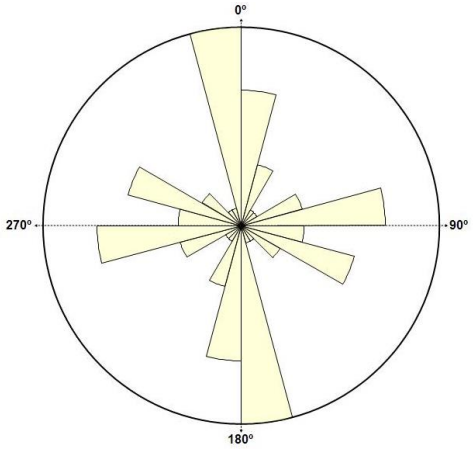


Figure 4.2: Rose diagram of joint trends in quartz-mica schist of the study area

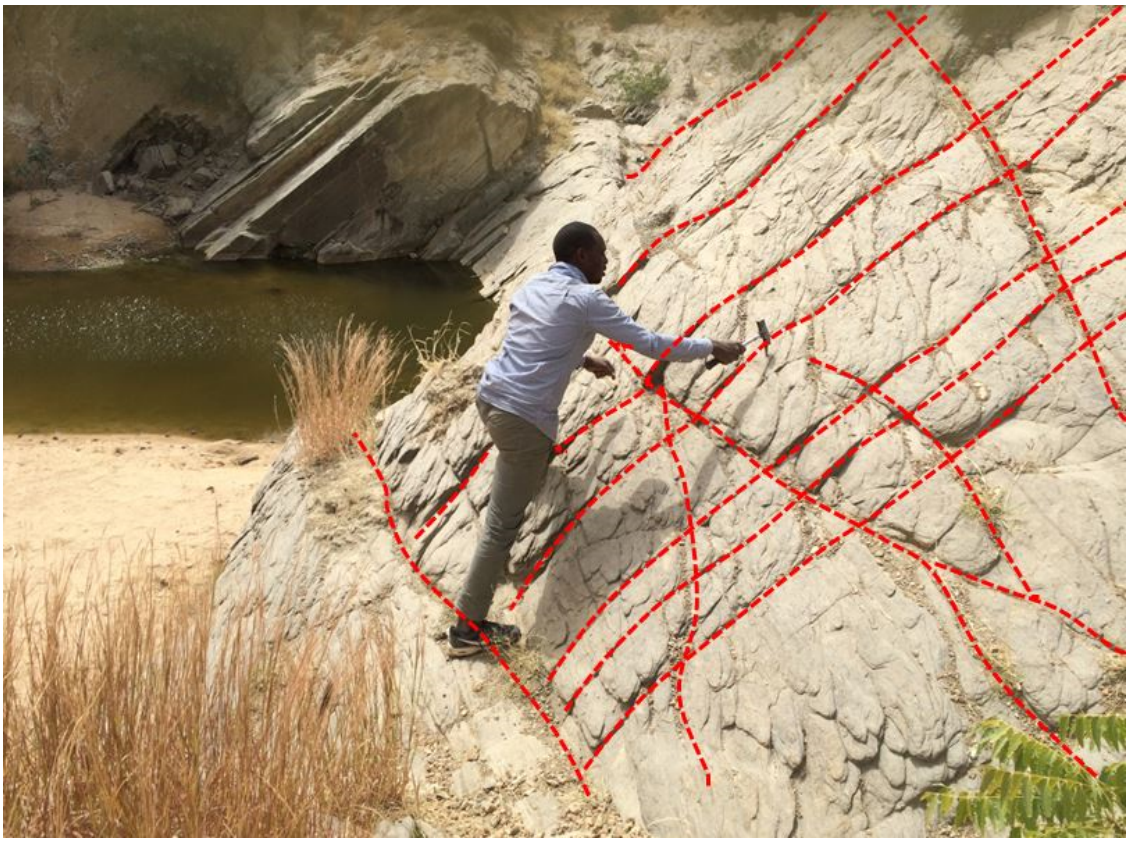


Plate 4.20: Photograph of quartz-mica schist with NE-SW trending parallel joint sets in ($N12^0$ 12' 06.6", $E06^0$ 57' 55.8")

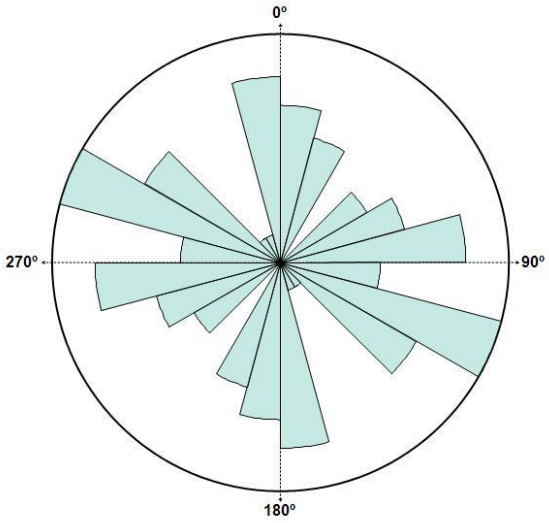


Figure 4.3: Rose diagram of joints observed within phyllite of the study area

On the intrusive rocks, the fracturing in general is relatively less, especially on the diorite. Some of the joints and fractures generally are filled by quartz or quartzo-feldspathic minerals, quartz boudins also occur in the schist and phyllite. Trend plots using rose diagrams were constructed for joints occurring on all the rocks in the study area, on which subsequent trend analysis was made and correlation of fracture pattern with the regional lineament observed.



Plate 4.21: Photograph of metasandstone with conjugal joints (N12^0 05' 51.6", E06^0 51' 12.7")

Predominantly NW-SE trending vertical to sub vertical joints and fractures are widespread in the metasediments (Figs. 4.2, 4.3), while the intrusive rocks have largely NE-SW trending fractures (Fig. 4.4 and Fig. 4.5).

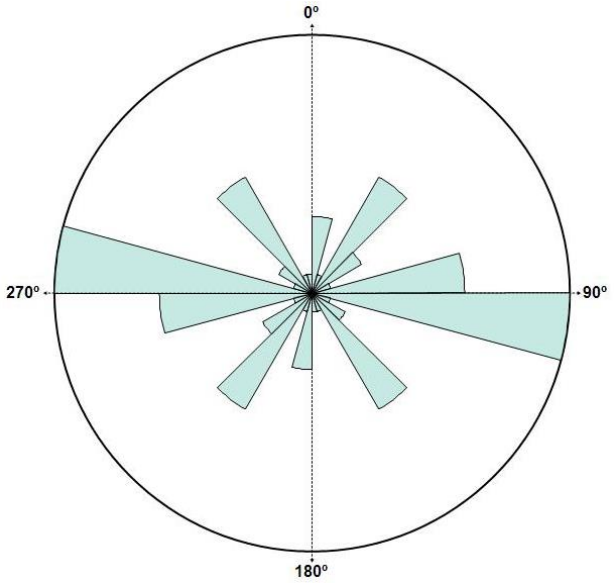


Figure 4.4: Rose diagram of joint trends of the granite gneiss of the study area

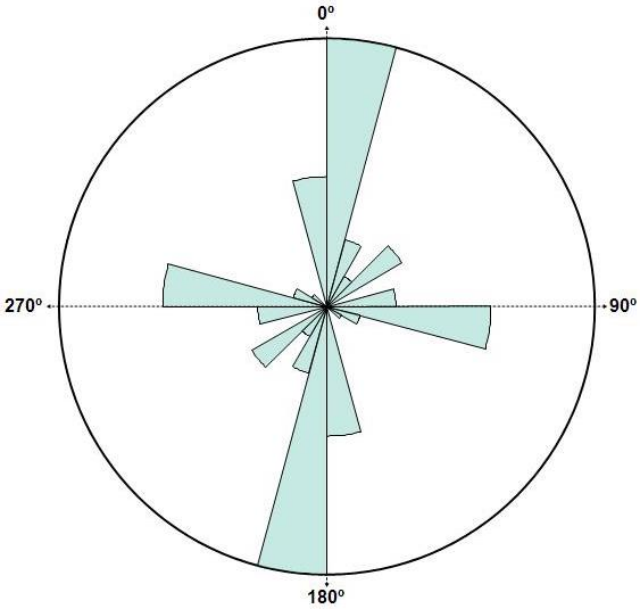


Figure 4.5: Rose diagram of joint trends within porphyritic granite in the study area.

4.2.3 Faults

Few fault structures were observed in the study area. At Takasaba, strike-slip faults occurs in the medium grained granite outcrops, with some having displacement of up to 13 cm. North of Mada, faults were observed on the medium grained granites in the area, displaced dextrally to up to 45 cm

(Plate 4.22). similar faults were encountered, however, they are minor with the maximum displacement of 3 cm.

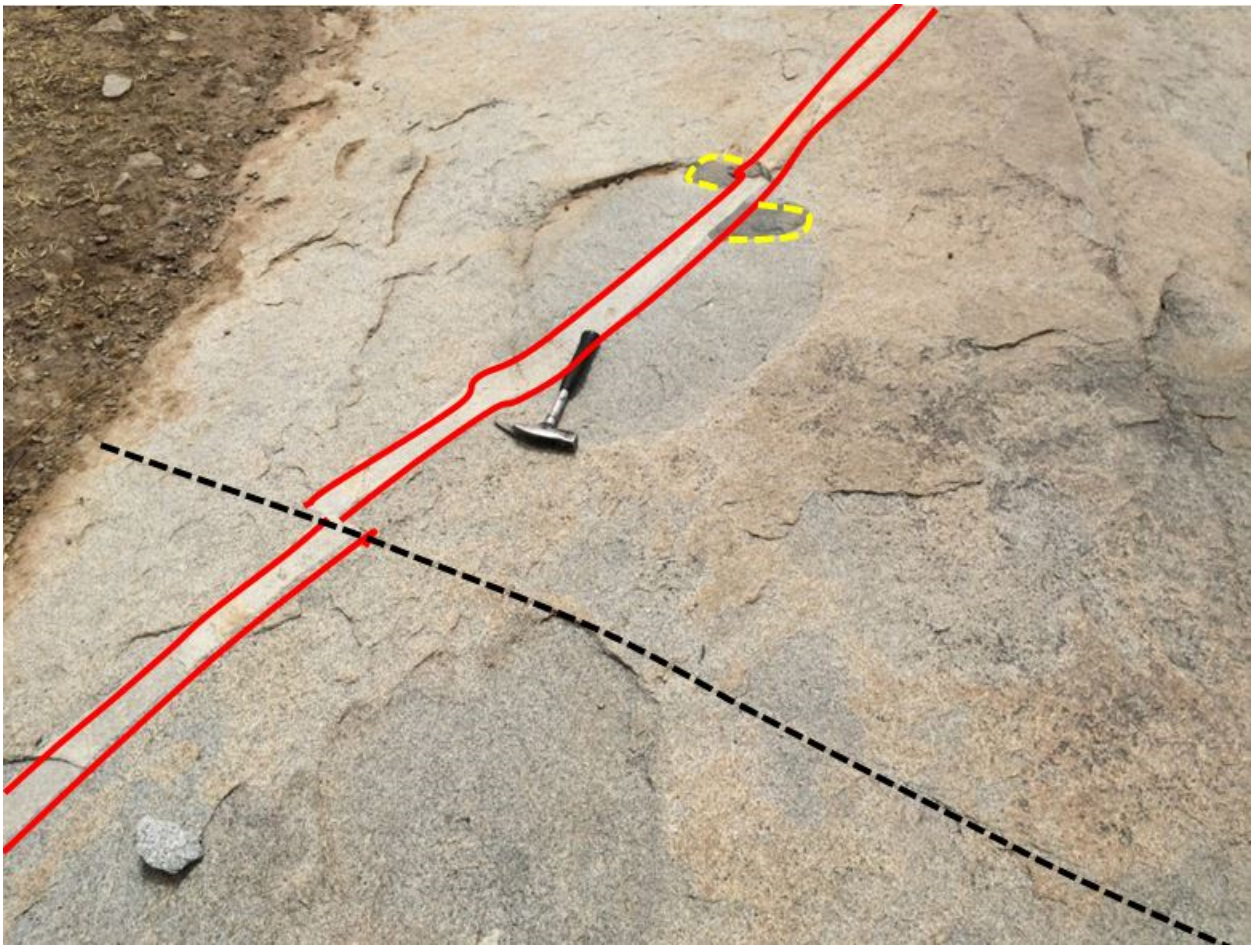


Plate 4.22: Photograph of a mafic xenolith, displaced by an aplite dyke which was subsequently faulted within low lying medium grained granite at Takasaba (N 12^0 17' 48.6", E 6^0 48' 54.6").

4.2.4 Folds

Ptygmatitic folding was observed within the granite gneissic with most occurring in the more gneissic part of the rock (Plate 4.23a). Slightly folded metasediments, and even so not widespread. Most of the occurrences are limbs of fold with dip varying between 67^0 to almost vertical. Parasitic *S* folds were observed in low lying phyllitic outcrops at Fura Girke (Plate 4.23b).



Plate 4.23: A) Ptygmatitic folding within granite gneiss (N12^0 10' 30.1", E06^0 50' 11.2"). B) Folded phyllite exposed along stream channel (N12^0 14' 50.3", E06^0 59' 14.5")

4.2.5 Lineament Analysis

The presences of large scale geologic structures in the study area were inferred using lineament interpreted from Digital Elevation Model (DEM). They were produced using RS images by semi-automatic method of extraction for the lineament generation, visual interpretation and subsequent manual digitization. These were generated from data obtained by Shuttle Radar Topographic Mission (SRTM). The DEM was processed to eight shaded relief images using ErDas imaging software by varying the direction of the azimuth of 0^0, 45^0, 90^0, 135^0, 180^0, 225^0, 270^0 and 315^0. These correspond to N, NE, E, SE, S, SW, W, and NW respectively (Appendixes 1.5 and 1.6). For good contrast and better interpretability, an ambient light setting of 0.2 and solar elevation of 30^0 were preferred. The shaded relief images were then combined into two. The first consist of N, NE, E, SE (Appendix 1.7), while the second was the combination of S, SW, W and NW direction relief images to enhance the lineament (Appendix 1.8). These combined shaded relief images led to better interpretation of lineaments since they superimposed the information contained in various single shaded relief images. PCI Geomatica was used to automatically extract lineaments using the two

composite shaded relief images, from which, rose diagrams were constructed using the lineaments from these images (Appendixes 1.9 and 1.10). Buffering was then carried out on the extracted lineaments and subsequently, the buffered images were reclassified into two classes and combined to produce a thematic image better known as the level of coincidence image (Appendix 1.11).

After further reclassification, manual extraction of lineament was carries out by digitization and a final lineament map was produced for the study area (Fig. 4.6). After the extraction, the orientation, length, frequency and density of the lineaments as well as lineament intersection density were evaluated.

The azimuthal distribution indicated that most of the lineaments are trending in the N-S direction, with local preferred directions being NE-SW and NW-SE (Fig. 4.6). The N-S trend observed at different scales on the lithologies with the exception of the diorite is further confirmed by the lineament. This in turn, confirms the moderate level of deformation that affected the region.

Areas with high lineament densities include the topographically complex granite gneiss of Kotorkoshi, porphyritic granite of Dakace and Gamawa and the steeply dipping quartz-mica schists around Dunkulakulli-lilu and Wonaka (Fig. 4.7; Fig. 4.8). The dominant trends in the study area are N-S, NW-SE and NE-SW. The lineaments not only have influence on the smaller structural features but also control the drainage pattern in the area, including the main rivers (Gagare and Kutiri).

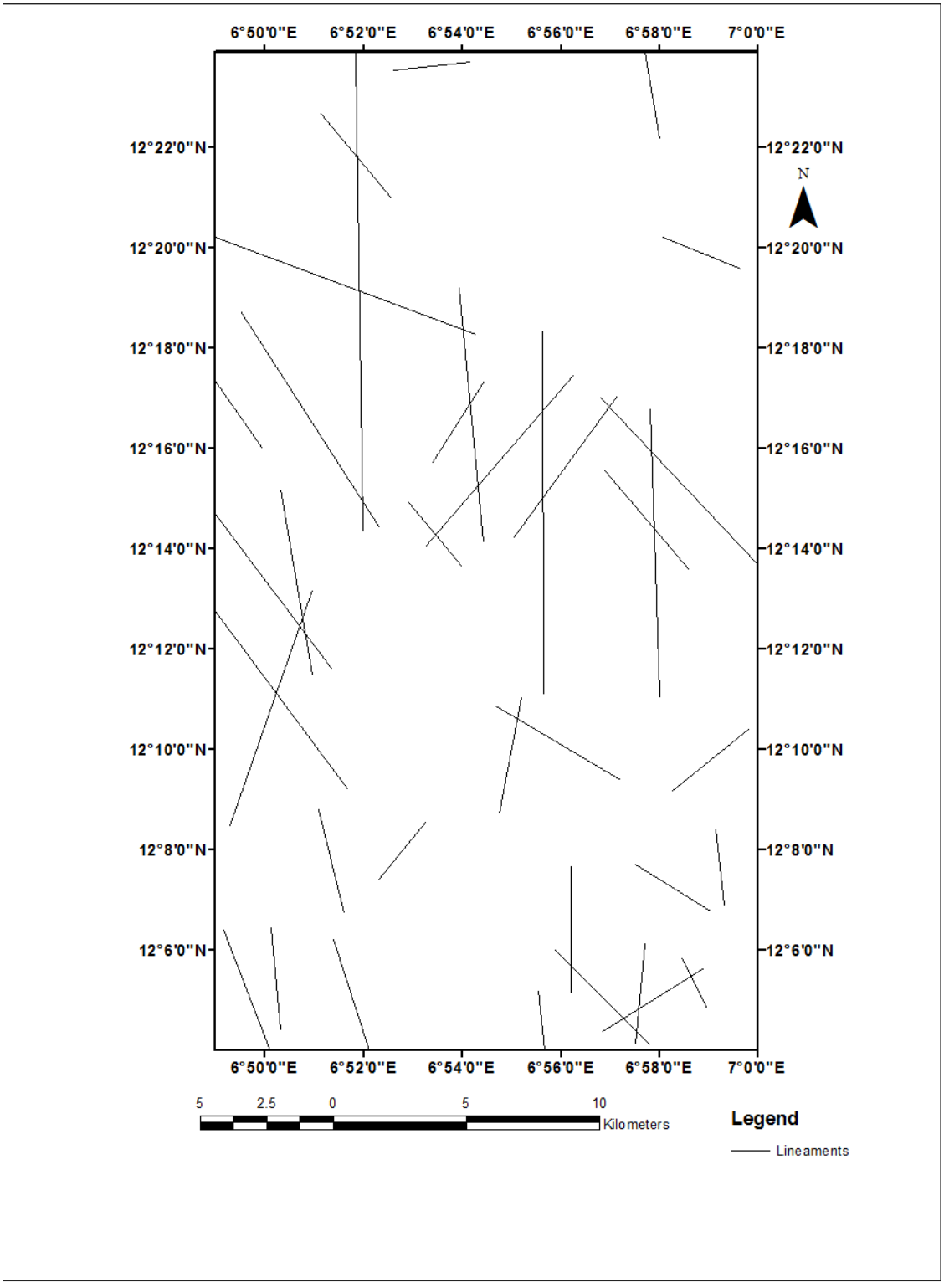


Figure 4.6: Lineament trends of structures in the study area.

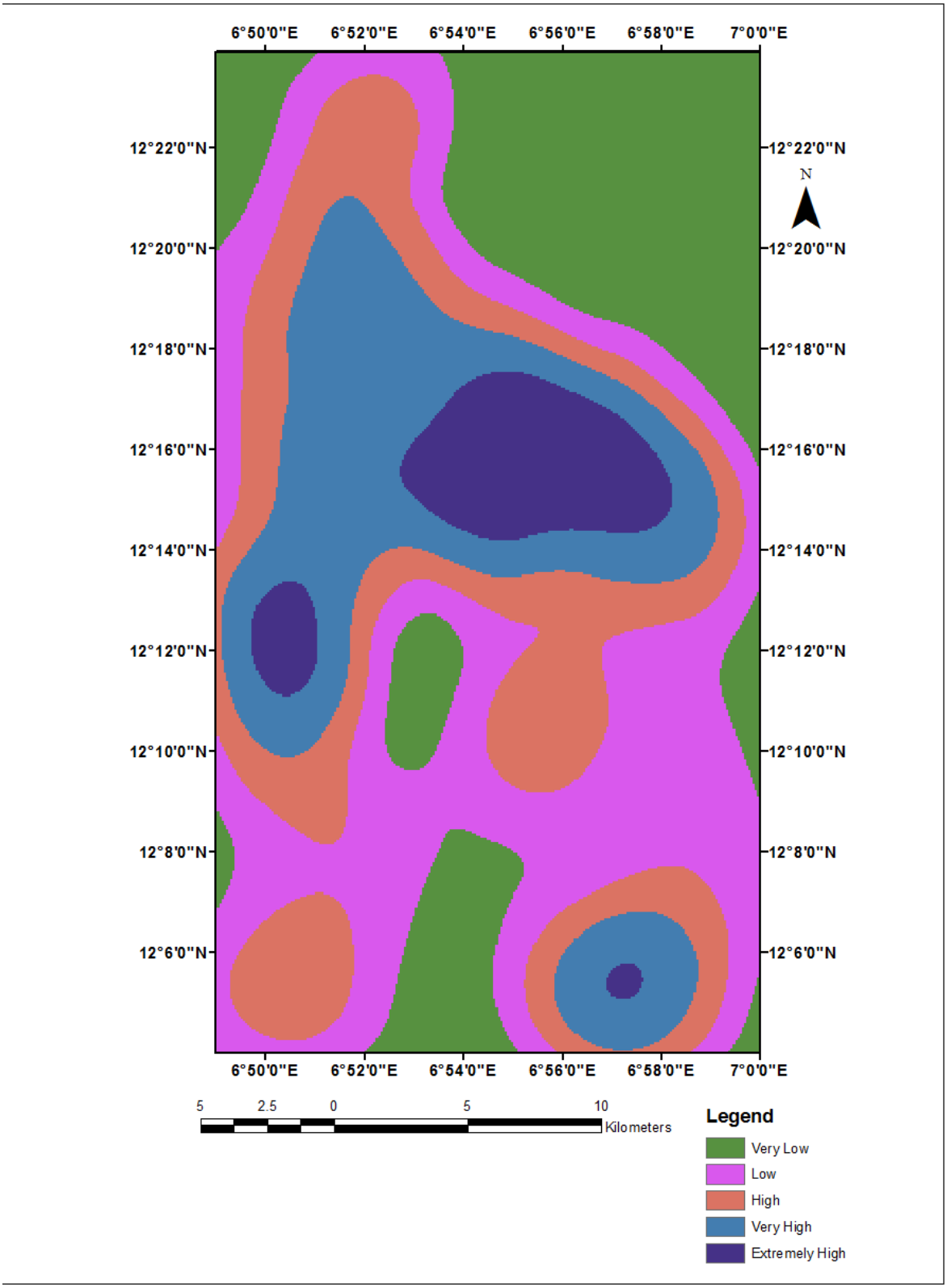


Figure 4.7: Lineament density map of the study area

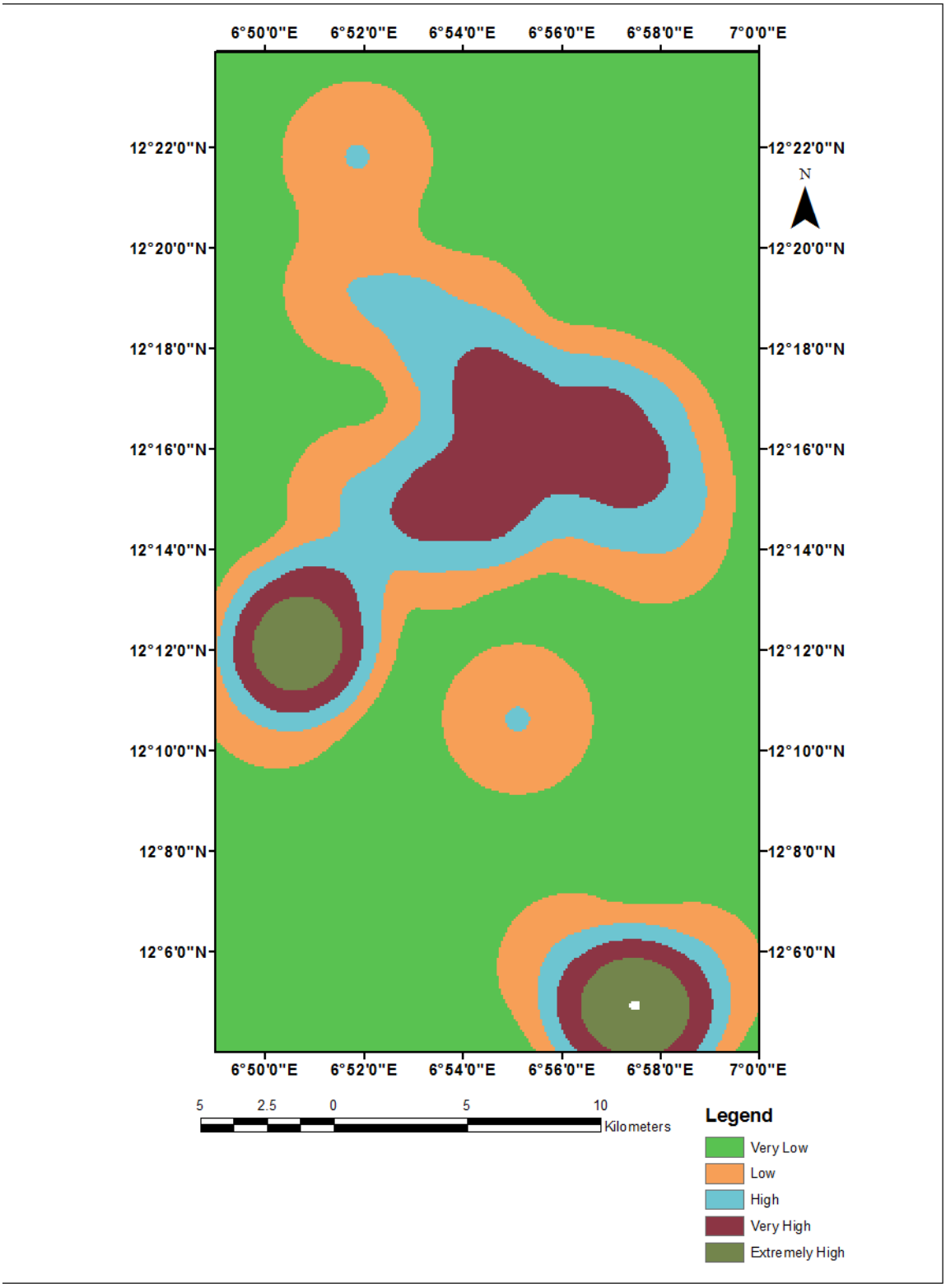


Figure 4.8: Lineament intersection density map of the study area.

4.3 SEDIMENTOLOGY OF GOLD BEARING STREAM SEDIMENTS

Endeavor has been made to make use of the grain size characteristics of the gold-bearing stream sediments to determine the environment of deposition and transport medium and regime.

The results obtained are presented in a tabular form (Appendix 2.1). The grain size data were plotted on Cumulative frequency curves (Appendix 3.1). Here, the total amount of grain by weight which are larger than a given ϕ value are plotted.

Mean

In the study area, mean values ranges from fine sand (1.8ϕ) to coarse sand (3.4ϕ), indicating a prominent distribution of medium sand (average size grains of 1.14). The distribution of medium sand in this region might be an indication of moderately higher energy environment.

Sorting

In the study area, the sediments sorting range from very poorly sorted (2.23ϕ) to moderately well sorted (0.69ϕ), indicating control of the size distribution of the source material on the sediment sorting.

Skewness

The sediments are strongly fine skewed (0.32ϕ) to near symmetrical (-0.03ϕ).

Kurtosis

Kurtosis are described as mesokurtic, while they range from very platykurtic to very leptokurtic within the study area.

The univariate analysis confirm the fluvial nature of the sediments, dominated by streams and rivers in the study area with the medium sediments indicate overall depositional environment transported

by suspension. Bivariate plots of mean and sorting indicates poorly sorted sediments with no regard to grain sizes, confirming that sorting is independent of grain size within fluvial environment.

4.4 GOLD-BEARING HEAVY MINERALS

Heavy minerals that occur together with the gold were visually recovered and subsequently examined using binocular microscope to obtain information that was used in determining transport distance and nature of the bedrock (e.g. McClenaghan, 2011). A total of 1564 heavy minerals were analyzed and counted using Galehouse (1971) ribbon counting technique.

Ultra-stable grains of opaque and non-opaque heavy minerals dominate with most of the grains still retaining their shapes and are well formed indicating multiple sources for the minerals (Fig. 4.9). These minerals are more resistant to weathering, hence survive greater distances of fluvial transport and are little affected by degradation or physical breakdown. They include – in order of abundance – zircon (26%), tourmaline (16%), rutile (15%), and garnet (7%).

Figure 4.9: Pie charts illustrating the distribution of heavy minerals per slide. (Z=zircon; T=tourmaline; R=rutile; S= staurolite; K=Kyanite; M=magnetite; G=garnet; A=amphiboles; E=Epidote; I=ilmenite; O= others)

4.4.1 Description of Heavy Minerals

Amphiboles

Occur as elongated dark green to brownish coloured striated minerals with some displaying strong lustre. Most of the occurrences of the minerals were from 1st order and 2nd order streams.

Garnet

This occurs as red to pink equant minerals, it occurs within streams draining from quartz-mica schist within which primary occurrence was also observed (Plate. 4.25) and in classifying the grains as almandine (iron-rich variety)

Ilmenite

This occurs as dark greyish tabular grains with metallic lustre which were not magnetic when subjected to magnetic mineral separator; a distinguishing feature used to differentiate it from magnetic (Plate.4.24)

Plate 4.24: incident light images of heavy mineral concentrate. Pink circle = Kyanite; yellow

Kyanite

This occurs as colourless elongate grain (Plate 4.24) with striated lines showing its good multidirectional clearage.

Magnetite

This occurs as mostly euhedral to subhedral grains (but also rounded anhedral) showing the characteristics octahedral crystal shape (Plate 4.25). The grains occur relatively smaller in the samples

Rutile

Rutile occur as elongated reddish brown (Plate 4.25) grains with metallic lustre. They occur mostly as small grains with some occurring as sub rounded.

Staurolite

These are elongated grains that appear orange and dark brown in colour that look similar to garnet but having smaller and elongated grains

Zircon

This occurs as relatively the smaller grains of light to colourless, mostly sub rounded mineral. They are mostly elongated

Tourmaline

Mostly euhedral and well-formed crystals commonly in a wide range of colours such as pink, brown, black and green.

Plate 4.25: incident light images of heavy mineral concentrates. Yellow circle = magnetite; Blue circles = garnets; Red circles = tourmaline; white circles = rutile; green circles = zircon.

Epidote

This mineral occurs as light green with some larger crystals of it occurring as dark green. This only occurs in two of the samples analysed and relatively less within these samples (Table 4.2). Occurring as elongate grains which differentiate it from similar green minerals e.g. olivine, pumpellyite, chloride, pyroxene etc.

Table 4.2: Heavy minerals within gold-bearing samples in the study area

6.2 RECOMMENDATIONS

1. Geochemical analyses of the stream sediments and the quartz veins should be carried out using technique(s) with high precision and low detection limit in order to detect particulate Au grains that were not recoverable by the method employed in this study. This is to further delineate areas of high Au potential and also identify possible primary mineralization in the areas highlighted by this study.
2. This study also recommends the sampling of the extreme northeastern part of the study area which for security reasons, was not covered in the course of this work.

REFERENCES

Abrams, M., (2000): ASTER User Handbook (version 2). Jet Propulsion Laboratory, Pasadena, CA-91109, USA. 135 pp.

Abubakar, Y.I. (2012): An Integrated Technique in Delineating Structures: A Case Study of the Kushaka Schist Belt Northwestern Nigeria. International Journal of Applied Science and Technology, **Vol. 2, No. 5**, pp 165-173.

Ajibade, A. C. (1976): Provisional Classification and Correlation of the Schist Belts of Northwestern Nigeria. In: Kogbe, C. A. (Ed). Geology of Nigeria, Elizabethan Publishing Co. Lagos. pp 85-90.

Ajlbade, A. C. (1980): Geotectonic Evolution of the Zungeru Region, Nigeria. Ph.D. Dissertation, University Of Wales, Aberystwyth UK.

Ajibade, A.C. and **Fitches, W.R.** (1988): The Nigerian Precambrian and the Pan-African Orogeny. A publication of the Geological Survey of Nigeria.

Ajibade, A.C., and **Wright, J.B.** (1988): The Togo-Benin Nigeria Shield: Evidence of Crustal Aggregation in the Pan African Belt. Tectonophysics **165**, 125-129.

Ajibade, A. C, Anyanwu, N. P. C., Okoro, A. U. and **Nwajide, C. S.** (2008): The Geology of Minna Area. Nigerian Geological Survey Agency Bulletin **No. 43**.

Akande, S.O., and **Fakorede, O.** (1988): Au Mineralization in the Nigerian Schist Belts. Bicentennial Au 88, Melburne, Australia pp 140-142.

Akande, A.O and **Kinnaird, J**. (1990): Characterization and origin of ore–forming fluids in the Nigerian mineral belts. Proceedings of the Eighth Quadrennial IAGOD Symposium, Ottawa, Canada, pages 199 – 218

Amuda, A.K., Dambatta, U.A., and **Najime, T.** (2013): Geology and Au Mineralization around Kutcheri, Northwestern Nigeria. Iosr Jour. Of App. Geo. And Geophy. **Vol. 1, Issue 6**. Pp18-24.

Azizi, H., Rsaouli, A.A., and **Babaei, K**. (2007): Using SWIR bands from ASTER for Discrimination of hydrothermal altered minerals in the northwest of Iran: a key for exploration of copper and Au mineralization. Research Journal of Applied Sciences 2 (6): 763-768

Blenkinsop, T., (2002): Deformation Microstructures and Mechanisms in Minerals and Rocks. Kluwer Academic Publishers. New York, USA

Bourke, M.C, Brearly, J.A., Haas, R., and Viles, H.A., (2007): A photographic atlas of rock breakdown features in geomorphic environments. Planetary Science Institute, Arizona, USA.

Bowden P, and **Kinnaird J. A.** (1984): Geology and Mineralization of the Nigerian Anorogenic Ring Complexes. Geologisches Jahrb (Hannover) **B56**, 3–65.

Bungwon A. D. (1983): The Geology And Preliminary Soil Geochemical Investigation Of Possible Au Bearing Features In The Tserita-Tungan Kudaku Area Near Anka, Sokoto State. Unpublished M.Sc. Thesis, Ahmadu Bello University, Zaria, Nigeria.

Bungwon, A. D. (1984): The Geological Setting of Au and Chromite Mineralization in the Tsareta-Tungan Kudaku Area, Near Anka, Sokoto State. **20th** Annual Conference of the NMGS.

Burke, K. C., and **Dewey, J. F.** (1972): Orogeny in Africa. In: Dessauvagie Tfj, Whiteman Aj (Eds), Africa Geology. University Of Ibadan Press, Ibadan, Pp 583–608.

Cailleux, A. and **Tricart, J.,** (1959): Initiation à l'étude dessables et des galets, vol. 1, Paris, Centre de Documentation Universitaire, 369 p.

Carranza, E.S.M., (2002): geologically-constrained mineral potential mapping (examples from the Philippines), PhD. Thesis, Delft University of Technology, Delft, The Netherlands

Chapman, R.J. and Mortensen, J.K., 2006. Application of microchemical characterization of placer Au grains to exploration for epithermal Au mineralization in regions of poor exposure. Journal of Geochemical Exploration, vol. 91, p. 1-26.

Chapman, R.J., Leake, R.C., Moles, N.R., Earls, G., Cooper, C., Harrington, K., Berzins, R., 2000. The application of microchemical analysis of Au grains to the understanding of complex local and regional Au mineralization: a case study in Ireland and Scotland. Econ. Geol. 95, 1753 - 1773.

Chapman, R., Leake, B., Styles, M., 2002. Microchemical characterization of alluvial Au grains as an exploration tool. Au Bull. 35, 53e65.

Chapman, R.J., Leake, R.C., Bond, D.P.G., Stedra, V., Fairgrieve, B., 2009. Chemical and mineralogical signatures of Au formed in oxidizing chloride hydrothermal systems and their significance within populations of placer Au grains collected during reconnaissance. Econ. Geol. 104, 563e585.

Chapman, R.J., Mortensen, J.K., Crawford, E.C., LeBarge, W., 2010. Microchemical studies of placer and lode Au in the Klondike District, Yukon, Canada: 2. Constraints on the nature and location of regional lode sources. Econ. Geol. 105, 1369e1392.

Chapman, R.J., Mortensen, J.K., LeBarge, W., 2011. Styles of lode Au mineralization contributing to the placers of the Indian River and Black Hills Creek, Yukon Territory, Canada as deduced from microchemical characterization of placer Au grains. Min. Depos. http://dx.doi.org/10.1007/s00126-011-0356-5.

Dada, S. S. (2006): Proterozoic Evolution of Nigeria. In: Oshi O (Ed) the Basement Complex of Nigeria and Its Mineral Resources (A Tribute to Prof. M. A. O. Rahaman). Akin Jinad & Co. Ibadan, Pp 29–44.

Danbatta, U. A. (2002): Rb/Sr Isochron Dating of Granitoids from the Kazaure Schist Belt, NW Nigeria. Global Journal of Pure and Applied Sciences **8 (3)**. 319-322.

Danbatta, U. A. (2006): Geochemistry of Au Deposits in Anka Schist Belt Northwestern Nigeria. Unpublished Paper. Ahmadu Bello University, Zaria. Pp16.

Danbatta, U.A. (2008): Precambrian Crustal Development in the Northwestern Part of Zuru Schist Belt, Northwestern Nigeria. Journal of Mining and Geology. **44** (1), P 45-56.

de Palomera, R. P. A., (2006): application of Remote Sensing and Geographic Information Systems for mineral predictive mapping, Deseado massif, Southern Argentina. M. Sc. Thesis, International Institute for Geo-information Science and Earth Observation. Enschede, the Netherlands.

Dilabio, R. (1991): Classification and interpretation of the shape and surface textures of Au grains from tills. In: **Hérail, G.** and **Fornari, M**. (eds) Gisements alluviaux d'or (Alluvial Au Placers/Yacimientos aluviales de oro). ORSTOM, Paris, 297–313.

Dunstan, W.R (1911): Reports on the results of mineral survey of Northern Nigeria, 1907 – 1908. Colon. Rep. Miscel. Series Number 79.

Egbuniwe, I.G. (1982). Geotectonic evolution of the Maru Belt, NW Nigeria. Unpublished Ph.D. Thesis, University of Wales, Aberystwyth.

Elueze, A. A. (1981): Petrographic Studies of Metabasic Rocks and Meta-Ultramafites In Relation To Mineralization in Nigeria Schist Belts. Nigerian Journal of Min. Geol. **18**, 53-58.

Elueze, A. A. (1984): Mineralogical and Chemical Variations in Ore Minerals-Bearing Metabasites in the Precambrian Basement Complex of Nigeria, In Relation To Cataclasis. Natural Res. Develop., Tubingen, F. R. Germany **19**. 63-70.

Evans A.M. (1993) Ore Geology and Industrial Minerals: an introduction. Blackwell Scientific Publications, Oxford.

Fargher, M. N. (1966): The Basement Complex Geology of Sheet **32** (Kaura Namoda) and **54** (Gusau). Unpublished Report. Geol. Sur. Nigeria.

Fitches, R.W., Ajibade, A.C., Egbuniwe, I.G., Hole, R.W., Wright, J.B., (1985). Late Proterozoic schist belts and Plutonism in NW Nigeria. Journal Geological Society London, 142, 319-337.

Folk, R. L. and Ward, W. C. (1957): Brazos River bar: a study in the significance of grain size parameters. Journal of Sedimentary Petrology, 28, 3-26.

Fossen, H., (2010): Structural Geology. Cambridge University Press. Cambridge, UK

Galehouse, J. S. (1971**):** Point counting": In Carver, R. E. (Ed.), Procedures in Sedimentology, Wiley, New York, pp 385 – 407.

Garba, I. (1992a): Rare Earth Element Study of Bin Yauri Au Deposit, Nigeria. Transactions Institution Mining Metallurgy (Section B: Applied Earth Sciences) **101**, 158- 161.

Garba, I. (1992b): Geology, Geochemistry and Origin of Au Mineralization at Bin Yauri, Nigeria. Ph.D. Dissertation, University Of London, UK, 264p.

Garba, I. (1996) Tourmalinization related to Late Proterozoic-Early Palaeozoic lode Au mineralization in the Bin Yauri area, Nigeria. Mineralium Deposita 31,201 - 209

Garba, I. (2000a): Au Prospects of the Nigeria Pan African Terrain of West Africa. Journal of Mining and Geology, **Vol. 36 (2)**, P123 – 135.

Garba, I. (2000b): Origin of Pan-African Mesothermal Au Mineralization at Bin Yauri, Nigeria. Jour .Afri. Earth. Sci. **31**, Pp 433-449.

Garba, I. (2002a): Geochemical Characteristics of the Au Mineralization near Tsohon Birnin Gwari, Northwestern Nigeria. Chemie Der Erde/Geochemistry, **Vol. 62, No. 2**, Pp160-170

Garba, I. (2002b): Late Pan-African Tectonics and Origin of Au Mineralization and Rare Metal Pegmatite in the Kushaka Schist Belt, Northwestern Nigeria. Journ. Of Mining and Geology, **Vol.38 (1)**, Pp.1-12.

Garba, I. (2003): Geochemical Characteristics of Mesothermal Au Mineralization in the Pan African (600 + 150 Ma). Basement of Nigeria. Applied Earth Science, Volume **36 (2)**, P123 – 135.

Geoprobe Limited (2014a): Au Prospecting and Pre-feasibility Assessment in Exploration Licenses 15979EL and 13960EL of Bilson Nigeria Limited, Gusau L.G.A., Zamfara State, Nigeria. Unpublished Report. P57.

Geoprobe Limited (2014b): Placer Au Prospecting in Exploration License 18259EL of Crescent Mines and Exploration Limited, Gusau L.G.A., Zamfara State, Nigeria. Unpublished Report. P45.

Gleeson, C.F. and **Boyle, R.W.** (1980): Minor and trace element distribution in the heavy minerals of rivers and streams of the Keno Hill District, Yukon Territory. Geological Survey of Canada. **76-31.**

Goldschmidt, V.M. (Ed. A. Muir); (1954): Geochemistry. Oxford: Clarendon Press, Pp 730.

Grant, N.K. (1970): Geochronology of Precambrian Basement Rocks from Ibadan, Southwestern Nigeria. Earth Planetary Science Letters **10**, 29-38.

Grant, N. K. (1978): Structural Distinction between A Metasedimentary Cover and an Underlying Basement in the 600-M.Y.Old Pan-African Domain of Northwestern Nigeria, West Africa. Geological Society of American Bulletin, **89**. 50-58.

Grant, N.K., Hickman, M., Burkholder, F.R. and **Powell, J.L.** (1972): Kibaran Metamorphic Belt in the Pan African Domain of W. Africa. Nature (Physical Sciences) **238**, 90-91.

Grant, A.H., Lavin, O.P. and **Nichol, I**. 1991. The morphology and chemistry
Of transported Au grains as an exploration tool. Journal of Geochemical
Exploration, 40, 73–94.

Grema, H.M. (2016) Au mineralization within the Northwestern Schist Belts of Nigeria. Unpublished M. Sc. Seminar. Dept. of Geology, Ahmadu Bello University, Zaria – Nigeria. Pp40.

Groen, J.C., Craig, J.R. and **Rimstid, D.** 1990. Au-rich rim formation on Electrum grains in placers. Canadian Mineralogist, 28, 207–228.

Groshong, R. H. Jr. 1988. Low-temperature deformation mechanisms and their interpretation. Bull. Geol. Soc. Am. 100, 1329-1360.

Harper, C.T., Sherrer, G., McCurry, P. and **Wright, J.B.** (1973): K-AR Retention Ages from the Pan-African of Northern Nigeria. Geological Society of America Bulletine **84**, P919-926.

Higgins, M. (2012) Placer Au Provenance in the Black Hills Creek, West-Central Yukon: Insight from Grain Morphology and Geochemistry. Unpublished thesis Department of Earth Sciences, Dalhousie University, Halifax, Nova Scotia pp102

Holt, R.W. (1982): The Geotectonic Evolution of the Anka Belt in the Precambrian Basement Complex of N.W. Nigeria. Ph.D. Dissertation, Open University, Milton Keynes.

Igbankwe, C. K. (2010) Geochemistry of Platinum Group Elements in the Serpentinite Body at Maimesa, Wonaka Schist Belt, NW Nigeria: Genetic Implications. Unpublished M. Sc. Thesis, Dept. of Geology, Ahmadu Bello University, Zaria – Nigeria. Pp 104.

Keulen, N., Frei, D., Riisager, P., Knudsen, C., (2012): Analysis of Heavy Minerals in Sediments by Computer-Controlled Scanning Electron Microscopy (CCSEM): Principles and Applications. Mineralogical Association of Canada Short Course 42, St. John's NL, May 2012, p. 167-184.

Keunen, P. H. (1956). Experimental abrasion of pebbles, 2. Rolling by currents. Journal of Geology **64,** 336-368.

Knight, J.B., Morison, S.R. and Mortensen, J.K., 1999. Lode and placer Au composition in the Klondike district, Yukon Territory, Canada: implications for the nature and genesis of Klondike placer and lode Au deposits. Economic Geology, vol. 94, p. 649-664.

Kroner, A. (1984): Fold Belt and Plate Tectonics in the Precambrian. Proceeding Of The **27th** International Geological Congress, Precambrian Geology. **5**, 247-284.

Lakin, H.W., Curtin, G.C. and **Hubert, A.E.** (1973): Geochemistry Of Au in the Weathering Cycle. U S Geol. Sv -V. Buff. **1330**, 80 Pp.

Leake R.C., Cameron D.G., Bland D.J., Styles M.T. and **Rollin K.E**. (1991) Exploration for Au in the South Hams District of Devon. Mineral Reconnaissance Programme Report 121. British Geological Survey.

Leake, R.C., Bland, D.J., and **Cooper, C.,** (1993) Source characterization of alluvial Au from mineral inclusions and internal compositional variation. Transactions of the

Institute of Mining and Metallogeny, section B. Appl. Earth Sci. 102, 65-82.
Leake , R C, Styles, M T, Bland, D J, Henney, P J, Wetton, P D and Naden J (1995): the interpretation of alluvial Au characteristics as an exploration technique, BGS Technical Report WC/95/22.

Li, Z. and **Peters, S.G**., (1998) Comparative geology and geochemistry of sedimentary-rock-hosted (Carlin-Type) Au deposits in the People's Republic of China and in Nevada, USA. United States Geological Survey Open-File Report 98–466, 104 p.

Loen, J.S., 1994. Origin of placer Au nuggets and history of formation of glacial Au placers, Au Creek, Granite County, Montana. Economic Geology, vol. 89, p. 91-104.

Mars, J.C. and **Rowan, R.C**. (2006). Regional mapping of phyllic-and argillic-altered rocks in the Zagros magmatic arc, Iran, using ASTER data and logical operator algorithms. Geosphere 2(3): 161-186

Marshall, P. (1927). The wearing of gravels. Transactions of the New Zealand Institute **58,** 507-532

Marshal, C. P. and **Fairbridge, R. W**. (Ed) (1999): Encyclopedia of Geochemistry; Encyclopedia of Earth Sciences Series. Kluwer Academic Publishers, London 747p.

Matheis, G. and **Caen-Vachette, M.** (1983): Rb-Sr Isotopic Study of Rare-Metal bearing And Barren Pcgmatites in the Pan-African Reactivation Zone of Nigeria. Journal Of African Terrify Science, I, 35-40.

McClenaghan, M.B., 2011. Review of common processing methods for recovery of indicator minerals from sediment and bedrock in mineral exploration. Geochemistry: Exploration, Environment, Analysis, **11**, 265–278.

McClenaghan, M. B., and Cabri, L. J. (2011): review of Au and platinum group element (PGE) indicator minerals method for surficial sediment sampling. Geochemistry: Exploration, Environment, Analysis, Vol. **11** 2011, AAG/Geological Society of London, pp. 251–263

McCready, A.J., Parnell, J. and Castro, L., 2003. Crystalline placer Au from the Rio Neuquén, Argentina: Implications for the Au budget in placer Au formation. Economic Geology, vol. 98, p. 623-633.

McCurry, P. (1970): The Geology of the Degree Sheet 21, Zaria. Unpublished M. Sc. Thesis, Ahmadu Bello University, Zaria.

McCurry, P. (1976): The Geology of the Precambrian to Lower Palaeozoic Rocks of Northern Nigeria - A Review. In: Kogbe, C.A. (Ed.), Geology of Nigeria. Elizabethan Publication Company, Lagos.

McDonald, E. H. (2007): Handbook of Au Exploration and Evaluation. Wood head Publishing Ltd. Cambridge, England. 664p.

Moles, N.R., Chapman, R.J., Warner, R.B., 2013. The significance of copper concentrations in natural Au alloy for reconnaissance exploration and understanding Au-depositing hydrothermal systems. Geochem. Explor. Environ. Anal. http://dx.doi.org/10.1144/geochem2011-114.

Moon, C. J., Barrett, W. L., Bell, T., Evans, A. M., Milsom, J., Scott, B. C., and **Whateley, K. G. M** (2006) Introduction to Mineral Exploration: 2nd Edn. Blackwell Publishing. U K.

Mortensen, J.K., Chapman, R., LeBarge, W. and Jackson, L., 2004. Application of placer and lode Au geochemistry to Au exploration in western Yukon. In: Yukon Exploration and Geology 2004, D.S. Emond, L.L. Lewis and G.D. Bradshaw (eds.), Yukon Geological Survey, p. 205-212.

Mortensen, J., R. Chapman, LeBarge, W., and L.Jackson. (2005). Application of placer and lode Au geochemistry to Au exploration in western Yukon. Yukon Exploration and Geology 2004. pp 205-212

Ninomiya, Y., (2004). A stabilized vegetation index and several mineralogic indices Defined for ASTER VNIR and SWIR data. Proceedings of IEEE 2004 International Geoscience and Remote Sensing Symposium: IGARSS'03, 3, pp. 1552–1554.

Obaje, N. G. (2009): Geology and Mineral Resources of Nigeria. Springer-Verlag Berlin Heidelberg. 219p.

Ogezi, A.E.O., (1977): Geochemistry and Geochronology of Basement Rocks from Northwestern Nigeria. Ph.D. Dissertation, University Of Leeds UK.

Oke, S. A., Abimbola, A. F., and **Rammlmair, D**. (2014) Mineralogical and Geochemical Characterization of Au Bearing Quartz Veins and Soils in Parts of Maru Schist Belt Area, Northwestern Nigeria. Journal of Geological Research. Hindawi Publishing Corporation. Vol. 2014, Article ID 314214, pp17

Olade, M. A. and **Elueze, A. A.** (1979): Petrochemistry of the Ilesha Amphibolites and Precambrian Crustal Evolution in the Pan-African Domain of SW Nigeria. Precambrian Research, 8. 303-318.

Oluyide, P.O., (1988). Structural trends in the Nigerian Basement Complex. Nigerian Mining, Geol. and Metall. Soc., 1, pp. 87-102.

Oyawoye, M. O. (1964): The Contact Relationship of Charnokite and Biotite Gneiss at Bauchi, Northern Nigeria. Geol. Mag. **No. 2**, Pp 138-144.

Oyawoye M. O. (1972): The Basement Complex of Nigeria. In: Dessauvagie Tfj, Whiteman Aj (Eds) African Geology. Ibadan University Press, Pp 66–102.

Palacios,C. and Herail,G. (2001) The composition of Au in the Cerro Casale Au-rich porphyry deposit, Maricunga belt, northern Chile. Canadian Mineralogist, 39, 907–915.

Passchier, C. W. & Trouw, R. A. J. 1996. Microtectonics. Springer-Verlag, Berlin Heidelberg New York.

Potter M, and **Styles MT** (2003) Au characterization as a guide to bedrock sources for the Estero Hondo alluvial Au mine, western Ecuador. Trans Inst Min Metall B Appl Earth Sci.112:297–304

Rahaman, M. A (1976): Review of the Basement Geology of South-Western Nigeria. In: Kogbe Ca (Ed) Geology of Nigeria, **2nd Edn**, Elizabethan Publishers, Lagos. Pp 41–58.

Rahaman, M. A. (1988): Recent Advances in the Study of the Basement Complex of Nigeria. In: Geological Survey of Nigeria (Ed) Precambrian Geol Nigeria, Pp 11–43.

Rahaman, M. A., Emofurieta, W. O., and **Caen-Vachette, M.** (1983): The Potassic-Granites of the Igbeti Area: Further Evidence of the Poly-Cyclic Evolution of the Pan-African Belt in Southwestern Nigeria. Precambrian Research, **22**, 75-92.

Ramadan, T. M., and **Abdel Fattah, M. F.** (2010): Characterization of Au Mineralization in Garin Hawal Area, Kebbi State, NW Nigeria, Using Remote Sensing. The Egyptian Journal of Remote Sensing and Space Sciences, **13**, 153-163.

Rasmussen, K.L., Mortensen, J.K. and Falck, H., 2007. Morphological and compositional analysis of placer Au in the South Nahanni River drainage, Northwest Territories. In: Yukon Exploration and Geology 2006, D.S. Emond, L.L. Lewis and L.H. Weston (eds.), Yukon Geological Survey, p. 237-250.

Rein, B., and Kauftman, H., (2003): exploration for Au using panchromatic stereoscopic intelligence satellite photographs and Landsat TM data in Hebei area, China: International Journal of Remote Sensing, Vol. 24, p. 2427-2438.

Richards, K. (1982). "Rivers: Form and Process in Alluvial Channels." Methuen, New York.

Rokos, D., Mavrantza, R., Vamvoukakis, St.-Seymour, Kouli, M., Karfakis, I., and Denes, G., (2000): Localization of alteration zoning for the detection of epithermal Au by interpretation of remote sensing and geochemical techniques: Lesvos Island, Aegean Sea, Hellas: proceedings of the Fourteenth International Conference on applied Geological Remote Sensing, Nevada, USA. P. 161-168.

Rutter, E. H. (1983). Pressure solution in nature, theory and experiment. J. geol. Soc. Lond. 140, 725-740.

Sabins, F.F., (1999): Remote Sensing for mineral exploration. Ore Geology Reviews, vol. 14, p. 157-183

Salau S. L. (2000): The Geology, Geochemistry and Possible Origin of Au Mineralization at Duki Old Mine, Maru, Zamfara State, Nigeria. M. Sc. Thesis, Ahmadu Bello University, Nigeria.

Seward, T.M. (1973): Thio Complexes of Au and the Transport of Au in Hydrothermal Ore Solutions. Geochim. Cosmochim. Acta, **37**, 379-99.

Tommaso, I. D. and **Rubinstein, N**. (2007). Hydrothermal alteration mapping using ASTER data in the Infiernillo porphyry deposit, Argentina. Ore Geology Reviews 32: 275-290

Toteu, S.F., Bertrand, J.M., Penaye, J., Macaudi, J., Angoua, S., and **Barbey, P**., (1991) Cameroon: a tectonic keystone in the Pan-African network. In: Lewry, J.F., Stauffer, M.R. (Eds.), The Early Proterozoic Trans-Hudson Orogen of North America, Geological Association of Canada, Special Paper, vol. 37, pp. 483e496.

Townley, B.K., Herail, G., Maksaev, V., Palacios, C., de Parseval, P., Sepuldeva, F., Orellana, R., Rivas, P., Ulloa, C., 2003. Au grain morphology and composition as an exploration tool: application to Au exploration in covered areas. Geochemistry: Exploration, Environment, Analysis. 3, 29-38.

Truswell, J.F. and **Cope, R.N.** (1963): The Geology of Part of the Niger and Zaria Provinces, Northern Nigeria. Geol. Surv. Nigeria Bull. **29**, 54p.

Turner, D.C. (1983): Upper Proterozoic Schist Belts in the Nigerian Sector of the Pan-African Province of West Africa. Precambrian Research **21**, 55-79.

Turner, D. C. and **Webb, P. K.** (1974): The Daura Igneous Complex Northern Nigeria; a Link between the Younger Granite District of Nigeria and Southern Niger. Jour. Geol. Soc. London, **130**:71-77.

Usman, A. (2014): Geology and Geochemistry of Rocks and Banded Iron Formation of Northern Part of Wonaka Schist belt, Northwestern Nigeria. Unpublished M. Sc. Dissertation, Ahmadu Bello University, Zaria Nigeria.

Van Breeman, O., Pidgeon, R.T., and Bowden, P. (1977): Age and Isotopic Studies of Some Pan-African Granites from North-Central Nigeria. Precambrian Research **4**, 307- 319.

Vincent, R. (1997). Fundamentals of geological and environmental remote sensing. USA: Prentice-hall

Vishiti, A., Suh, C.E, Lehmann, B, Egbe, J.A, Shemang, E.M (2015) Au grade variation and particle microchemistry in exploration pits of the Batouri Au district, SE Cameroon. Journal of African Earth Sciences. 111. 1-13.

Waziri, N. M., (2014): Environment Geochemistry of Soils and Stream Sediments from the Birnin-Gwari Artisinal Au Mining Area, Northwestern Nigeria. Universal. Journal of Geoscience **2(1)**: Pp18-27.

Weibel, R. (2003): Alteration of detrital Fe-Ti oxides in Miocene fluvial deposits, central Jutland, Denmark. Bull. Geol. Soc. Denmark **50**, 171-183.

Woakes, M. and **Bafor, B.E.** (1984): Primary Au Mineralisation in Nigeria. In: Foster, R.P. (Ed.), Au '82. A.A. Balkema, Rotterdam, Pp. 661-671.

Woakes, M. Ajibade, C.A and **Rahaman, M. A.** (1987): Some metallogenic features of the Nigerian Basement, J. Afr. Sci., 5: 655-664.

Wright, J.B., Hastings, D.A., Jones, W.B., and **Williams, H.R**. (1985): Geology and Mineral Resources of West Africa. Allen and Unwin, London, 187p.

Youngson, J., and Craw, D. (1999). Variation in Placer Style, Au Morphology, and Au Particle Behavious Down Gravel Bed-Load Rivers: An Example from the Shot over/Arrow-Kawarau-Clutha River System, Otago, New Zealand. Economic Geology Vol. 94, 615-634.

Youngson, J.H., Woperies, P., Kerr, L.C. & Craw, D. 2002. Au-Ag-Hg and Au-Ag alloys in Nokomai and Nevis valley placers, northern Southland, and Central Otago, New Zealand, and implications for placer-source relationships. New Zealand Journal of Geology and Geophysics, **45,** 53–69.

Zaborski P.M. (2000): The Cretaceous and Paleocene Transgression in Nigeria and Niger. Elm Bank. Gardens Barnes, London, UK.

APPENDIXES

Appendix 1.1: Joint readings on granite

094	130	094	040	088	182	086	136	136	140
096	044	030	034	038	094	092	088	088	048
136	050	134	150	155	138	040	136	092	092
088	100	102	088	044	060	070	044	182	184
182	180	088	092	100	102	080	100	088	112

Appendix 1.2: Joint reading on quartz-mica schist

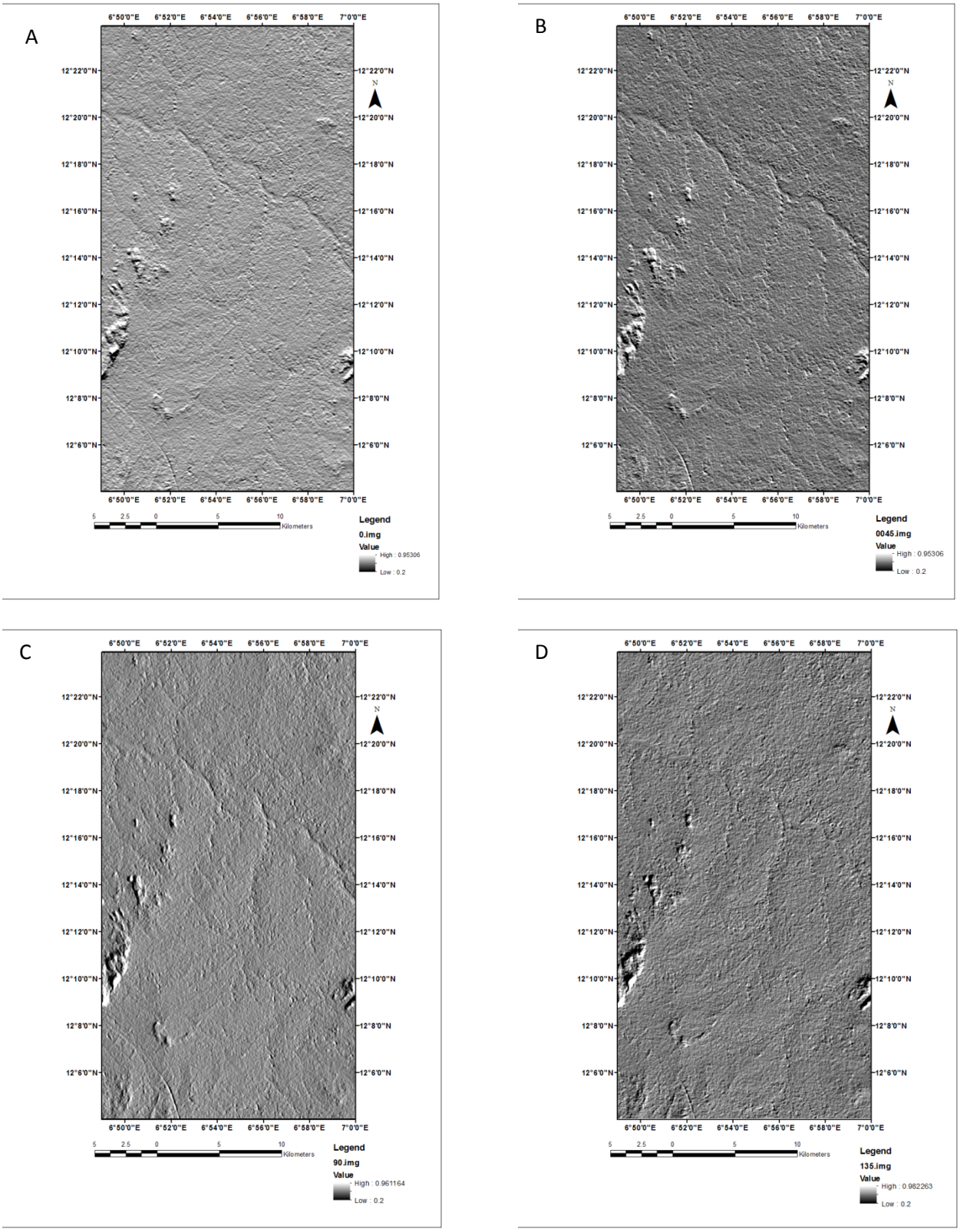
170	252	300	302	218	252	262	268	300	191
062	058	188	340	360	090	120	090	094	084
170	180	210	350	090	280	276	182	300	300
082	090	170	355	270	176	178	170	120	182
180	189	180	176	192	092	272	005	002	020
180	210	130	132	208	140				

Appendix 1.3: Joints reading on phyllite

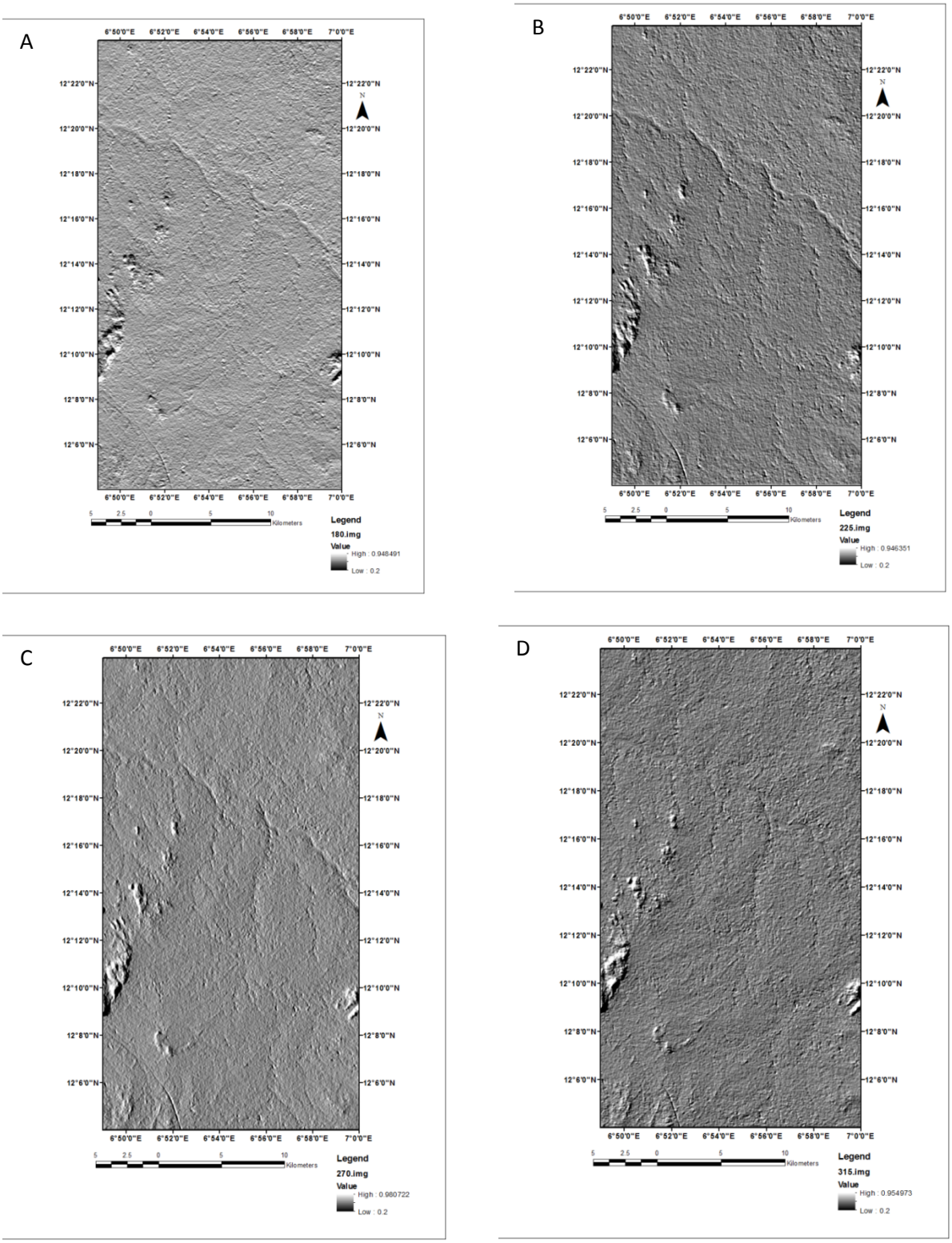
080	180	090	176	188	186	280	270	180	268
300	300	062	182	180	176	092	210	092	090
355	110	356	010	005	052	290	110	156	210
025	024	292	066	070	050	130	128	128	135
288	070	210	156	270	280	092	024	180	

Appendix 1.4: Joints reading on granite gneiss

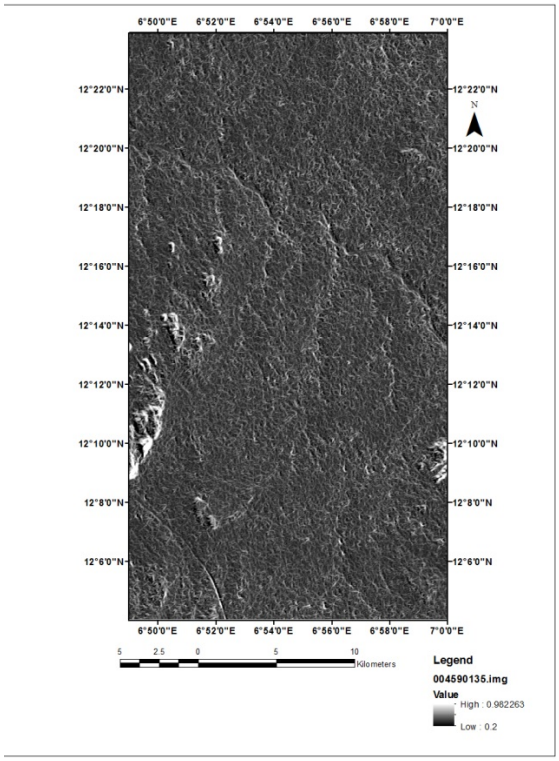
182	010	050	005	008	100	046	100	354	096
088	180	184	186	102	036	010	188	014	310
188	180	094	092	082	012	020	351	280	358
348	280	012	040	032	026	184	084	054	022
010	354	300	110	350	090	014	046	192	080
098									



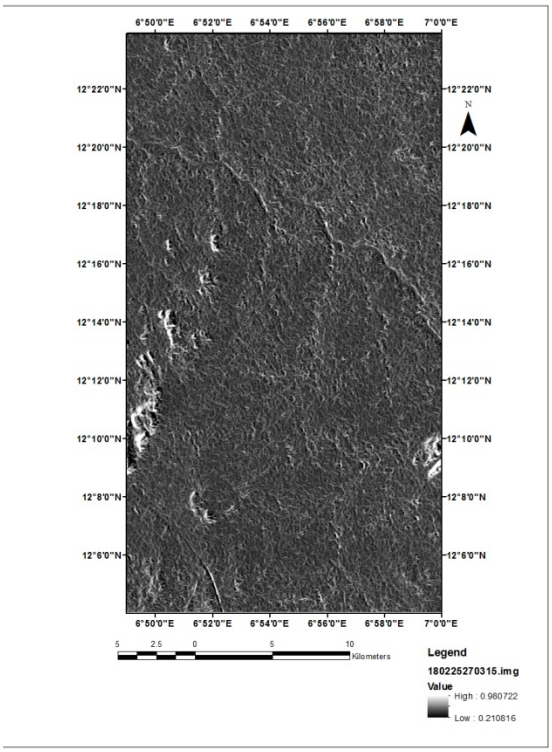
Appendix 1.5: DEM shaded relief images of A: 0^0 (N), B: 45^0 (NE), C: 90^0 (E), and D: 135^0 (SE)



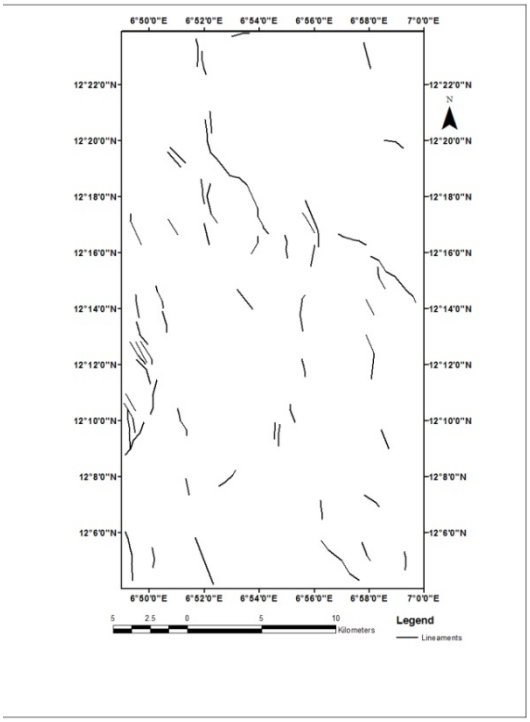
Appendix 1.6: DEM shaded relief images of A: 180^0 (S), B: 225^0 (SW), C: 270^0 (W) and D: 315^0 (NW)



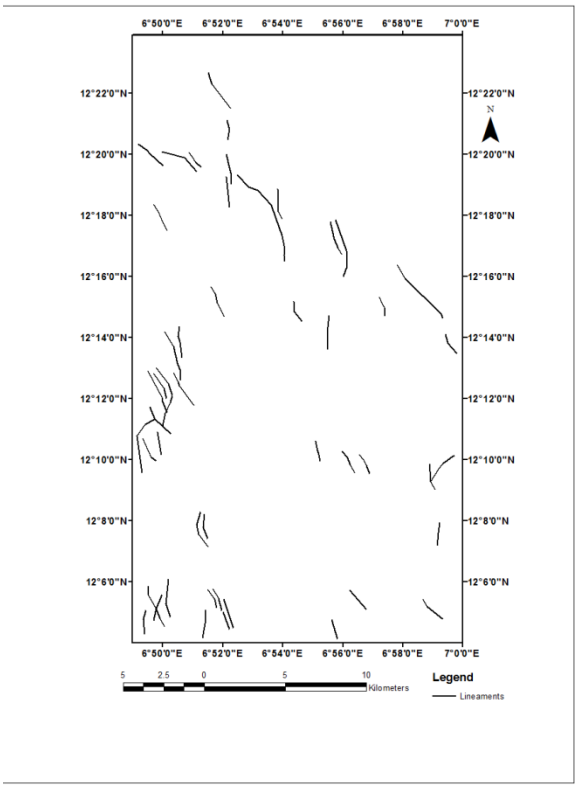
Appendix 1.7: combined shaded relief images of N, NE, E, and SE



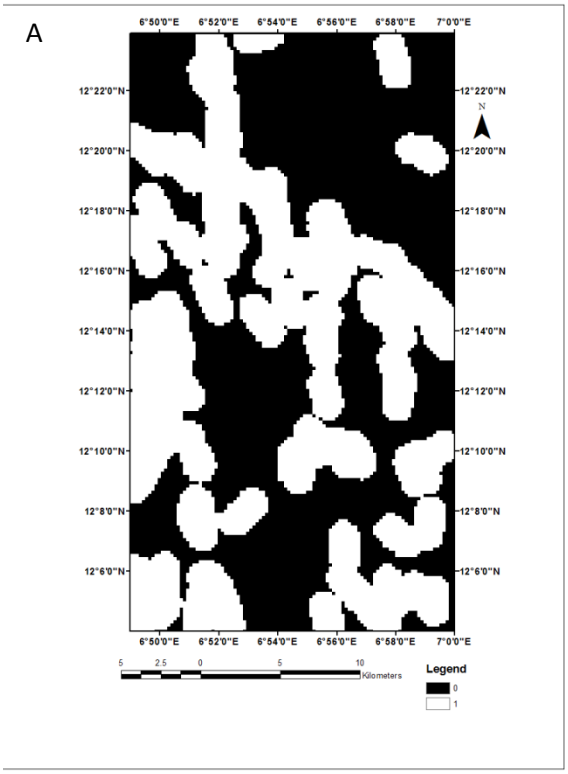
Appendix 1.8: combined shaded relief images of S, SW, W and NW

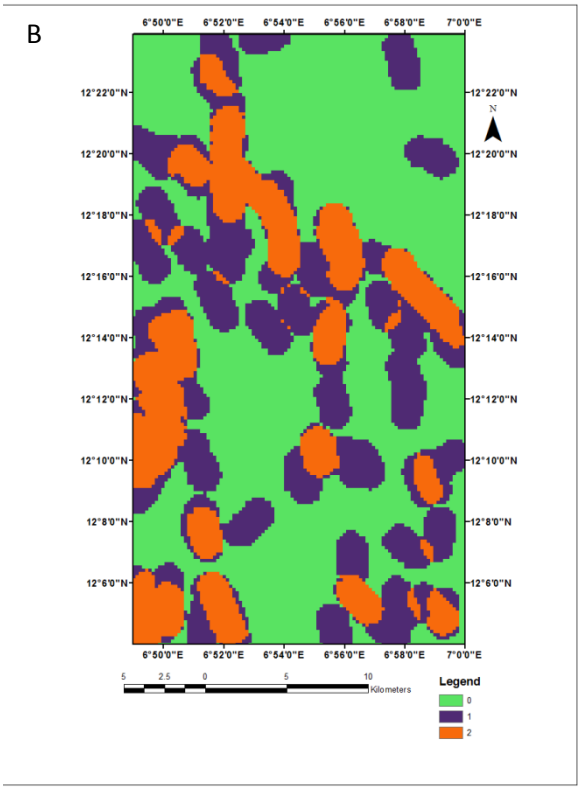


Appendix 1.9: Automatically extracted lineament from shaded relief images of N, NE, E, and SE



Appendix 1.10: Automatically extracted lineament from shaded relief images of S, SW, W and NW





Appendix 1.11: A; Final reclass and B; Level of coincidence image

Appendix 2.1: Sieve analysis data from the stream sediments samples

WT

sieve size	phi values	weight retained	cumulative weight %
1.18	-1	57	57
0.6	0	14	71
0.3	1	14	85
0.15	2	6	91
0.075	3	5	96
<0.075	4	4	100
TOTAL		100	

ZO7

sieve size	phi values	weight retained	cumulative weight %
1.18	-1	38	38
0.6	0	45	83
0.3	1	7	90
0.15	2	6	96
0.075	3	3	99
<0.075	4	1	100
TOTAL		100	

T05

sieve size	phi values	weight retained	cumulative weight %
1.18	-1	48	48
0.6	0	16	64
0.3	1	13	77
0.15	2	11	88
0.075	3	7	95
<0.075	4	5	100
TOTAL		100	

W02

sieve size	phi values	weight retained	Cumulative wt.%
1.18	-1	51	51
0.6	0	23	74

0.3	1	8	82
0.15	2	4	86
0.075	3	7	93
<0.075	4	6	99
TOTAL		99	

T01

sieve size	phi values	weight retained	cumulative weight %
1.18	-1	42	42
0.6	0	30	72
0.3	1	18	90
0.15	2	5	95
0.075	3	3	98
<0.075	4	2	100
TOTAL		100	

W04

sieve size	phi values	weight retained	cumulative weight %
1.18	-1	38	38
0.6	0	25	63
0.3	1	27	90
0.15	2	6	96
0.075	3	0	96
<0.075	4	3	99
		99	

MM

sieve size	phi values	weight retained	cumulative weight %
1.18	-1	59	59
0.6	0	14	73
0.3	1	14	87
0.15	2	2	89
0.075	3	4	93
<0.075	4	6	99
TOTAL		99	

ML

sieve size	phi values	weight retained	cumulative weight %
1.18	-1	61	61
0.6	0	15	76
0.3	1	10	86
0.15	2	8	94
0.075	3	3	97
<0.075	4	2	99
TOTAL		99	

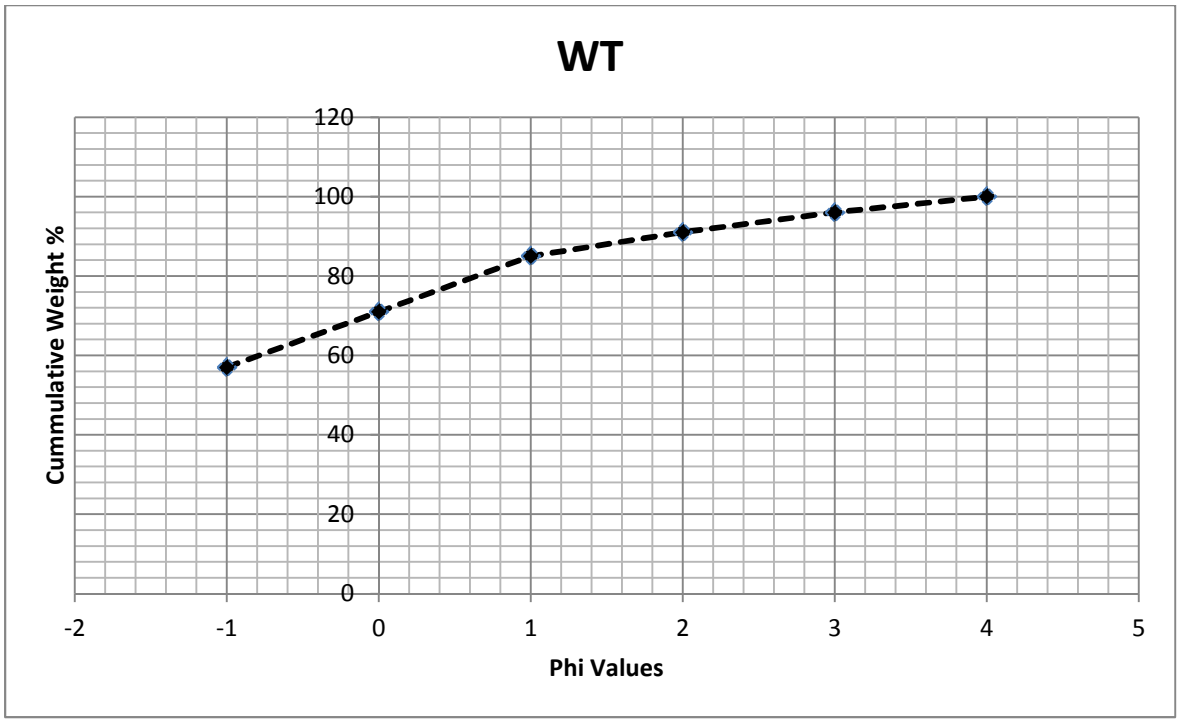
KO2

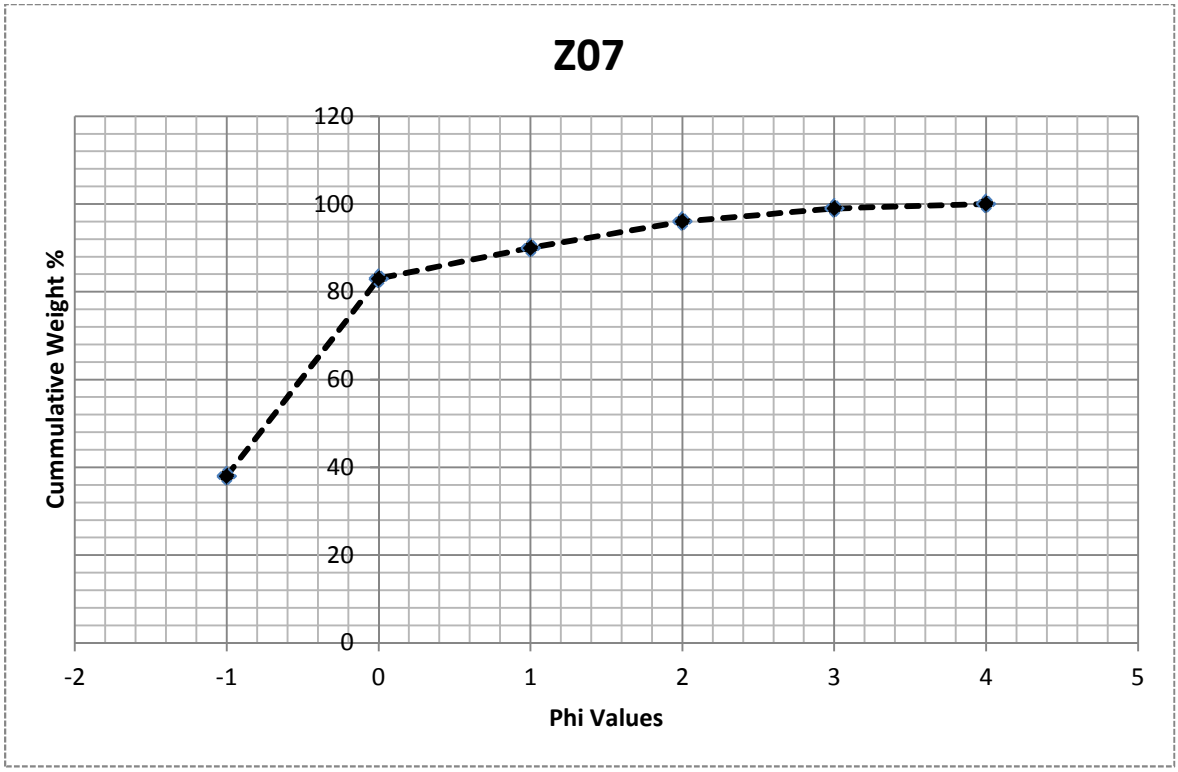
sieve size	phi values	weight retained	cumulative weight %
1.18	-1	45	45
0.6	0	14	59
0.3	1	21	80
0.15	2	10	90
0.075	3	8	98
<0.075	4	2	100
		100	

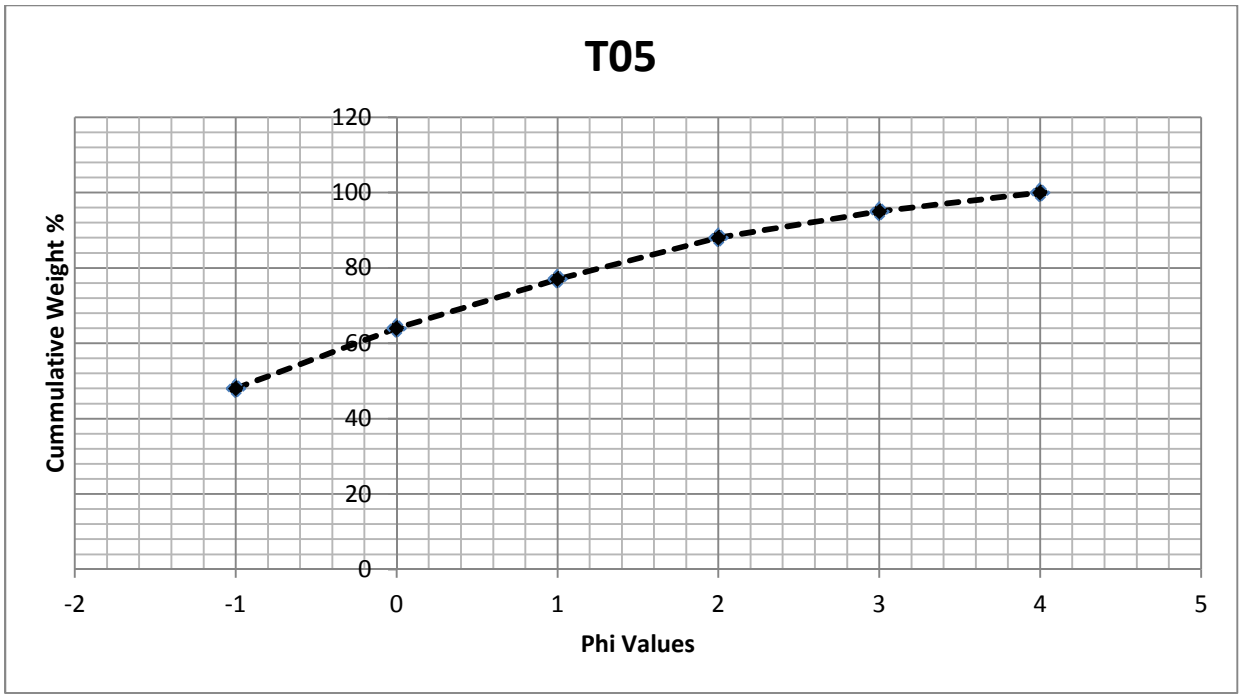
Z01

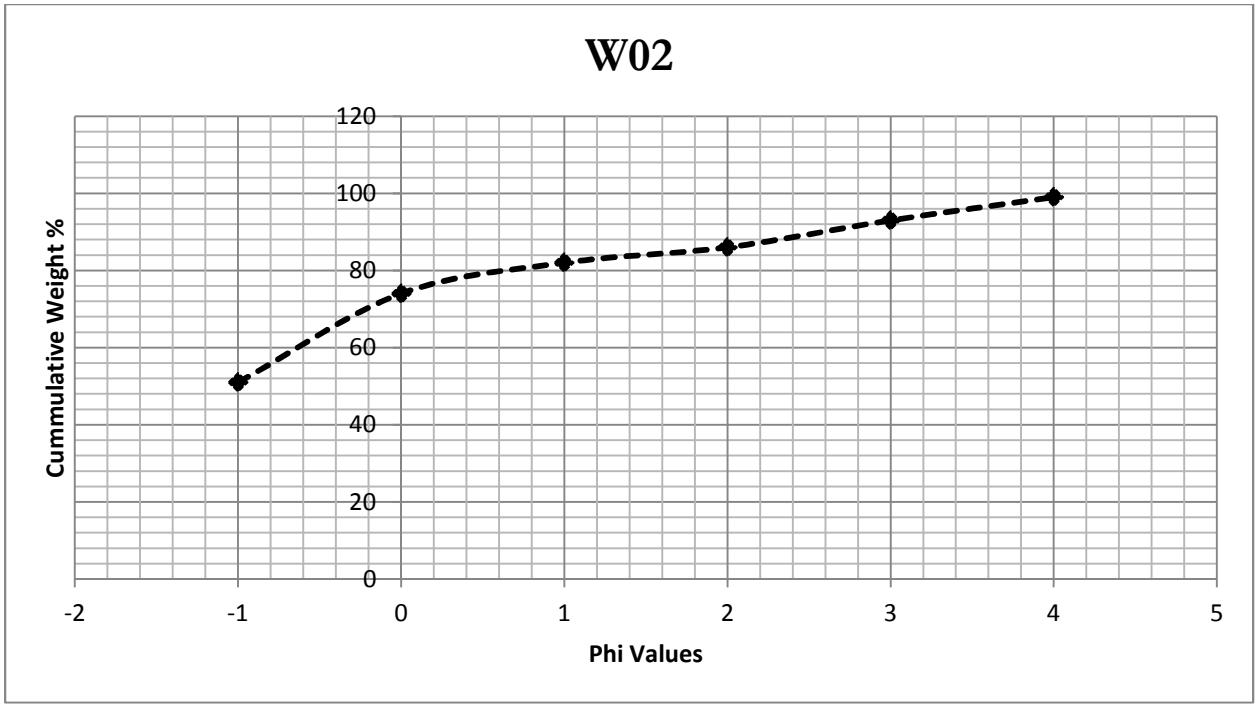
sieve size	phi values	weight retained	cumulative weight %
1.18	-1	70	70
0.6	0	7	77
0.3	1	7	84
0.15	2	6	90
0.075	3	3	93
<0.075	4	7	100
TOTAL		100	

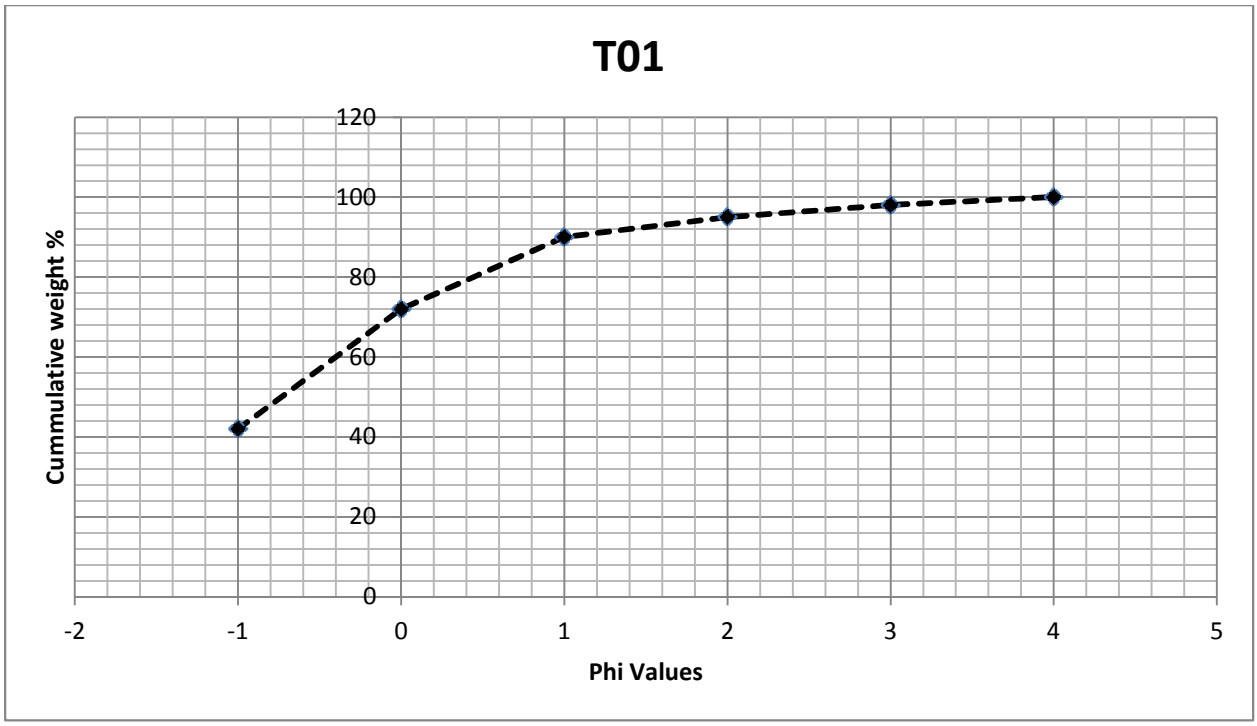
Appendix 3.1: Cumulative frequency curves of weight % vs. phi values

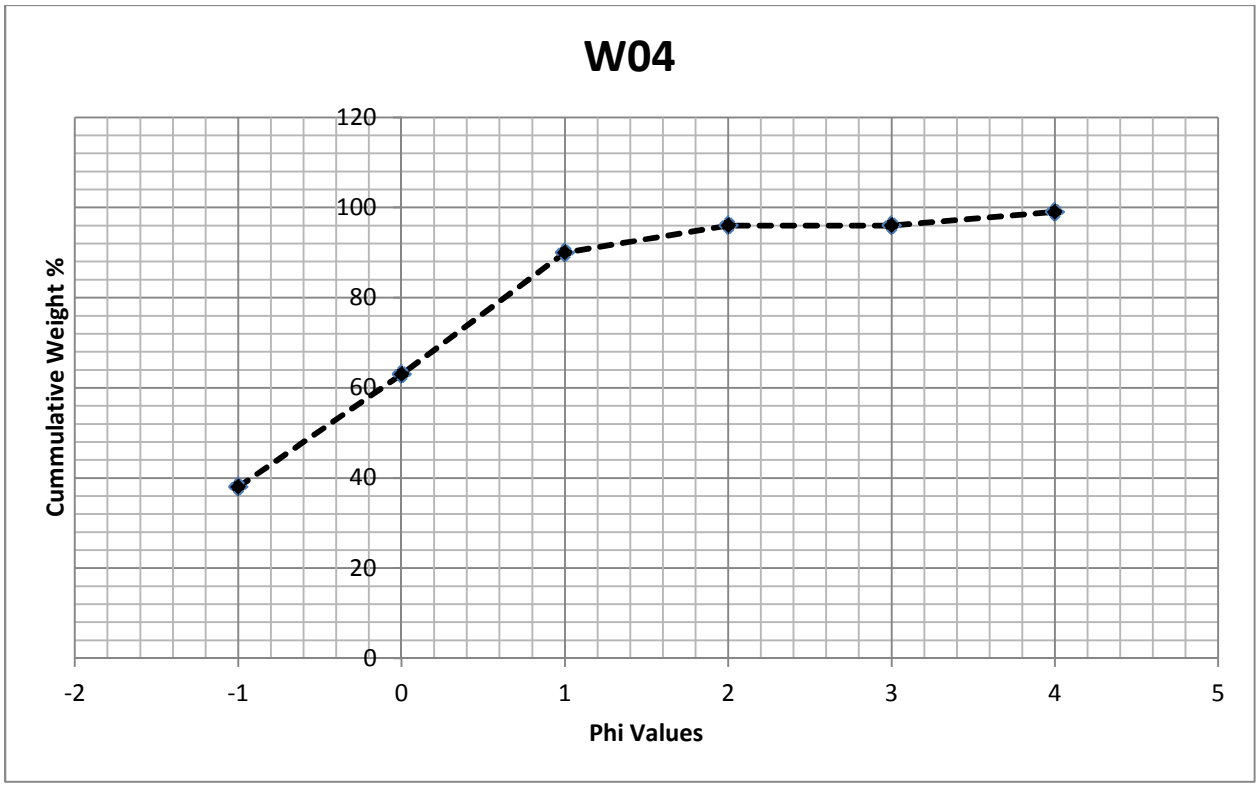


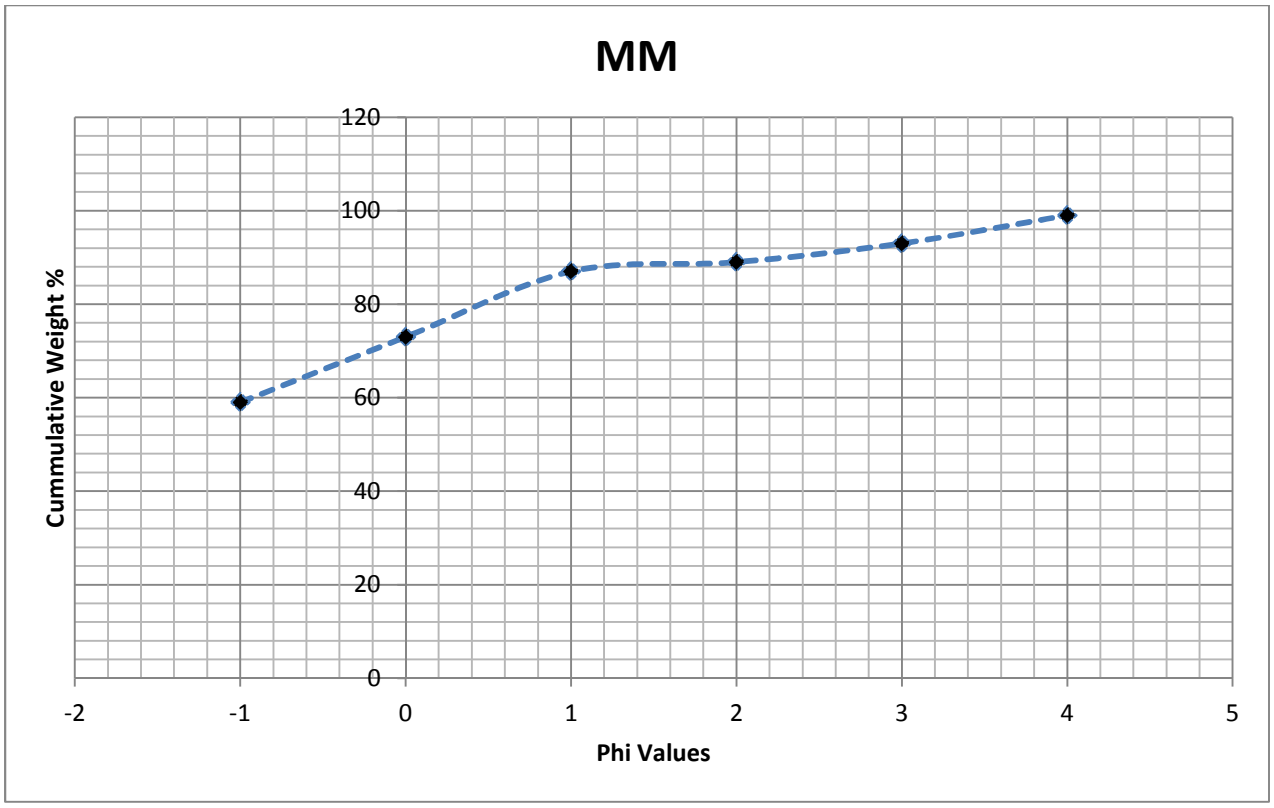


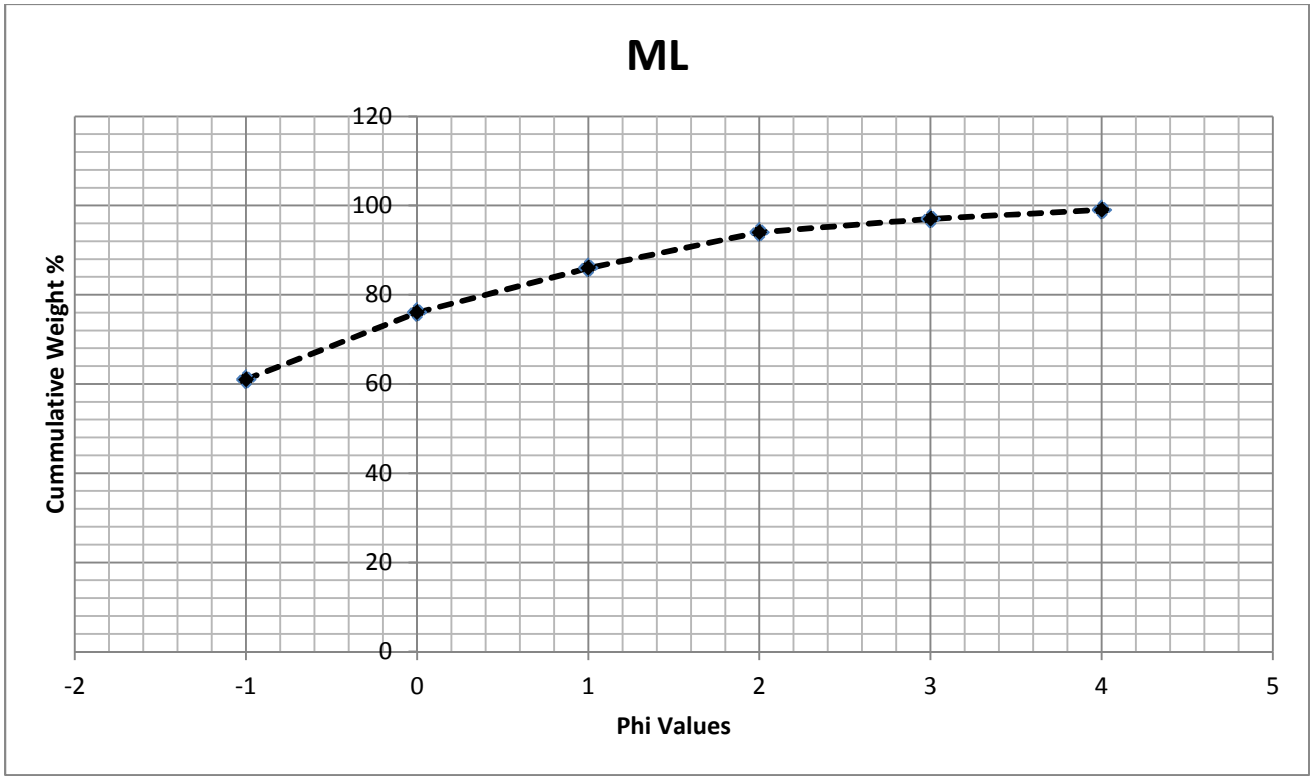

T05
120
100
80
60
40
20
0
Cummulative Weight %
-2
-1
0
1
2
3
4
5
Phi Values

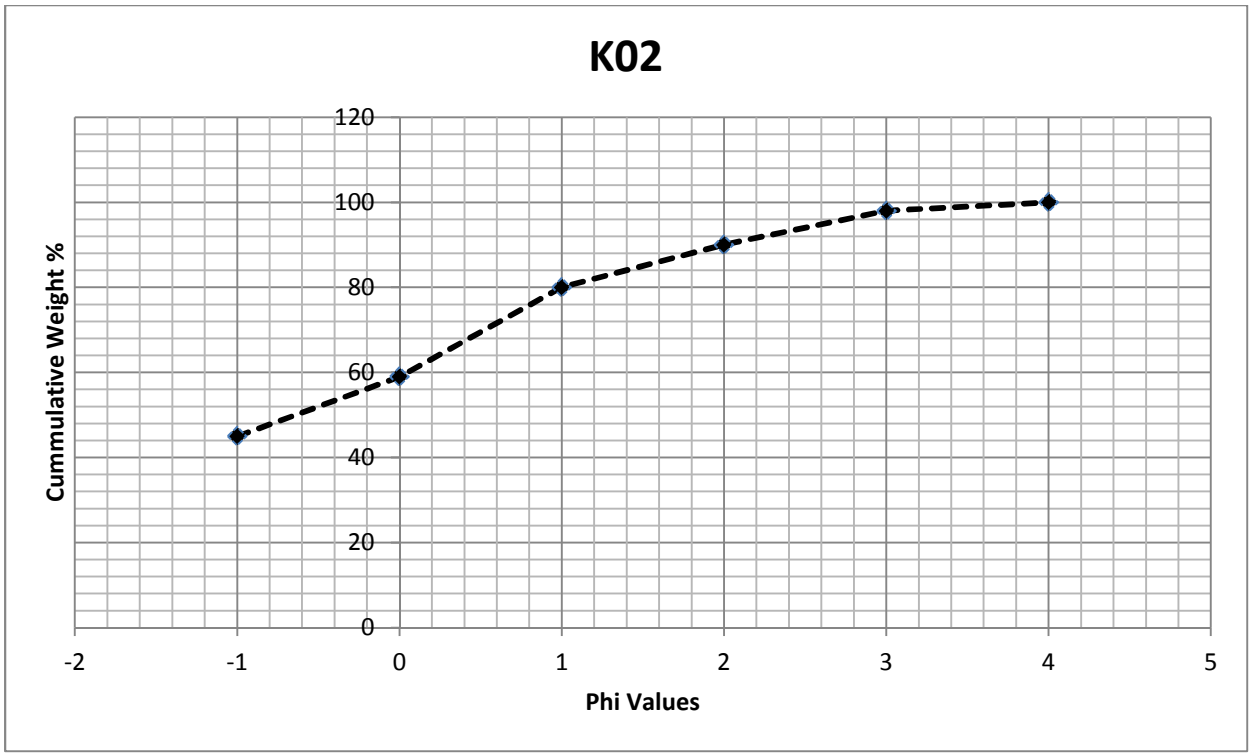

W02
120
100
80
60
40
20
0
Cummulative Weight %
-2
-1
0
1
2
3
4
5
Phi Values

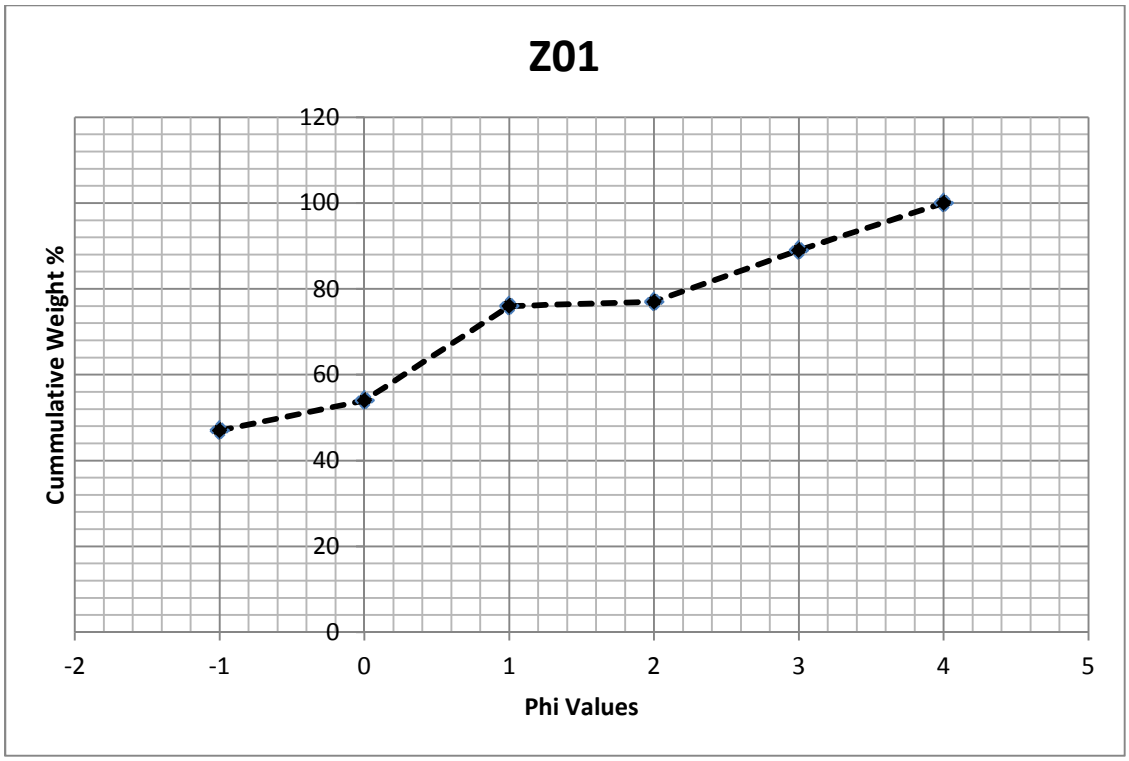

T01
120
100
80
60
40
20
0
Cummulative weight %
-2
-1
0
1
2
3
4
5
Phi Values


W04
120
100
80
60
40
20
0
Cummulative Weight %
-2
-1
0
1
2
3
4
5
Phi Values


MM
120
100
80
60
40
20
0
Cummulative Weight %
-2
-1
0
1
2
3
4
5
Phi Values


ML
120
100
80
60
40
20
0
Cummulative Weight %
-2
-1
0
1
2
3
4
5
Phi Values


K02
Cummulative Weight %
120
100
80
60
40
20
0
-2
-1
0
1
2
3
4
5
Phi Values


Z01
Cummulative Weight %
120
100
80
60
40
20
0
-2
-1
0
1
2
3
4
5
Phi Values